IMPACT OF IRRIGATION AND SOIL COMPACTION ON AGRICULTURAL LANDS WITH SHALLOW GROUND WATER TABLE

by

Sina Maghami Nick

B.Sc. in Liberal Arts and Sciences, Maastricht University, 2008

Submitted to the Institute of Environmental Sciences

in partial fulfilment of the requirements for the degree of

Master of Science

in

Environmental Technology

Boğaziçi University

2021

IMPACT OF IRRIGATION AND SOIL COMPACTION ON AGRICULTURAL LANDS WITH SHALLOW GROUND WATER TABLE

APPROVED BY:

Prof. Dr. Nadim Copty Thesis Advisor	. . . . .
Prof. Dr. Burak Demirel Thesis Co-Advisor	. . . . .
Prof. Dr. Işıl Balcıoğlu	. . . . .
Prof. Dr. Hasan Sabri Öztürk	. . . . .
Dr. Masoud Babaei	. . . . .

DATE OF APPROVAL: 24/06/2021

ACKNOWLEDGEMENTS

I would like to express my deepest appreciation to one of the best, kindest and smartest professors in the world, Prof. Dr. Nadim Copty, who did not only supervise my thesis project but also supported me in all directions during my master studies at the institute of environmental sciences in Bogazici University. Without his guidance and persistence help pursuing this research would have not been possible.

I would like to show my special appreciation to my beautiful family. I owe my parents and siblings for enduring all the hardships for me while giving unconditional support. I am standing here strong because I have them beside me.

I would like to thank all the staff who helped me and supported me during my thesis project, especially Filiz Ayılmaz, the laboratory supervisor who greatly assisted me with my lab work, Prof. Burak Demirel who guided me as the secondary advisor. I also thank Prof. Dr. Işıl Balcıoğlu, Prof. Dr. Hasan Sabri Öztürk and Dr. Masoud Babaei for being the jury members assessing my thesis project.

Many friends and colleagues helped me in different ways to make this project happen, I would like to send my gratitude to Prof. Dr. Gunay.Erpul, Dr. Manoj Menon, Dr. Selen Deviren Saygin, Dr. Mehdi Emadian, Mehmet Can Tunca, Buse Yetişti and Yağmur Ongar.

This research was supported by The Scientific and Technological Research Council of Turkey (TUBITAK 118Y343).

ABSTRACT

IMPACT OF IRRIGATION AND SOIL COMPACTION ON AGRICULTURAL LANDS WITH SHALLOW GROUNDWATER TABLE

Salt accumulation in agricultural soils is a long-lived problem for farmers in many regions of the world, leading to a decrease in crop yields and threatening food security. The salinity challenge amplifies in absence of proper soil water drainage in areas with shallow groundwater table. Hence, this study was carried out by examining the impact of irrigation pattern and soil compaction on the salt dynamics within a soil profile with a shallow aquifer. A series of laboratory-scale column experiments were conducted to examine the impact of different irrigation patterns, water quality and soil compaction conditions on salt dynamics. Two water qualities were applied: fresh (DI water) and saline (~3.4 mS/cm). The soil columns (60 cm height and 16 cm diameter) were packed with agricultural soil from a 10-year non-tilled profile of an apple farm located in the Konya plain, Turkey. A saline shallow water table was maintained at the bottom of the columns. The experiments were numerically modelled with the HYDRUS-1D computer program which can simulate water and solute movement in unsaturated soils. Results showed that without having proper drainage the salinity within the profile would only accumulate in the presence of a shallow saline aquifer. Furthermore, the numerical simulations showed that short-term solutions such as the application of freshwater during the critical plant growth period can limit the accumulation of salts in agricultural soils. The type of soil, the kind of plant and the availability of freshwater all play a role in the practicability of such short-term solution.

ÖZET

IMPACT OF IRRIGATION AND SOIL COMPACTION ON AGRICULTURAL LANDS WITH SHALLOW GROUNDWATER TABLE

Tarım topraklarında tuz birikmesi, dünyanın birçok bölgesinde çiftçiler için uzun süredir devam eden bir sorun olup, mahsul veriminin düşmesine neden olmakta ve gıda güvenliğini tehdit etmektedir. Tuzluluk sorunu, sığ yeraltı suyu tablasına sahip alanlarda uygun toprak suyu drenajının olmadığı durumlarda artar. Bu nedenle, bu çalışma, sığ akiferli bir toprak profilinde, sulama düzeninin ve toprak sıkışmasının tuz dinamikleri üzerindeki etkisi incelenerek gerçekleştirilmiştir. Farklı sulama modelleri, su kalitesi ve toprak sıkıştırma koşullarının tuz dinamikleri üzerindeki etkisini incelemek için bir dizi laboratuvar ölçekli kolon deneyi yapıldı. İki su kalitesi uygulandı: taze (DI su) ve tuzlu su (~3.4 mS/cm). Toprak sütunları (60 cm yüksekliğinde ve 16 cm çapında), Türkiye, Konya ovasında bulunan bir elma çiftliğinin 10 yıllık işlenmemiş profilinden tarım toprağı ile dolduruldu. Sütunların dibinde tuzlu bir sığ su tablası muhafaza edildi. Deneyler, doymamış topraklarda su ve çözünen hareketini simüle edebilen HYDRUS-1D bilgisayar programı ile sayısal olarak modellendi. Sonuçlar, uygun drenaj olmadan profil içindeki tuzluluğun sadece sığ tuzlu akifer varlığında birikeceğini gösterdi. Ayrıca, sayısal simülasyonlar, kritik bitki büyüme döneminde tatlı su uygulaması gibi kısa vadeli çözümlerin tarım topraklarında tuz birikimini sınırlayabileceğini gösterdi. Toprağın türü, bitkinin türü ve tatlı suyun mevcudiyeti, bu tür kısa vadeli çözümlerin uygulanabilirliğinde rol oynar.

TABLE OF CONTENTS

ACKNOWLEDGEMENTS iii

ABSTRACT iv

ÖZET v

TABLE OF CONTENTS vi

LIST OF FIGURES viii

LIST OF TABLES xii

1. INTRODUCTION 1

2. BACKGROUND 3

2.1. Soil Salinity 3

2.2. Soil Sodicity 4

2.3. Soil Texture and Salt-affection 5

2.4. Shallow Saline Groundwater and Salt-affection 6

2.5. Irrigation 8

2.6. Agricultural Soil Compaction 10

2.7. Numerical Modelling of Salinization and HYDRUS-1D 11

2.8. Literature Review 13

3. STATEMENT OF THE PROBLEM 17

4. METHODOLOGY 18

4.1. Sample Preparation 18

4.2. Laboratory Setup 19

4.2.1. Initial Conditions 22

4.3. Column Experiments 23

4.3.1. Experiment 1: Capillary Rise without Irrigation 24

4.3.2. Experiment 2: Capillary Rise with Saline Water Flood Irrigation 24

4.3.3. Experiment 3: Capillary Rise with Saline Water Drip Irrigation 26

4.3.4. Experiment 4: Capillary Rise with Freshwater Flood Irrigation....26
4.3.5. Experiment 5: Capillary Rise with Freshwater Drip Irrigation....27
4.3.6. Experiment 6: Freshwater Flood Irrigation with Free Drainage....27
4.4. Numerical Modelling....27
5. RESULTS AND DISCUSSIONS....29
5.1. Soil Characterization....29
5.2. Soil Moisture....31
5.3. Surface Soil Bulk Electrical Conductivity....44
5.4. Pressure/Tension Sensors....49
5.5. Soil Moisture Analysis....52
5.6. HYDRUS-1D Numerical Simulations....62
5.6.1. Hydraulic Simulations....64
5.6.2. Solute Transport Simulations....71
6. CONCLUSIONS....79
REFERENCES....83

LIST OF FIGURES

Figure 1.1. A global demonstration of salt-affected soils. 1

Figure 2.1. Soil texture classification triangle.....6

Figure 2.2. Process of salinization due to capillary rise from a shallow saline aquifer. 7

Figure 2.3. Relation between soil type (indicated by porosity, α, and hydraulic conductivity, K_s) and capillary rise (indicated as suction head). 7

Figure 2.4. Left: the bulk density distribution of a compacted sandy loam soil before and after ploughing. Right: An example of a compacted agricultural soil profile. 11

Figure 2.5. The number of publications related to soil salinity presented in the Web of Science database. 14

Figure 4.1. Left: sampling location. Right: 60 cm deep sample collection.....18

Figure 4.2. Dried and sieved (2mm mesh) samples 19

Figure 4.3. Soil columns after filling the soil samples. The right column is CA, and the left is CB. The compaction layer is vivid in the picture on column CB.....20

Figure 4.4. Soil columns after equipping the sensors. 21

Figure 4.5. Soil columns in dark having infrared lamps controlling the soil surface temperature. ..22

Figure 4.6. Hyprop soil retention curve analysis setup 23

Figure 4.7. Soil water collection using the suction cups.....25

Figure 5.1. Hyprop analysis results from L1 with a dry bulk density of ~1.15 g/cm^3. This analysis applies to both CA and CB columns. 30

Figure 5.2. Hyprop analysis results from L2 with a dry bulk density of ~1.15 g/cm^3 which applies to the bottom layer in the CA column. 30

Figure 5.3. Hyprop analysis results from L2 with a dry bulk density of ~1.25 g/cm^3 which applies to the compacted layer of the column CB. 31

Figure 5.4. Moisture sensor measurements from column CA during experiment 1 (capillary rise without irrigation).....32

Figure 5.5. Moisture sensor measurements from column CB during experiment 1 (capillary rise without irrigation)…….. 33

Figure 5.6. Moisture sensor measurements from column CA during experiment 2 (capillary rise with saline water flood irrigation).....34

Figure 5.7. Moisture sensor measurements from column CB during experiment 2 (capillary rise with saline water flood irrigation). 35

Figure 5.8. Moisture sensor measurements from column CA during experiment 3 (capillary rise with saline water drip irrigation). 36

Figure 5.9. Moisture sensor measurements from column CB during experiment 3 (capillary rise with saline water drip irrigation). 37

Figure 5.10. Moisture sensor measurements from column CA during experiment 4 (capillary rise with freshwater flood irrigation). 38

Figure 5.11. Moisture sensor measurements from column CB during experiment 4 (capillary rise with freshwater flood irrigation).....39

Figure 5.12. Moisture sensor measurements from column CA during experiment 5 (capillary rise with freshwater drip irrigation).....39

Figure 5.13. Moisture sensor measurements from column CB during experiment 5 (capillary rise with freshwater drip irrigation).....40

Figure 5.14. Moisture sensor measurements from column CA during experiment 6 (freshwater flood irrigation with free drainage).....40

Figure 5.15. Moisture sensor measurements from column CB during experiment 6 (freshwater flood irrigation with free drainage). 41

Figure 5.16. Comparison between moisture sensor measurements of column CA and CB throughout all the experiments. 43

Figure 5.17. Comparison between surface moisture of columns CA and CB throughout all the column experiment.....43

Figure 5.18. Surface bulk electrical conductivity measured by the Teros 12 sensor for columns CA and CB during experiment 1 (capillary rise without irrigation).....44

Figure 5.19. Surface bulk electrical conductivity at every irrigation instance measured by the Teros 12 sensor for columns CA and CB during experiment 2 (capillary rise with saline water flood irrigation).....47

Figure 5.20. Surface bulk electrical conductivity at every irrigation instance measured by the 12 sensors for columns CA and CB during experiment 3 (capillary rise with saline water drip irrigation). 47

Figure 5.21. Surface bulk electrical conductivity at every irrigation instance measured by the Teros 12 sensor for columns CA and CB during experiment 4 (capillary rise with freshwater flood irrigation). 48

Figure 5.22. Surface bulk electrical conductivity at every irrigation instance measured by the Teros 12 sensor for columns CA and CB during experiment 5 (capillary rise with freshwater drip irrigation). 48

Figure 5.23. Surface bulk electrical conductivity at every irrigation instance measured by the Teros 12 sensor for columns CA and CB during experiment 6 (freshwater flood irrigation with free drainage).....49

Figure 5.24. Soil tension measurements from middle and bottom sensors in column CA during experiment 1 to 6. 50

Figure 5.25. Soil tension measurements from middle and bottom sensors in column CB during experiment 1 to 6. 51

Figure 5.26. Soil tension comparison between surface sensors in column CA and CB during experiment 3 to 6. 51

Figure 5.27. Comparison between CA, CB and bottom tank magnesium concentrations after each experiment at various depths. 56

Figure 5.28. Comparison between CA, CB and bottom tank calcium concentrations after each experiment at various depths. 57

Figure 5.29. Comparison between CA, CB and bottom tank sodium concentrations after each experiment at various depths.....58

Figure 5.30. Comparison between CA, CB and saline bottom tank potassium concentrations measured by AAS after each experiment at various depths. 59

Figure 5.31. Comparison between CA, CB and bottom tank SAR values after each experiment at various depths. 60

Figure 5.32. Calibrated HYDRUS-1D hydraulic model for column CA at depth of 8cm for experiments 1 to 5. 66

Figure 5.33. Calibrated HYDRUS-1D hydraulic model for column CA at depth of 18cm for experiments 1 to 5. 67

Figure 5.34. Calibrated HYDRUS-1D hydraulic model for column CB at depth of 8cm for experiments 1 to 5. 67

Figure 5.35. Calibrated HYDRUS-1D hydraulic model for column CB at depth of 18cm for experiments 1 to 5. 68

Figure 5.36. HYDRUS-1D hydraulic model simulation for column CA at depth of 8cm for experiment 6. 68

Figure 5.37. HYDRUS-1D hydraulic model simulation for column CA at depth of 18cm for experiment 6. 69

Figure 5.38. HYDRUS-1D hydraulic model simulation for column CB at depth of 8cm for experiment 6. 69

Figure 5.39. HYDRUS-1D hydraulic model simulation for column CB at depth of 18cm for experiment 6. 70

Figure 5.40. Comparisons between simulated and measured Mg^{2+} concentration profiles. 74

Figure 5.41. Comparisons between simulated and measured Ca^{2+} concentration profiles. 75

Figure 5.42. Comparisons between simulated and measured Na^{+} concentration profiles. 76

Figure 5.43. Simulated Mg^{2+} concentration in soil water through experiments 1 to 5. 77

Figure 5.44. Simulated Ca^{2+} concentration in soil water through experiments 1 to 5.....77

Figure 5.45. Simulated Na^{+} concentration in soil water through experiments 1 to 5.....78

LIST OF TABLES

Table 2.1. Irrigation water quality salinity and sodicity guidelines 8

Table 4.1. The ionic concentration of the tanks below the soil columns. 23

Table 4.2. Summary of the six soil column experiments. 24

Table 5.1. Soluble cation concentration from 1:10 soil water extracts measured by AAS. The value in brackets represents the standard deviation from two replicas. 29

Table 5.2. Exchangeable cation concentration using calcite saturated cobalt hexamine trichloride method. The value in brackets represents the standard deviation from two replicas. 29

Table 5.3. Magnesium concentrations measured by AAS after each experiment at various depths. The standard deviations from the two replicates are shown in brackets when available. 53

Table 5.4. Calcium concentrations measured by AAS after each experiment at various depths. The standard deviations from the two replicates are shown in brackets when available. 53

Table 5.5. Sodium concentrations measured by AAS after each experiment at various depths. The standard deviations from the two replicates are shown in brackets when available. 54

Table 5.6. Potassium concentrations measured by AAS after each experiment at various depths. The standard deviations from the two replicates are shown in brackets when available.54

Table 5.7. SAR values after each experiment at various depths. The standard deviations from the two replicas are shown in brackets when available. 55

Table 5.8. List of key parameters used in the HYDRUS-1D simulations 63

Table 5.9. Initial estimate of soil hydraulic parameters used for HYDRUS-1D reverse modelling.64

Table 5.10. Non-linear least-squares analysis for column CA by HYDRUS-1D model. 65

Table 5.11. Non-linear least-squares analysis for column CB by HYDRUS-1D model. 66

LIST OF SYMBOLS/ABBREVIATIONS

Symbol	Explanation	Unit
K_s	Hydraulic conductivity	cm/seconds
α	Porosity	

Abbreviation	Explanation
AAS	Atomic absorption spectroscopy
EC	Electrical conductivity
EC_e	EC measured from saturated soil extract
EC_w	EC measured from irrigation water
EC_b	Soil bulk EC measured by salinity sensors
CEC	Cation exchange capacity
DI	De-ionized
dS	Deci Simens
ESP	Exchangeable sodium percentage
Kg	Kilogram
m	Meter
cm	Centimetre
mm	Milli meter
L	Litre
mEq	Milliequivalent
RSC	Residual Sodium Carbonate
SAR	Sodium absorption ratio
SD	Standard deviation
TDS	Total dissolved salts

1. INTRODUCTION

Salinization of agricultural soils is one of the soil chemical phenomena that induce a significant risk to the sustainability of earth's arable lands, expressly in dry and semi-dry environments (Pessarakli and Szabolcs 1999). Salinization is defined as the process of salts accumulation within the soil which results in a decline of agricultural yield when the salinity exceeds some threshold (P. Rengasamy 2006). More than 800 million hectares of land are known to be salt-affected on a global basis. Moreover, every year about ten million hectares of arable soils are becoming unfunctional due to the emergence of salinization (P. Rengasamy 2010, Shahid, Zaman and Heng 2018). Irrigated lands in arid and semi-arid environments with poor precipitation and high evapotranspiration are the most vulnerable to become salt-affected. Figure 1.1 shows the worldwide distribution of salinity affected lands illustrating the widespread nature of this problem (Pessarakli and Szabolcs 1999). A total of 831 million hectares of global salt-affected land has been reported in the year 2000 (P. Rengasamy 2006). Yadav et al. (2011) report an estimated annual income loss of 11.4 billion US dollars at irrigated farms in drylands due to soil salinity. Despite the vast investigations conducted to address this problem, countless farmers and governments continue to struggle with the management of their agricultural activities to prevent encountering soil salinity.



Figure 1.1. A global demonstration of salt-affected soils (Pessarakli and Szabolcs 1999).

The susceptibility of agricultural soils to salinization has been attributed to several natural and anthropogenic factors such as 1) poor drainage of salts from the top to the deeper soil levels, 2) usage of low-quality irrigation waters which contain high ionic concentrations and 3) capillary movement of salty soil water from the lower soil layers to the root zone (Van der Zee, et al. 2010). Consequently, soil physical properties (i.e., particle size distribution, bulk density and porosity) and chemical characteristics (such as alkalinity, ion exchange capacity and organic content), play an important role in the salinization of soils (Ezlit, Smith and Raine 2010). Therefore, any agricultural practices that may impact these soil properties can become crucial for the management of soil salinity.

The large impact of soil salinity and the vast worldwide demand for sustainable agriculture motivated this study to systematically analyse the interactions between agricultural activities and soil salt dynamics. By emphasising on lands with shallow groundwater tables, this research focused on irrigation and soil compaction as the two factors of conventional farming which have substantial influences on the physical and chemical properties of agricultural soils. Irrigation is determined as the main source of salt input to most agricultural lands (Van der Zee, et al. 2010), while soil compaction is broadly considered as the main parameter influencing soil physical properties (McGarry 2003). Irrigation practices were examined by their method of application (flooding or sprinkling), water quality and irrigation frequency. On the other hand, agricultural soil compaction was studied by varying the bulk density distribution of a soil profile to represent agricultural land undergoing soil compaction, in contrast to the bulk density distribution of a virgin soil profile.

2. BACKGROUND

2.1. Soil Salinity

Soil salinity is defined in terms of the concentrations of soluble salts present in the soil. The main mineral salt ions encountered in agricultural soils are Na^+, Ca^{2+}, Mg^{2+} and K^+ as cations, and Cl^-, NO^{3-}, HCO_3^- and SO_4^{2-} as anions (Shahid, Zaman and Heng 2018). Soil salinity is commonly determined by measuring the electrical conductivity from the soil saturated paste extract EC_e, which provides a quick and precise measure of soil salinity (Rhoades 1993). EC_e is measured in deci Simens per meter (dS/m) at 25 degrees Celsius, which is widely used to present soil salinity measurements (Shahid, Zaman and Heng 2018). Common soil sensors which measure salinity can only record the electrical conductivity of the soil, known as EC_b that is the soil bulk electrical conductivity. EC_b is a function not only to soil water salinity but also to soil water content, temperature, and tortuosity of the soil pores (Malicki and Walczak 1999). Therefore, these measurements can only indirectly give information about the actual soil salinity.

Vargas et al. (2018) states that soils having EC_e greater than 4 dS/m are considered saline salt-affected soils. Soil salinity values above this threshold can lead to significant yield reduction of typical agricultural plants (Chhabra 2004). The yield reduction because of soil salinity is explained by the physical disability of root systems to uptake soil water. The incapability of roots is due to the negative osmotic pressure which occurs above a certain ionic concentration of the soil water, or in other words when the soil becomes saline (Rengasamy and Olsson 1993).

Soluble salts can be readily transported to the lower soil layers if the soil allows infiltration, and salinity would only induce a negative impact on agricultural soil if it were significant in the topsoil (root zone). Hence, saline salt-affected soils can be treated by proper management of soil water drainage in agricultural lands (Hoffman 1985). Nevertheless, acquiring a proper water drainage structure is costly and requires a dedicated design process which is often not available to farmers and landowners that encounter salinity (Seelig 2000).

2.2. Soil Sodicity

Besides salinity, sodicity is another substantial issue that can occur in non-sandy soil profiles (Van der Zee, et al. 2010). Sodicity is the dominance of sodium ions among the other salts (mainly Ca^{+2} and Mg^{2+}) that are available to be bonded to the soil particles (Seelig 2000). Hence, sodicity can be considerable even at a low concentration of total dissolved salts (TDS). Above a certain significance of soil sodicity, the soil is classified as sodic salt-affected soil. The magnitude of sodicity at which the soil becomes sodic is recognized by the dispersion of soil particles which is an undesirable physical change leading to infertility of the land (Vargas, et al. 2018). Sodicity driven soil dispersion occurs when the attraction of electromagnetic forces between clay particles are overcome due to the large size of the sodium ions, which contrasts with the smaller sized magnesium and calcium ions (Warrence, Bauder and Pearson 2002). Consequently, soil dispersion allows smaller soil particles to clog the pores in the soil structure, causing an extensive reduction in soil infiltration rate and hydraulic conductivity, leading to an impermeable soil structure for the plants rooting systems, which is also affirmative to waterlogging (Shainberg, Letey and others 1984).

Soil sodicity is commonly measured in exchangeable sodium percentage (ESP), which is the ratio between the bonded exchangeable sodium ions and the cation exchange capacity (CEC) of the certain soil (see Eq. 2.1) (Weil and Brady 2017). However, due to the difficulties involved in direct measurement of the ESP from a soil sample, sodium absorption ratio (SAR), which is closely correlated to ESP, is measured from the soil water (e.g. soil saturated extract) to determine sodicity. SAR is directly obtained from the concentrations of soluble sodium, magnesium, and calcium ions available in the soil water (see Eq. 2.2); SAR can be converted to ESP using Eq. 2.3 (Weil and Brady 2017, Shahid, Zaman and Heng 2018).

$$ESP = \frac{Exchangeable\ Sodium}{CEC} \times 100 \tag{2.1}$$

where ‘Exchangeable Sodium’ and CEC are measured in mEq per 100 g soil

$$SAR = \frac{[Na^{+}]}{0.4\times\sqrt{[Ca^{+2}][Mg^{+2}]}} \tag{2.2}$$

where the concentrations are measured in mEq/L

$$ESP = \frac{100\times(-0.0126+0.01475\times SAR)}{1+(-0.0126+0.01475\times SAR)} \tag{2.3}$$

Sodic soils are characterised by Vargas et al. (2018) as having ESP of more than 15% and EC of less than 4 dS/m. Sodic soils are also referred to as alkali or alkaline soils (Richards 1954). This is because of the alkali nature of the sodic soils, which is the result of the hydrolysis of sodium ions from clay particles (see Eq. 2.4). In addition, the presence of sodium carbonate and sodium bicarbonate in a sodic profile enhances the alkaline nature of the soil (see Eq. 2.5 and Eq. 2.6). Consequently, due to this alkali nature of sodic soils, a high pH of above 8.5 has become an indicator to detect sodic conditions, although, this is a general assumption and there can be cases (i.e. in the absence of sodium carbonates) where sodic soils have a low pH value (Richards 1954).

$$Clay - Na + H_2O = Clay - H + Na^+ + OH^- \quad (2.4)$$

$$Na_2CO_3 + 2H_2O = 2Na^+ + 2OH^- + H_2CO_3 \quad (2.5)$$

$$NaHCO_3 + H_2O = Na^+ + OH^- + H_2CO_3 \quad (2.6)$$

2.3. Soil Texture and Salt-affection

Soil texture is an indication of the relative size of individual soil grains (Kellogg 1937). Accordingly, the soil grain size divides soil texture into three principal texture classes: sand, loam and clay. Finer soil classes are described depending on the percentage of each principal class within the soil (Figure 2.1).

There is a direct relationship between the significance of sodification and soil texture since the sodium ions only become a concern when they attach to clay particles. On the other hand, what becomes important regarding salinity and the effect of soil texture, is the hydraulic relations between soil-water and the soil, or in other words, the transportability of soluble salts within the soil layers. Hence, soil texture induced characteristics such as bulk density, porosity, infiltration rate, permeability and soil moisture retention are essential in analysing salinity and sodicity in a certain soil profile.

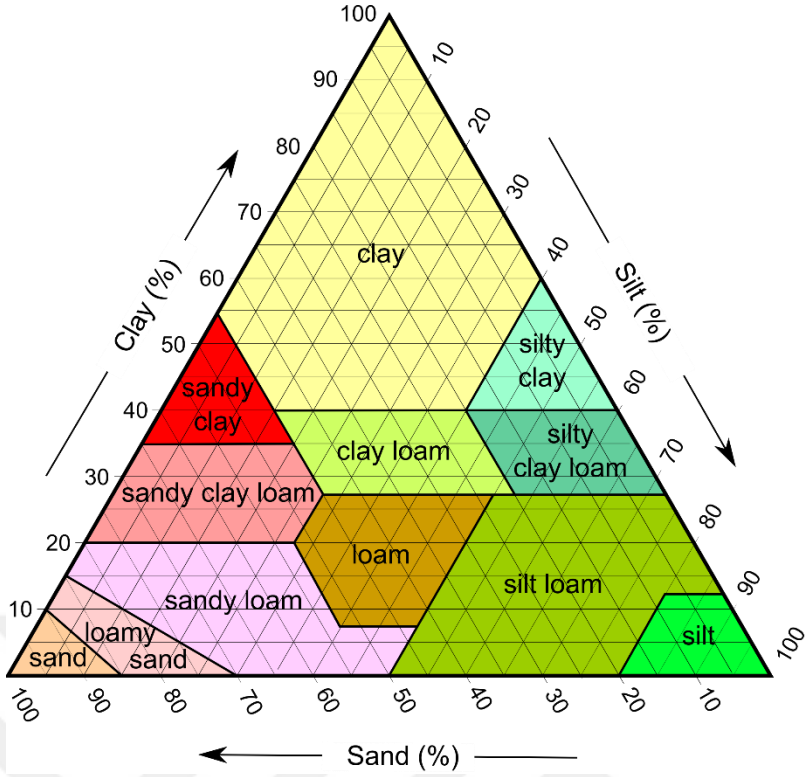

Figure 2.1. Soil texture classification triangle adapted from Rhoades (1993)

2.4. Shallow Saline Groundwater and Salt-affection

Capillary rise of saline soil water is a major cause for salinization in soil profiles that are located above a shallow saline groundwater table (P. Rengasamy 2010). Saline water can transfer to the soil surface due to the capillary phenomena, which can be described as the upward movement of soil-water from the (moist) underlying layers to the (dry) upper layer of the soil due to the negative pressure induced by the dry upper layers (Lu and Likos 2004). This phenomenon leads to the accumulation of salts on the surface as the saline water evaporates from the topsoil while crystalizing the salts in the topsoil (Figure 2.2).

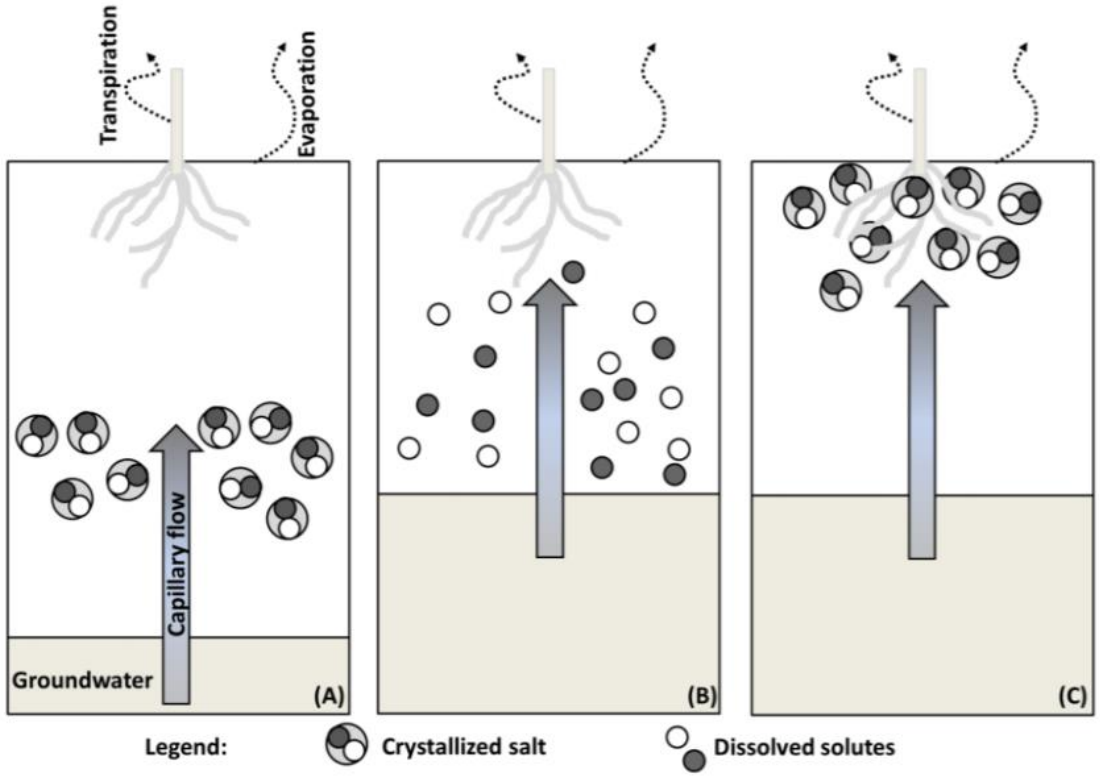

Figure 2.2. Process of salinization due to capillary rise from a shallow saline aquifer (Nachshon 2018).

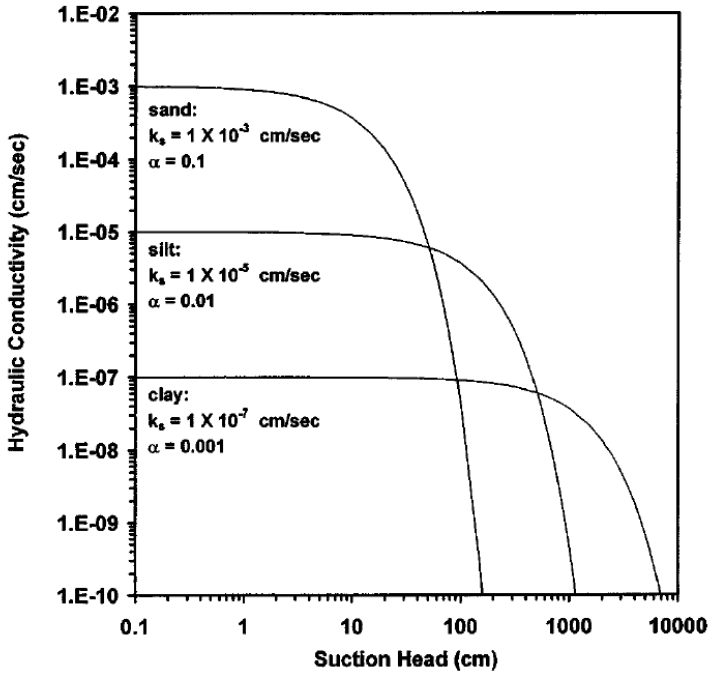

Figure 2.3. Relation between soil type (indicated by porosity, α, and hydraulic conductivity, K_s) and capillary rise (indicated as suction head) adapted from Lu and Likos (2004).

The significance and speed of the upward groundwater flow are dependent on soil texture, water table depth, level of groundwater salinity, soil drainage and climate (Blaine 1999). Lu and Likos (2004) further explain that hydraulic properties of the soil such as hydraulic conductivity and porosity which are classified by the soil texture directly influence the magnitude and velocity of capillary rise (Figure 2.3).

2.5. Irrigation

Irrigation is known as the main cause for the occurrence of salinity and sodicity in arid and semi-arid agricultural lands (Van der Zee, et al. 2010). Due to the insufficient rainfall particularly during the plant growing season, farmers are obliged to use lower quality waters (e.g. groundwater) which predominantly contain a considerable portion of impurities such as soluble salts. Subsequently to soil-water evaporation, the salts from the irrigation water precipitate within the soil which can trigger salinization and sodification. Abrol, Yadav and Massoud (1988) group irrigation water types to reference the risks involved in using a certain water quality for agriculture. Table 2.1 indicates a general guideline for water quality that can result in salinity, as well as, the reduction in soil infiltration rate due to sodification (Weil and Brady 2017).

Table 2.1. Irrigation water quality salinity and sodicity guidelines (Weil and Brady 2017).

		Degree of restriction on use		
Water property	Units	None	Slight to moderate	Severe
Salinity (affects crop water availability)				
ECw	dS/m	<0.7	0.7-3.0	>3
TDS	mg/L	<450	450-2000	>2000
Physical structure and water infiltration (evaluate using ECw and SAR together)				
SAR = 0–3 and ECw =	mS/cm	>0.7	0.7-0.2	<0.2
SAR = 3-6 and ECw =	mS/cm	>1.2	1.2-0.3	<0.3
SAR = 6-12 and ECw =	mS/cm	>1.9	1.9-0.5	<0.5
SAR = 12-20 and ECw =	mS/cm	>2.9	2.9-1.3	<1.3
SAR = 20-40 and ECw =	mS/cm	>5.0	5.0-2.9	<2.9

SAR has been a common indicator for irrigation water quality to prevent sodicity. However, other indicators have been also suggested since, at a high concentration of salts (EC > 4), SAR does not have a direct impact on soil dispersion (Weil and Brady 2017). For instance, Bauder et al. (2011) has mentioned the use of both EC and SAR at the same time, but studies such as Eaton (1950) have described Residual Sodium Carbonate (RSC) as a better indicator to measure the risk factors of

irrigation water regarding sodification (see Eq. 2.7). Abrol, Yadav and Massoud (1988) define RSC values above 2.5 mmol to be an indication of sodicity hazardous irrigation water.

$$RSC = (CO_3^{2-} + HCO_3^-) - (Ca^{2+} + Mg^{2+}) \quad (2.7)$$

As explained by Malash, Flowers and Ragab (2008), the method of irrigation contributes to the dynamics of irrigation induced salinization and sodification. The most known irrigation types are:

- Surface irrigation: also known as flood irrigation, at which the farmer runs off the water directly on the surface of the land and lets it infiltrate into the soil due to the force of gravity (Bjorneberg 2013). This method uses an extensive amount of water but in return, it is an inexpensive option as it does not require the use of any machinery or special equipment. However, in lands with insufficient infiltration capacity and when poor quality water is used for irrigation, surface irrigation can be hazardous for salt accumulation due to the substantial amount of salts added to the soil upon each irrigation.
- Sprinkler irrigation: an irrigation technique that requires special machinery which can uniformly distribute and spray water over the land. The advantage of this method is the vast reduction of water use and the salt infusion to the land in comparison to surface irrigation. Nevertheless, the costs involved with the purchasing and maintenance of the equipment, make this method only suitable to lands that acquire an adequate agricultural income.
- Drip irrigation: also known as micro-irrigation, is a localized irrigation method where each plant receives drips of water close to its roots just enough for its growth. Therefore, water usage is optimized in this type of irrigation in contrast to the previous methods. Nevertheless, due to limitations involved in the design of drip irrigation, it cannot be utilized with low-quality waters and it is not a suitable method for all type of plants (Bjorneberg 2013).

The recommended frequency of water application can differ following the irrigation method, soil type, climate and the development stage and the type of the cultivated plants. Abrol, Yadav and Massoud (1988) introduce three practices for the determination of irrigation frequency which are observation method, estimation method and calculation method. The observation method relies on the knowledge of the observation of the farmer on ‘when’ to irrigate. The estimation method is a simple and approximate procedure that utilizes data tables that indicate the required irrigation rate by plant type, soil texture and the climate profiles of the lands. And the calculation method can be noted

as the most sophisticated among the three methods which use several equations to output a comprehensive irrigation schedule following factors such as soil type, irrigation method, root depth, monthly climate (rainfall and evaporation rates) and aquifer depth.

2.6. Agricultural Soil Compaction

Among the negative environmental impacts of today's industrialized agriculture, soil compaction is judged as a major cause of agricultural soil degradation (McGarry 2003). Conventional agricultural soil compaction is mainly caused by the regularly inserted downward forces to the land surface by hoofs of grazing animals, tires of heavy machinery and the equipment loaded on them (Hamza and Anderson 2005). Figure 2.4 exposes the intensity of interactions between the machinery and the soil in conventional farming practices. Although agricultural traffic is applied to the surface of the soil, the compaction of soil occurs within the subsoil at some distance from the surface (Jones and Montanarella 2001). This is due to the frequent ploughing of the cultivated lands which results in the loosening of the topsoil. As a result, a hard-compacted layer of soil is left below the ploughing depth, often referred to as, hardpan, traffic pan, plough pan or tillage pan (Stitt, et al. 1982, Weil and Brady 2017). In this regard, Figure 2.4 illustrates the structure and formation of a typical hardpan (Weil and Brady 2017, USDA 2008).

The primary impact of compaction on a soil profile is the increase of its bulk density and decrease in porosity which directly influences the hydraulic properties of the soil. Accordingly, due to the comparability of bulk density measurements among all soil types, the bulk density of the compacted layer has become the most common unit of measure for the degree of soil compaction (Hamza and Anderson 2005).

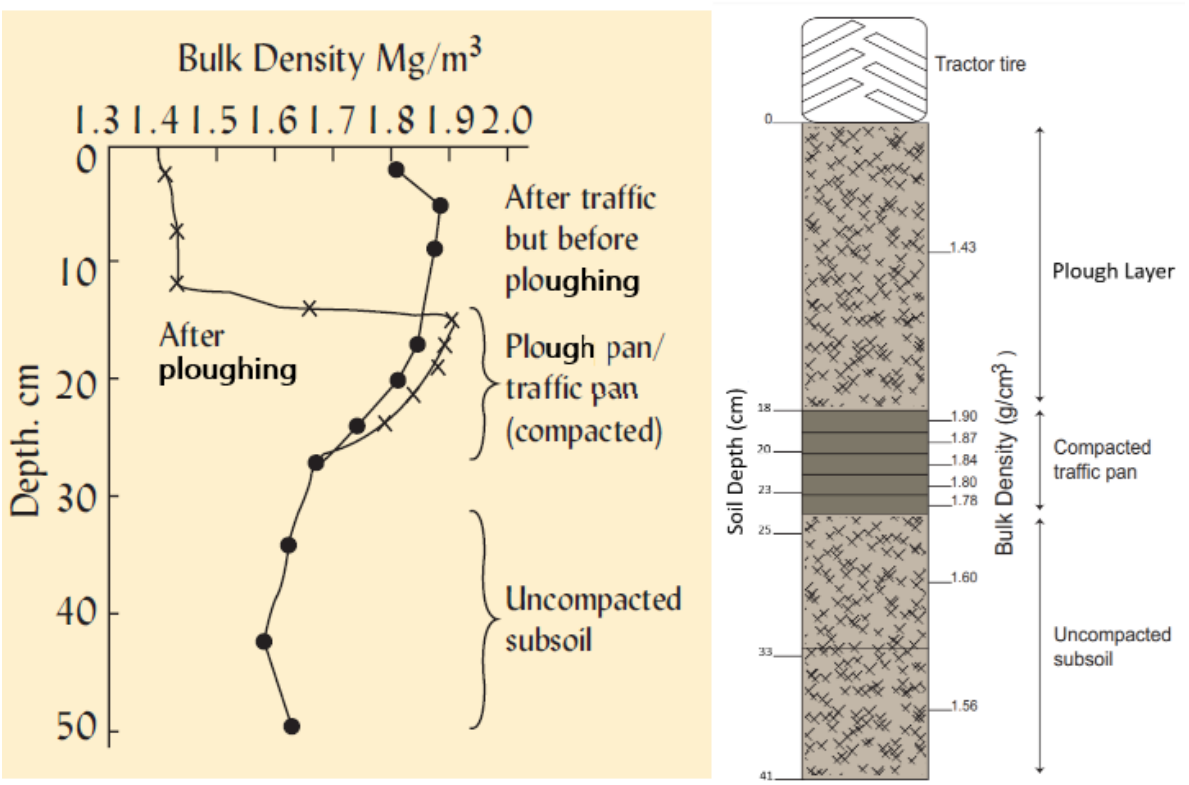

Figure 2.4. Left: the bulk density distribution of a compacted sandy loam soil before and after ploughing. Right: An example of a compacted agricultural soil profile (USDA 2008, Weil and Brady 2017).

2.7. Numerical Modelling of Salinization and HYDRUS-1D

Tiwari and Goel (2013), reviewed and compared seven existing numerical modelling tools that could be utilized to simulate soil salinity problems. These are HYDRUS (Simunek, et al. 2009), DRAINMOD (Skaggs, Youssef and Chescheir 2012), UNSATCHEM (Suarez and Šimůnek 1997), LEACHC (Bin 2005), SWAP (van Dam 2000), SALTMOD (Oosterbaan 2001) and SOWACH (Dudley and Hanks 1991). The core of these models which calculates the moisture flow through the soil is mainly governed by Richard's equation (Tiwari and Goel 2013):

$$\sigma(h)\frac{\partial h}{\partial t} - \vec{\nabla}.(K(h)\vec{\nabla}(h+z)) = q \qquad (2.8)$$

where

t	time [T]
h	pressure head [L]
z	elevation [L]
σ	specific volumetric storativity [L^{-1}]

h hydraulic conductivity [LT^{-1}]

q sink and/or source of water [T^{-1}].

Among the existing tools, HYDRUS has been globally known as one of the most prevalent and advanced numerical modelling in soil physics (Radcliffe and Simunek 2018). HYDRUS can simulate water, heat and solute movement of a saturated, partially saturated and non-saturated soil profile (Simunek, et al. 2009). In addition, the modelling package can be supplemented with modules that can allow an analysis of diverse chemical and physical properties of the modelled media. In this regard, a salinity module (SALTMODE) is appended to the HYDRUS package for simulating different ion solute movement and accumulation concerning soil salinization and sodification effects (Simunek, et al. 2009). The core solute transport equation used in HYDRUS models is given by (Simunek, et al. 2013):

$$\frac{\partial(\theta c+\rho_b s)}{\partial t} = \frac{\partial}{\partial z}\left(\theta D \frac{\partial c}{\partial z}\right) - \frac{\partial(qc)}{\partial z} - \theta c\mu_w - \rho_b s\mu_s + \rho_b\gamma_s + \theta\gamma_w - r \quad (2.9)$$

where

t time [T]

θ volumetric water content [L^3L^{-3}]

z spatial coordinate [L]

q volumetric flux density [LT^{-1}]

c dissolved concentration [ML^{-3}]

ρ_b bulk density [ML^{-3}]

D hydrodynamic dispersion coefficient [L^2T^{-1}]

μ_w 1st order degradation coefficient for liquid phase [T^{-1}]

μ_s 1st order degradation coefficient for solid-phase [T^{-1}]

γ_w zero-order product ion coefficient for liquid phase [$ML^{-3}T^{-1}$]

γ_s zero-order production coefficient for solid phase [T^{-1}]

s sorbed concentration [MM^{-1}]

r sink term for root solute uptake [$ML^{-3}T^{-1}$]

The cation exchange reactions calculated by the HYDRUS is based on Cation Exchange Capacity and Gapon equation (Simunek, et al. 2009). The CEC and Gapon equations for HYDRUS-1D major ion chemistry model are given by (Simunek, et al. 2009):

$$CEC = \overline{Mg}^{2+} + \overline{Ca}^{2+} + \overline{Na}^{+} + \overline{K}^{+} \quad (2.10)$$

where

CEC Cation Exchange Capacity mEq/Kg

$\overline{Mg}^{2+}$ soil exchangeable magnesium mEq/Kg

$\overline{Ca}^{2+}$ soil exchangeable calcium mEq/Kg

$\overline{Na}^{+}$ soil exchangeable sodium mEq/Kg

$\overline{K}^{+}$ soil exchangeable potassium mEq/Kg

$$\text{K}\left[\frac{Ca}{Mg}\right] = \frac{\overline{Mg}^{2+}}{\overline{Ca}^{2+}} \frac{\sqrt{Ca^{2+}}}{\sqrt{Mg^{2+}}}$$

$$\text{K}\left[\frac{Ca}{Na}\right] = \frac{\overline{Ca}^{2+}}{\overline{Na}^{+}} \frac{\sqrt{Na^{+}}}{\sqrt{Ca^{2+}}}$$

$$\text{K}\left[\frac{Ca}{K}\right] = \frac{\overline{Ca}^{2+}}{\overline{K}^{+}} \frac{\sqrt{K^{+}}}{\sqrt{Ca^{2+}}} \quad (2.11)$$

where

K[] Gapon constant

$\overline{Mg}^{2+}$ soil exchangeable magnesium mEq/Kg

$\overline{Ca}^{2+}$ soil exchangeable calcium mEq/Kg

$\overline{Na}^{+}$ soil exchangeable sodium mEq/Kg

$\overline{K}^{+}$ soil exchangeable potassium mEq/Kg

Mg^{2+} soil exchangeable magnesium mEq/Kg

Ca^{2+} soil exchangeable calcium mEq/Kg

Na^{+} soil exchangeable sodium mEq/Kg

K^{+} soil exchangeable potassium mEq/Kg

2.8. Literature Review

According to the Web of Science (2021), the number of studies relating to soil salinity and sodicity has consistently increased in the past 70 years, with at least a hundred thousand scientific papers published in this regard. Remarkably, almost no research was found that directly investigated the salinization in lands with shallow groundwater table concerning agricultural soil compaction under different irrigation regimes (Web of science. 2021).

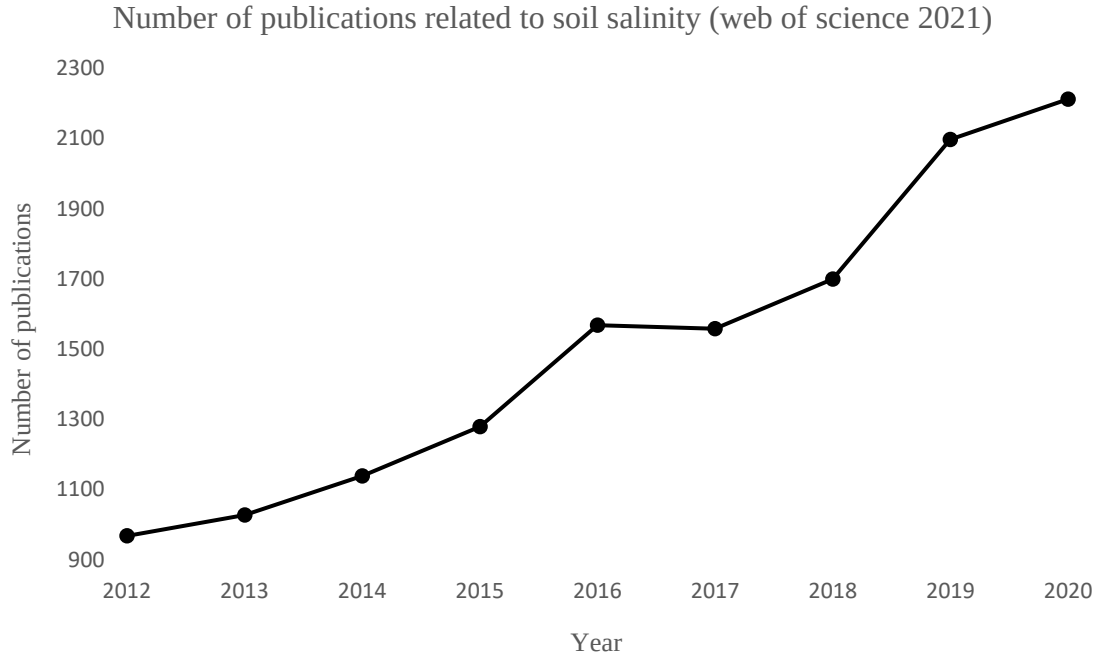

Figure 1.1. The number of publications related to soil salinity presented in the Web of Science database.

Various studies have developed soil column experiments to study different aspects of salinization of soil profiles under irrigation regimes with the presence of a shallow groundwater table. Among these studies, several looked at plant response to salinity stress under different conditions (Ghamarnia and Jalili 2014, Zhang, et al. 2019, Hutmacher, et al. 1996, Ding, et al. 2020), while some others only investigated the soil properties concerning salinization (Qadir, Qureshi and Ahmad 1996, Kobayashi, et al. 2008, Li, et al. 2021) and only a few numerically modelled their experiments (Ibrahimi, et al. 2014, Cardon and Letey 1992), yet no article was found which investigated the impacts of agricultural soil compaction in a column experiment with shallow groundwater table.

Hutmacher et al. (1996) conducted 3-year long column experiments with cotton crops having various depths of shallow ground waters with different levels of salinity. The authors used freshwater for irrigation and their main finding was that the level of shallow ground water salinity is directly proportional to the amount of water the cotton plants use for their growth. Ghamarnia and Jalili (2014) developed a similar experiment and conclusion as of Hutmacher et al. (1996) but with Black Cumin plants, in addition, they experimentally showed that the growth was also dependent on the depth of the saline aquifer. Zhang et al. (2019) on the other hand, performed in situ column experiments to experiment with wheat growth at a coastal site with a shallow saline water table induced from the sea. The authors placed the columns at a slope to generate scenarios with different column depths. Like

the other studies mentioned here, Zhang et al. (2019) concluded an inverse proportionality between salinity level and depth of the ground water with the wheat yield and quality.

In the column experiments conducted by Qadir, Qureshi and Ahmad (1996), Kallar Grass was cultivated and tested not to see the impacts of salinity on its growth, but this time the plant was used as a technique for remediation of a saline-sodic soil profile. Qadir, Qureshi and Ahmad (1996) also tested the impact of the conventional gypsum treatments on their saline-sodic columns. Their study found that the gypsum treatment was the most efficient, however, the biological treatment (Kallar Grass) was also impactful and sufficient to control a certain degree of salinity and sodicity problem. The study of Kobayashi et al. (2008) focused on various soil types packed in laboratory column experiments with the saline shallow ground. The study determined that finer-textured soils were more prone to salinization than coarse-textured soils in a scenario with heavy irrigation induced salinization. The most recent column experiment study found which analyzed a scenario with a shallow water table, irrigation and soil salinization was Li et al. (2021). However, the research did not investigate the impacts of a natural shallow aquifer but instead, it looked into soil profiles without proper drainage resulting in water logging and formation of a saline shallow water table.

Only two studies were encountered in the Web of Science database which tried to numerically model their column experiment while having a shallow water table. The first study was Cardon and Letey (1992) which focused on a solute movement in a profile with fluctuating shallow saline water. Cardon and Letey introduced a new numerical model based both on predicted and measurements from the greenhouse column experiments. The study focused on the implications of the model rather than the salinization process of their column experiments. Nonetheless, the later study by Ibrahimi et al. (2014), utilized a quite similar approach to our research by both column experiments and Hydrus one modelling of a 60 cm deep soil profile with a shallow ground water table. Ibrahimi et al. (2014) conducted experiments with bromine tracers and attempted to numerically model the solute transport of their setup. The authors further conducted different simulation scenarios to evaluate various soil management strategies. Firstly, the effect of changing the soil surface temperature was evaluated; it revealed that lowering the surface temperature reduced salt accumulation. Secondly, alternative irrigation management scenarios were numerically tested. Ibrahimi et al. (2014) concluded that the scenario without irrigation resulted in the highest surface salt accumulation in the outcome of the simulations.

The review of the existing literature revealed a very limited number of studies that directly relating salinity to soil compaction. The most relevant study found that in salinization and soil compaction was a 12-year field experiment on agricultural land in Southeast China which investigated the development of agricultural soil compaction and its long-term impacts on soil salinization and sodification (Wang, et al. 2014). The results from Wang et al. (2014) suggests that salt accumulation within the soil is one of the negative impacts of conventional farming practices on soil structure due to soil compaction.

Overall, the results attained from the Web of Science (2021) revealed a paucity of a scientific study that includes both an experimental component and a modelling component to comprehend salinization in lands with shallow groundwater table with a focus on irrigation and agricultural soil compaction.

3. STATEMENT OF THE PROBLEM

This master thesis project investigated the salinization of agricultural soils in the presence of a shallow saline groundwater table. The analysis consists of a series of laboratory experiments and numerical modelling. The overall research question asked by this study was: how do salinization take place in the top layer of soil in conventional agricultural lands in the presence of a shallow saline aquifer? The specific features examined in this study are:

(A) The transport of ions across an agricultural soil profile downwards due to irrigation and upwards due to capillary rise.

(B) The impact of farming-induced soil compaction on salinization.

(C) The effect of alternative irrigation practices with different water qualities on salinization patterns.

In order to answer the research questions, this study combined a laboratory-based soil experiment with HYDRUS-1D numerical modelling of the experimental setup. The experimental setups utilized agricultural soil samples from the Konya plain in Turkey which is classified as having a semi-arid climate (Ozbahce and Tari 2010). Besides, the lands of Konya are reported to be extensively used for conventional agricultural practices irrigated from non-renewable groundwater sources (Dıvrak, Is and Ayas 2007).

4. METHODOLOGY

This chapter reviews the laboratory and numerical methods used in this study. These include sample preparation to laboratory setup, experimental scenarios, and numerical simulation of the laboratory experiments.

4.1. Sample Preparation

The soil samples were collected from an apple farm (located at 3711’32.6” N 3308’48.4” E) at a close distance to the city of Karaman in the plain of Konya. The main reason for choosing this specific sampling location was due to the non-salinity and virginity of the soil profile structure, as it has not been disturbed within the last 10 years. The average EC and the pH of the soil were measured at the field to be within the range of 0.1-0.3 dS/m and 7.7-7.8, respectively. The samples were stored in ten 20L boxes each representing a 6 cm layer of a soil profile.



Figure 4.1. Left: sampling location. Right: 60 cm deep sample collection.

The collected soil samples were pre-treated before the packing of the columns following British Standards Institution procedures (2006). Specifically, the soils were dried in the oven overnight at 104 degrees Celsius. The total weight of the dried soil samples was measured to be 141.5 Kg. Thereafter, all the soil samples were grinded and sieved through a 2 mm mesh. The total remaining weight of soil ready for analysis was recorded to be 98 Kg.



Figure 4.2. Dried and sieved (2mm mesh) samples

The soluble and exchangeable cation concentration of the soil samples were measured using the calcite saturated cobalt hexamine trichloride method as described in British Standards Institution (2018) by using Atomic absorption spectroscopy (AAS). This analysis was performed to determine the cation (Na^{+}, Ca^{2+}, Mg^{2+} and K^{+}) concentrations and the salinity and sodicity of the soil samples. Two replicas from each soil sample were measured by AAS.

4.2. Laboratory Setup

This study utilized soil column experiments for examining moisture transport and soil dynamics in the soil column. Two plexiglass columns were tailored crafted and used for this study with a diameter of 18 cm and length of 60 cm. The diameter of the column was selected such that the sensors installed along the column had adequate space and would not interfere with each other.

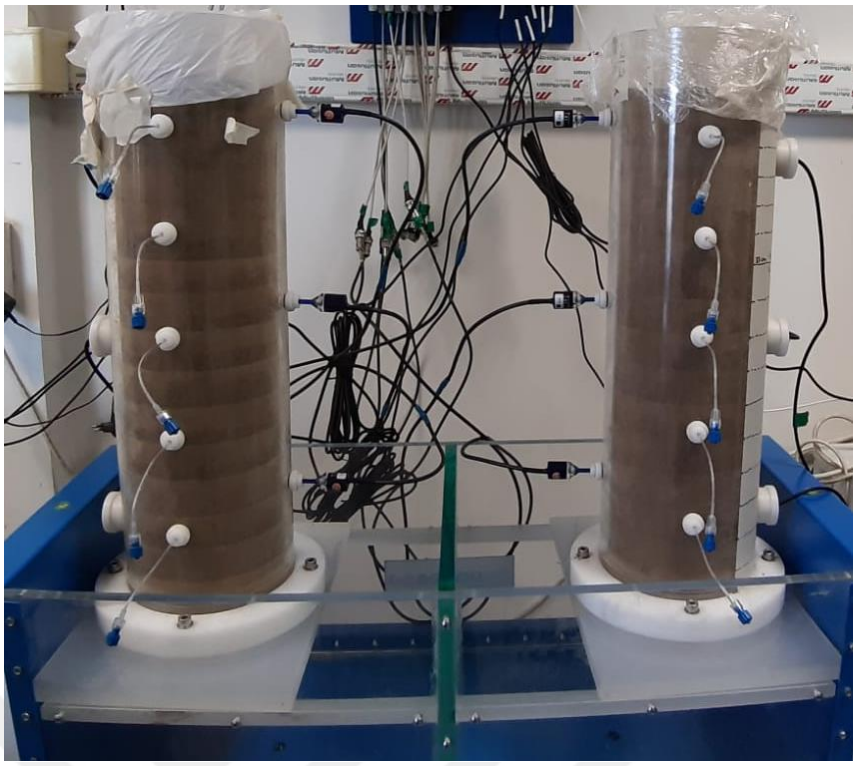

Figure 4.3. Soil columns after filling the soil samples. The right column is CA, and the left is CB. The compaction layer is vivid in the picture on column CB.

Two 55 cm deep soil profiles were devised to be synthesized one for each of the columns, one representing agricultural land undergoing soil compaction and the other representing a distribution of an undisturbed soil profile. Henceforth, the soil samples presented in Figure 4.2 were further divided into two layers: the topsoil (L1) that consisted of the top 18 cm of soil layer which was the soil available to the plant roots, the bottom soil layer (L2) which signified the soil below the depth of 18 to 55 cm. To achieve this composition, L1 was prepared by equally mixing dry weighted soil taken from boxes 1, 2 and 3. L2 was prepared in the same manner as L1 but from boxes 4 to 10. The first column labelled "CA", was filled with both L1 and L2 having 1.15 g/cm^3 dry bulk densities representing a non-compacted virgin soil. The second column, labelled "CB", was filled with L1 having 1.15 g/cm^3 and L2 having 1.35 g/cm^3 bulk densities. Therefore, "CB" was filled to mimic the compacted agricultural soils which had the topsoil ploughed leaving a compacted zone beneath it. Figure 4.3 shows the columns after filling the soil layers. Furthermore, as shown in Figure 4.4 each column was equipped with:

- A bottom with ~30 L volume water tank representing a shallow water table
- An advanced soil moisture sensor (Teros 12 from Meter Group) that measures EC_b, moisture and temperature, was installed on the top 5 cm of the soil. The accuracy of these

sensors was given by the manufacturer as ± 5% for conductivity measurements in the range of 0 to 10 mS/cm and ± 8% for 10 to 20 mS/cm.

- Three soil moisture sensors (EC-5 from Meter Group) mounted on each column at depths of 8, 28 and 48 cm, respectively. The accuracy of this sensor was given as ±0.03 m^3/m^3 in measuring the water content of the soil.
- Three pressure transducer tensiometers (T5 from Meter Group) respectively placed at depths of 4, 24 and 44 cm. These tensiometers were utilized to continuously measure the pressure that induced the vertical soil water transport within the columns. The accuracy of these sensor measurements was given by the Meter Group as ± 0.5 kPa.
- Five suction cups were used to collect soil water samples from equally segregated depths of the columns at 6, 16, 26, 36 and 46 cm.
- Infrared lamps were mounted at the top of the columns to regulate the soil surface temperature.
- A digital temperature sensor (DS18B20) was placed at a depth of 5 cm. The measurement of the topsoil temperature is used as input for the numerical model, and a point reference to regulate the heat applied by the infrared lamps.
- All sensors were connected to a GP2 from Delta-T and a ZL6 from Meter Group dataloggers.

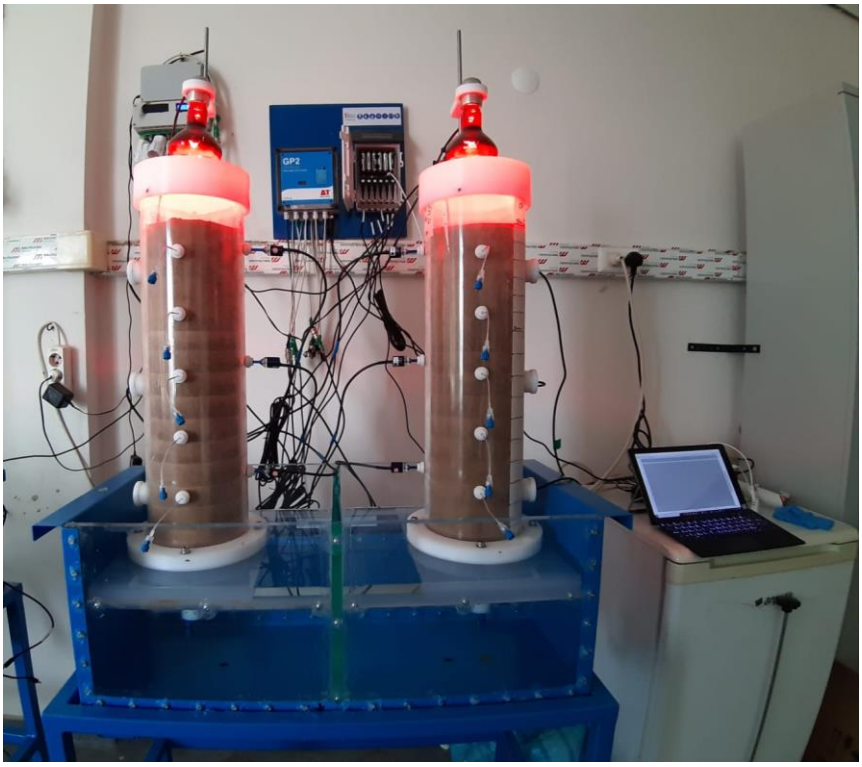

Figure 4.4. Soil columns after equipping the sensors.

4.2.1. Initial Conditions

The surface temperature was automatically moderated at 30 degrees Celsius using the infrared lamps regulated by the live data from the surface temperature sensor. This was done to increase surface evaporation for the experiment to guarantee the occurrence of sufficient capillary rise within the time scope of the project.

To emulate the impact of saline shallow aquifer, the tanks below both columns were filled with saline water with a high salinity level but with no sodicity. The saline water composition was based on groundwater data from a well in the region where the soil samples were taken as indicated by Bozdağ (2015). Table 4.1 gives information about the ionic composition of the synthesized saline waters used for the bottom tanks.

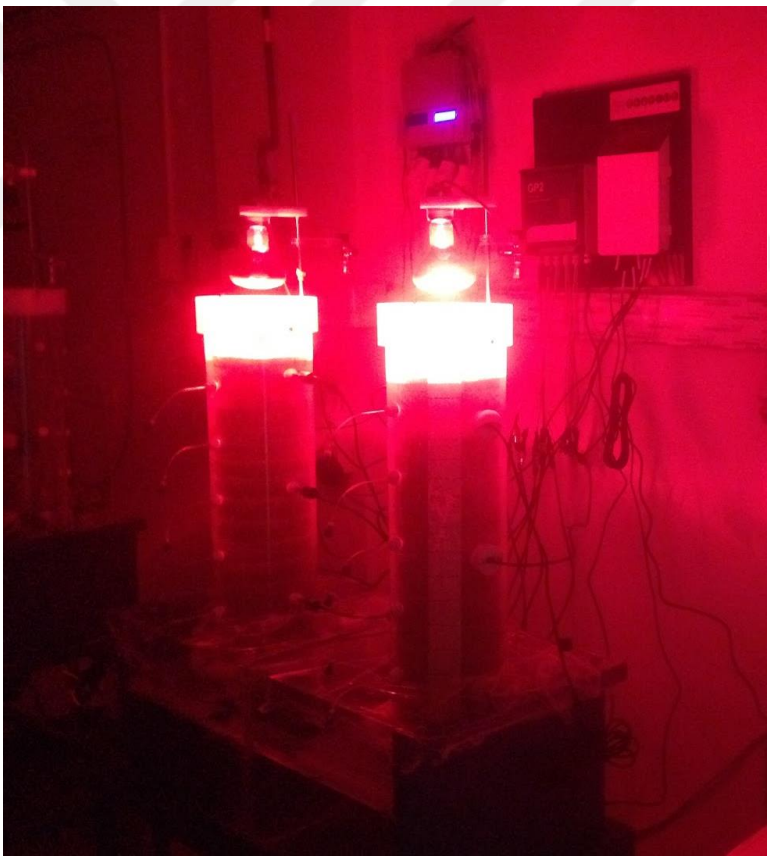

Figure 4.5. Soil columns in dark having infrared lamps controlling the soil surface temperature.

Table 4.1. The ionic concentration of the tanks below the soil columns.

Ca^{2+} (mEq/L)	Mg^{2+} (mEq/L)	Na^{+} (mEq/L)	SO_4^{2-} (mEq/L)	Cl^{-} (mEq/L)	HCO_3^{-} (mEq/L)	TDS (mEq/L)
9.28	16.54	13.05	16.52	27.32	6.52	89.24

The initial hydraulic properties of L1 and L2 under both dry bulk densities of 1.15 g/cm^3 and 1.35 g/cm^3 were analysed by the Hyprop soil moisture release curve measurement setup from the Meter Group (Figure 4.6). This analysis gave information about the water retention curve and the hydraulic conductivity vs saturation curve, parameters needed to solve Richard's equation in the HYDRUS numerical model as explained in Section 2.7.

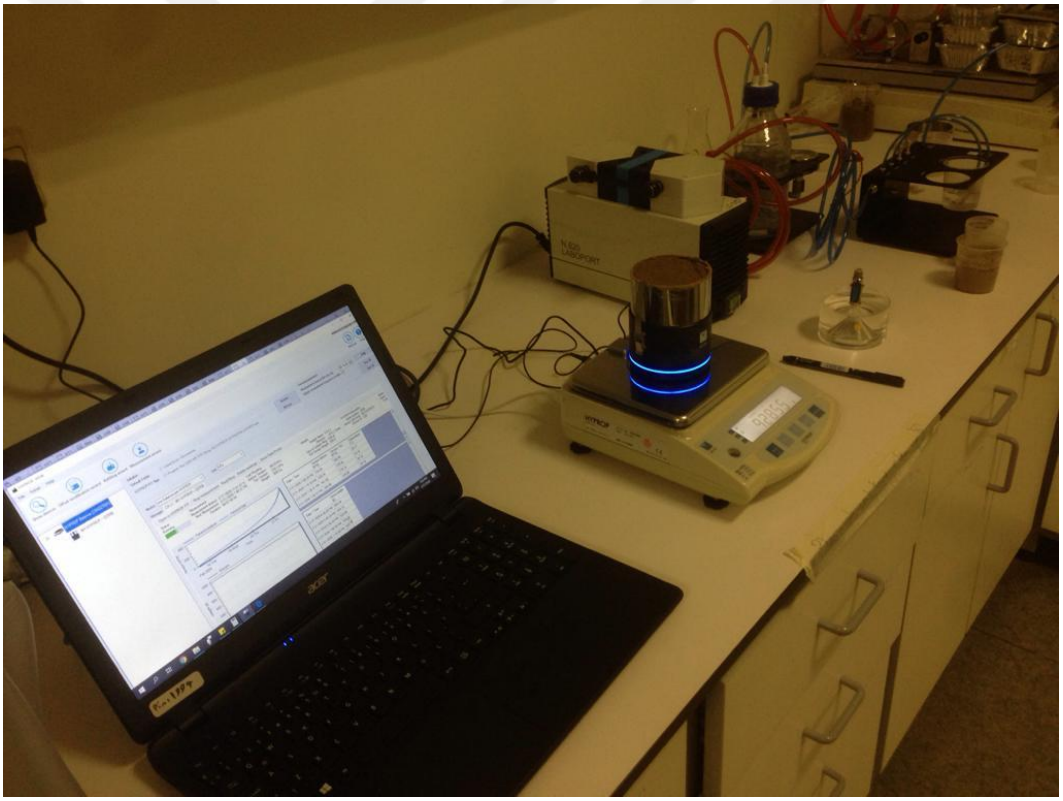

Figure 4.6. Hyprop soil retention curve analysis setup

4.3. Column Experiments

Six distinct experiments were conducted on the packed soil columns over a total period of fourteen months. The first experiment started on 20th February 2020 and the sixth one ended on 15 April 2021. This section describes each of the experiment runs. Table 4.2 summarizes all the experiments performed.

Table 4.2. Summary of the six soil column experiments.

Experiment	Irrigation type	Irrigation water	Bottom boundary	Number of irrigation cycles	Start date (day/month/year)	Duration (days)
1	None	N/A	Saline water tank at depth of 55 cm	N/A	20/02/2020	81
2	Flood	Saline		5	11/05/2020	135
3	Drip	Saline		4	23/09/2020	61
4	Flood	Deionized		4	23/11/2020	88
5	Drip	Deionized		4	19/02/2021	37
6	Flood	Deionized	Free drainage	4	28/03/2021	12

4.3.1. Experiment 1: Capillary Rise without Irrigation

The first experiment was performed without any irrigation for eighty days. The columns were maintained with no surface application of water but with the saline water tanks at the bottom boundary. This experiment was applied to both columns (without and with compaction layer, CA and CB, respectively). The surface salinity, the moisture level and soil pressure at three depths were continuously measured. This was done to evaluate the impact of capillarity on the transfer of moisture and ions upwards to the column surface. To induce evaporation from the soil surface, the temperature was maintained at 30 ^{o}C through the experiment using infrared lamps. In addition to the monitoring through the sensors installed along the column, soil samples were taken from the surface of each column before and after this cycle to be analyzed for changes in its salinity conditions.

4.3.2. Experiment 2: Capillary Rise with Saline Water Flood Irrigation

After the initial stationary period of about three months, cycles of saline water flood irrigation was performed on the columns CA and CB. The amount of saline water applied was designed as 1L

by estimating the porosity of each column not to over saturate and lead in water intrusion to the bottom water tanks. The initial application in experiment 1 consisted of 1.5L irrigation water. However, as this led to excess water reaching the bottom tanks, all subsequent flood irrigation applications were reduced to 1L which is equivalent to 5 cm of water. The salinity of the irrigation water was set to the salinity of the bottom tanks, consisting of the same salt composition as indicated in Table 4.1.

Five irrigation cycles were performed in this phase. Each irrigation run was performed every 4-5 days. This irrigation frequency was decided following the moisture data received from the sensors. The soil water samples were collected right before each irrigation and after each irrigation when there was no overhead water left right after each flood irrigation. The soil water collection was utilized using suction cups as indicated in Figure 4.7. Furthermore, salinity, moisture and pressure of the soil were continuously measured by the soil sensor in continuation from the beginning of the experiments at the initial step. Besides, soil samples were collocated from the surface similar to the first experiment as presented in the previous section.

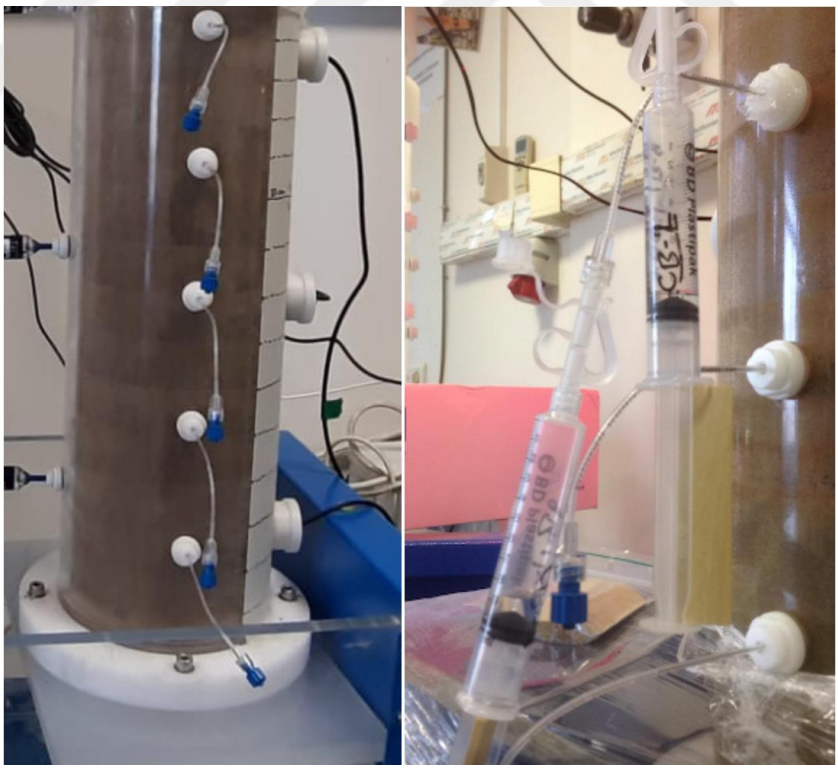

Figure 4.7. Soil water collection using the suction cups.

4.3.3. Experiment 3: Capillary Rise with Saline Water Drip Irrigation

Both columns were put at rest for about three months following experiments 2. This extensive delaying period was carried out unexpectedly due to the Covid-19 outbreak and the relevant restriction. Nonetheless, this waiting period did not impact the experiment due to fact that the columns tendency to get back to an equilibrium moisture profile and keep constant at that point. Besides, the salinity changes in the column were continuously measured and the data were used for model calibration as will be described in Section 4.4.

On 29th September 2020, the third experiment was started by imitating a saline water drip irrigation scenario for both columns. To apply the same amount of moisture and salts to the soil profile on every experiment, the drip irrigation cycles were designed to use a litre of saline water applied over four days similar to Experiment 2. Henceforth, 250 ml of water was applied over 50 minutes at a rate of 5mL per minute. This would be equivalent to about 1.25 cm of infiltration per day for 5 days. The 250 ml applications were performed over four consecutive days, followed by 3 days of rest. This sequence was decided upon the convenience of using the laboratory to perform the manual drip irrigations. The four days cycles were repeated four times resulting in a month of saline water drip irrigations. The irrigations were conducted using a 5ml automatic pipet that was used manually to apply the simulated drip irrigation on the soil surface distributed over the cross-sectional area.

Similar to experiment 2, this round also used saline water with an EC of ~3.40 dS/cm with the ionic composition of the bottom tanks as presented in Table 4.1. The same data collection techniques were performed for this round of the experiment as explained for the previous round in Section 4.2.2.

4.3.4. Experiment 4: Capillary Rise with Freshwater Flood Irrigation

To evaluate the impacts of saline water flood irrigation the same irrigation procedure as Section 4.2.2 was performed. However, this time the irrigation water was set to freshwater (DI water). One month of rest was dedicated before this experiment round. The first flooding with DI water was performed on 23rd November 2020 and the last irrigation in this experiment was completed on 30th December 2020.

4.3.5. Experiment 5: Capillary Rise with Freshwater Drip Irrigation

With the same rationality used for the fourth experiment, this experiment was conducted in the same setup as Experiment 3 described in Section 4.2.3. The only difference was the water quality of the drip irrigation. In this round freshwater (DI water) was utilized as the source of irrigation water. The freshwater drip irrigation cycles were started on 19 February 2021 after about 50 days of rest period after the fresh flood irrigation cycles.

4.3.6. Experiment 6: Freshwater Flood Irrigation with Free Drainage

The final experiment by removing the bottom tanks was started on 30 March 2021. This experiment was designed and performed to compare this scenario to the shallow groundwater table experiments and therefore, to evaluate the significant changes occurring due to the presence of the shallow aquifer. For this purpose, the same irrigation techniques as the fourth experiment (fresh water flooding, see Section 4.2.4) were conducted with the only difference that the water table was absent at the bottom of the columns. The surface soil samples and soil water samples were acquired following the same procedure used in the previous experiments. Furthermore, the first 5ml of the drainage water was collected after each flood irrigation for cation ion analysis using AAS.

4.4. Numerical Modelling

All the experimental column experiments conducted (see Section 4.2) were numerically simulated using the HYDRUS-1D simulation package version 4.17.0114 (Simunek, et al. 2009). The water flow experiments were numerically simulated using HYDRUS by solving the governing Richard's equation with the van Genuchten – Mualem pressure-saturation and permeability saturation relations. The simulations were initialized by the initial parameters measured from the columns and the soil samples. Moreover, the "Major Ion Chemistry" mode of HYDRUS-1D was utilized to simulate the solute transport within the column experiments. The column was discretized into 55 nodes, each 10 mm in size. Crank-Nicholson time weighting scheme was utilized together with the Galerkin Weighting Scheme to solve the numerical equations for the solute transport (Simunek, et al. 2009). Eq. 2.9 was given by Simunek et al. (2013) as the basis of the HYDRUS-1D solute transport model. However, due to the absence of crop modelling in the numerical model needed for this study "r" will be set as zero. In addition, "μ_w" and "μ_s" will be set to zero due to the use of only cations

which do not degrade. Henceforth, the solute transport equation solved for this study is shown in Eq 2.9.

The simulations were performed in four steps. At first, the water moisture behaviour of experiments 1 to 5 was modelled in a simulation run. This was followed by modelling the 6th experiment. The need for having two distinct simulation was due to the difference in the boundary conditions between the two; one having a constant pressure lower boundary condition (experiments 1 to 5) and the latter having a free drainage lower boundary condition (experiment 6). The upper boundary conditions were set to atmospheric pressure without a surface runoff. The same model setups were used for solute transport simulations. This four-step procedure was conducted to progressively calibrate the model with the data collected from the experimental runs. Calibration of the model was performed by minimizing the normalized root mean square of the error (NRMSE) between the observed and simulated data using the HYDRUS-1D Inverse Modelling Package. All the hydraulic variables were calibrated by the inverse modelling technique using the results from the sensor measurements.

Each column was modelled by having two soil profiles representing L1 and L2 as explained in Section 4.2. For experiments 1 to 5, the upper and lower boundaries for the water flow was set to atmospheric boundary condition with surface layer and constant water content, respectively. Whereas experiment 6 was set with a free drainage bottom boundary condition due to the absence of the shallow water table. The boundary conditions for the solute transport simulation were set as concentration flux boundary condition and concentration boundary condition, respectively as upper and lower boundaries for experiments 1 to 5. The same upper condition was set for experiment 6 simulation, but the zero gradients (free drainage) lower boundary was chosen for the lower boundary condition.

5. RESULTS AND DISCUSSIONS

This chapter presents the results obtained from the different experiments and their numerical simulation using the HYDRUS computer code. The interpretation from the various forms of results is further discussed in this chapter and finally, a comparative analysis is performed on the results which draw the findings and conclusions of this study.

5.1. Soil Characterization

Table 5.1 and Table 5.2 respectively show the cation composition of the 1:10 soil water extraction and exchangeable cation concentration from two packing layers of the columns at the initial stage. Figure 5.1 to Figure 5.3 show the analysis from the L1 and L2 soil samples for both CA and CB columns before the start of the experiments. These values were further utilized for modelling the solute transport of the column experiments.

Table 5.1. Soluble cation concentration from 1:10 soil water extracts measured by AAS. The value in brackets represents the standard deviation from two replicas.

	Soluble cations, mEq/Kg			
Depth (cm)	Mg^{2+}	Ca^{2+}	Na^{+}	K^{+}
0-18	3.04 *(0.06)*	17.87 *(0.61)*	0.64 *(0.00)*	3.20 *(0.16)*
18-55	2.02 *(0.1)*	14.16 *(0.68)*	1.28 *(0.02)*	1.13 *(0.08)*

Table 5.2. Exchangeable cation concentration using calcite saturated cobalt hexamine trichloride method (British Standards Institution 2006). The value in brackets represents the standard deviation from two replicas.

	Exchangeable cations, mEq/Kg			
Depth (cm)	Mg^{2+}	Ca^{2+}	Na^{+}	K^{+}
0-18	22.06 *(0.64)*	158.5 *(2.37)*	298.84 *(0.62)*	10.07 *(0.47)*
18-55	20.61 *(1.15)*	169.34 *(3.36)*	478.19 *(43.37)*	9.72 *(0.13)*

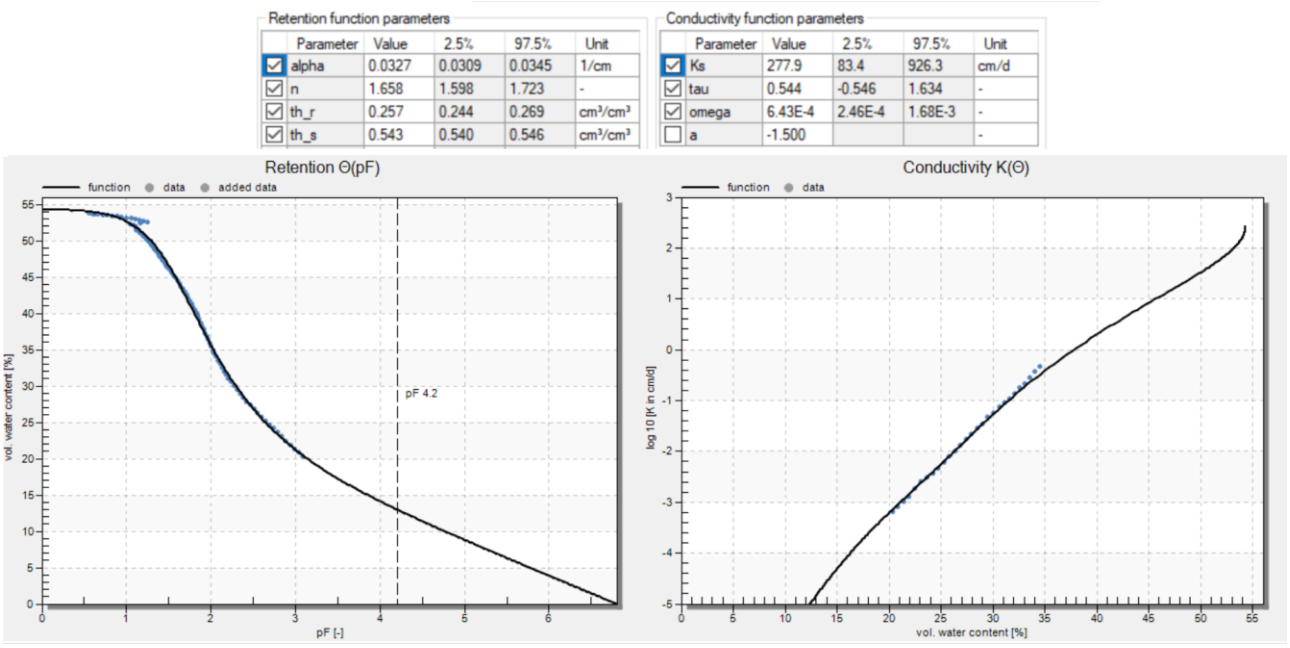

Figure 5.1. Hyprop analysis results from L1 with a dry bulk density of ~1.15 g/cm^3. This analysis applies to both CA and CB columns.

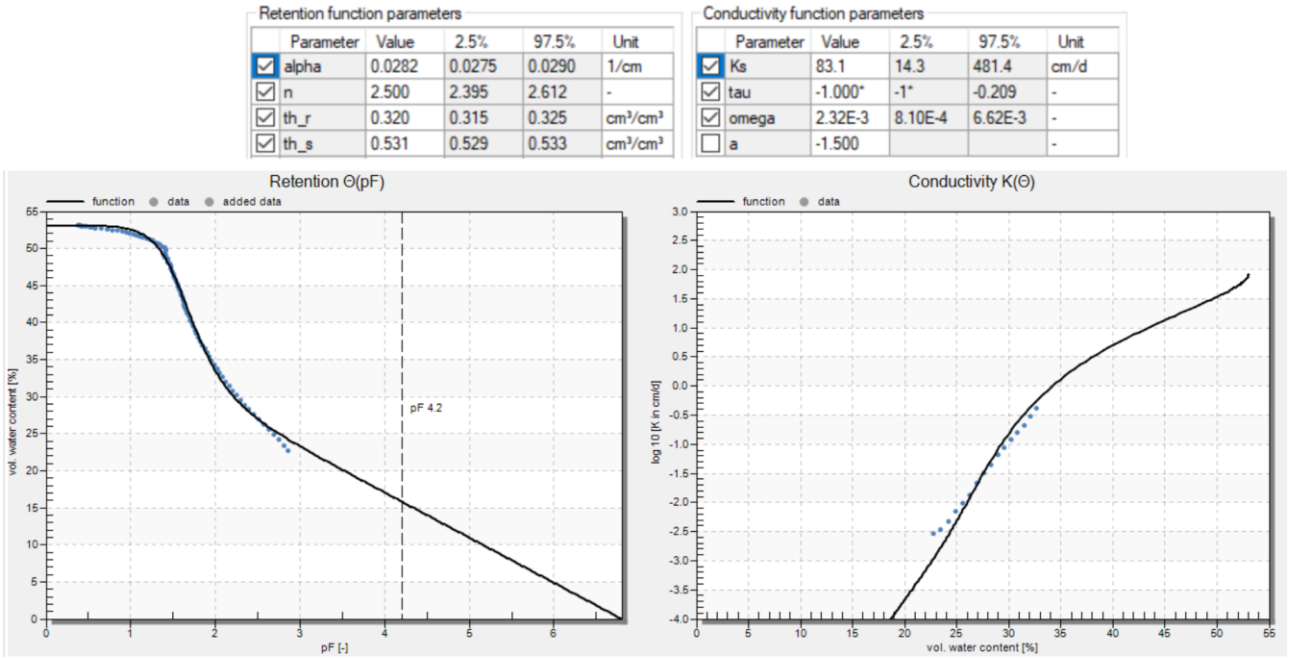

Figure 5.2. Hyprop analysis results from L2 with a dry bulk density of ~1.15 g/cm^3 which applies to the bottom layer in the CA column.

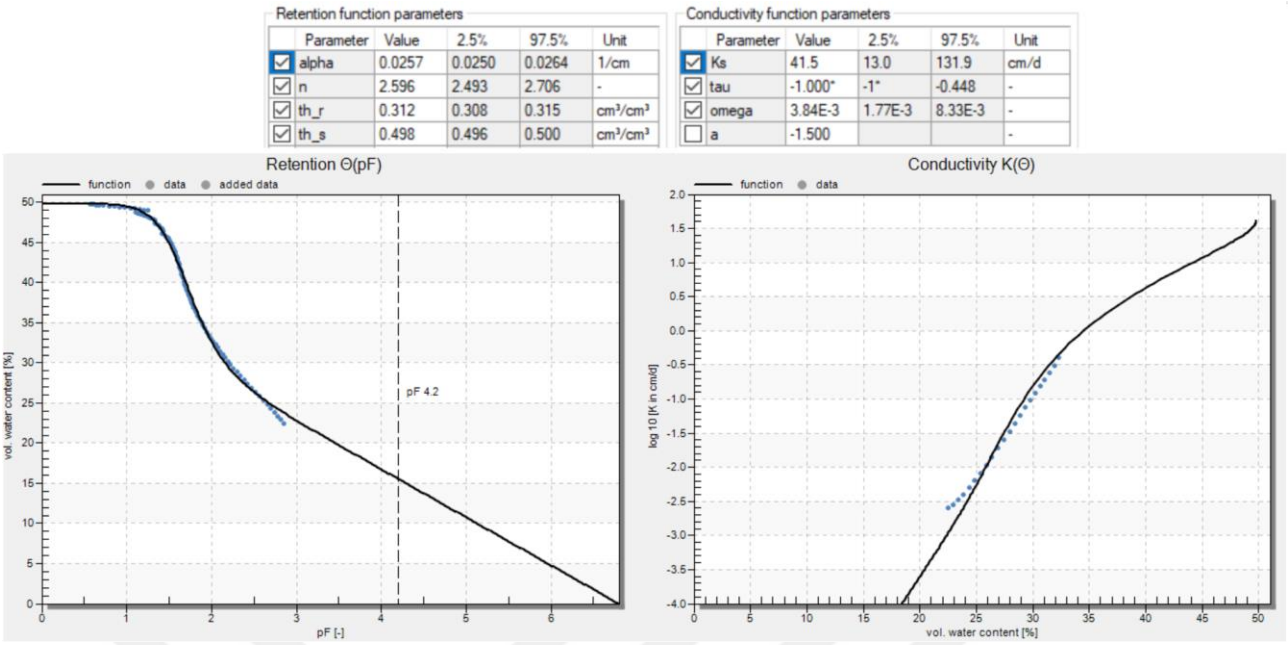

Figure 5.3. Hyprop analysis results from L2 with a dry bulk density of ~1.25 g/cm^3 which applies to the compacted layer of the column CB.

The Hyprop analysis is an estimation of the soil parameters by measuring the dynamic pressure and water content of the soil samples. However, as indicated in Figure 5.1 to Figure 5.3 the Hyprop's soil retention sensor measurements are only in the saturated zone upon which the whole retention curves are estimated. The limiting factor that created high uncertainties in this study's Hyprop measurement is the packing of the Hyprop sampling rings. In other words, it was not possible to pack the Hyprop sampling rings to correctly mimic the soil samples packed in the columns. Hence, the hydraulic parameters which were estimated by the Hyprop setup were only used as an initial estimate for further model calibration.

5.2. Soil Moisture

The soil moisture of both columns CA and CB was continuously recorded throughout the six-column experiments. The sensors encountered noise due to the void space around the probes, and this problem was fixed by pushing the sensors further into the centre of the soil columns. The blank parts of the graphs in this Section are the noises that were removed from the data set.

The column experiments started with dry soil packed in the columns. During experiment 1 the changes in soil water content at two different depths were recorded by the moisture probes for both columns CA (without compaction) and CB (with compaction) as indicated in Figure 5.1 and Figure

5.2. The measurements showed that both columns experienced a capillary rise from the bottom water tanks to the soil surface. The moisture of the soil surface sharply increased for both columns. This was followed by a relatively steady period of soil surface moisture for both columns.

Further analysing the moisture measurements during experiment 1 revealed that the sudden incline in moisture due to the capillary rise occurred about two weeks earlier for the column CB that consisted of a compaction layer with 1.35 g/cm^3 bulk density below 18 cm depth than CA which had a uniform bulk density of 1.15 g/cm^3. This behaviour indicated that the rate of capillary rise in column CB was higher than that of in CA. Besides, after the stabilization period during experiment 1, CB had about 0.45 m^3/m^3 higher moisture level than CA at the depth of 28 cm. This could be explained by the fact that the layer below 18 cm (L2) in each column had different hydraulic properties (see Section 4.2.1). This relation is shown in Section 2.3 where the rate and significance of capillary rise are a function of the soil properties, specifically the hydraulic conductivity and porosity. The impact of the velocity of the capillary rise on surface salinization in the column experiments will be discussed while analyzing the data from the other points of measurements in the coming sections.

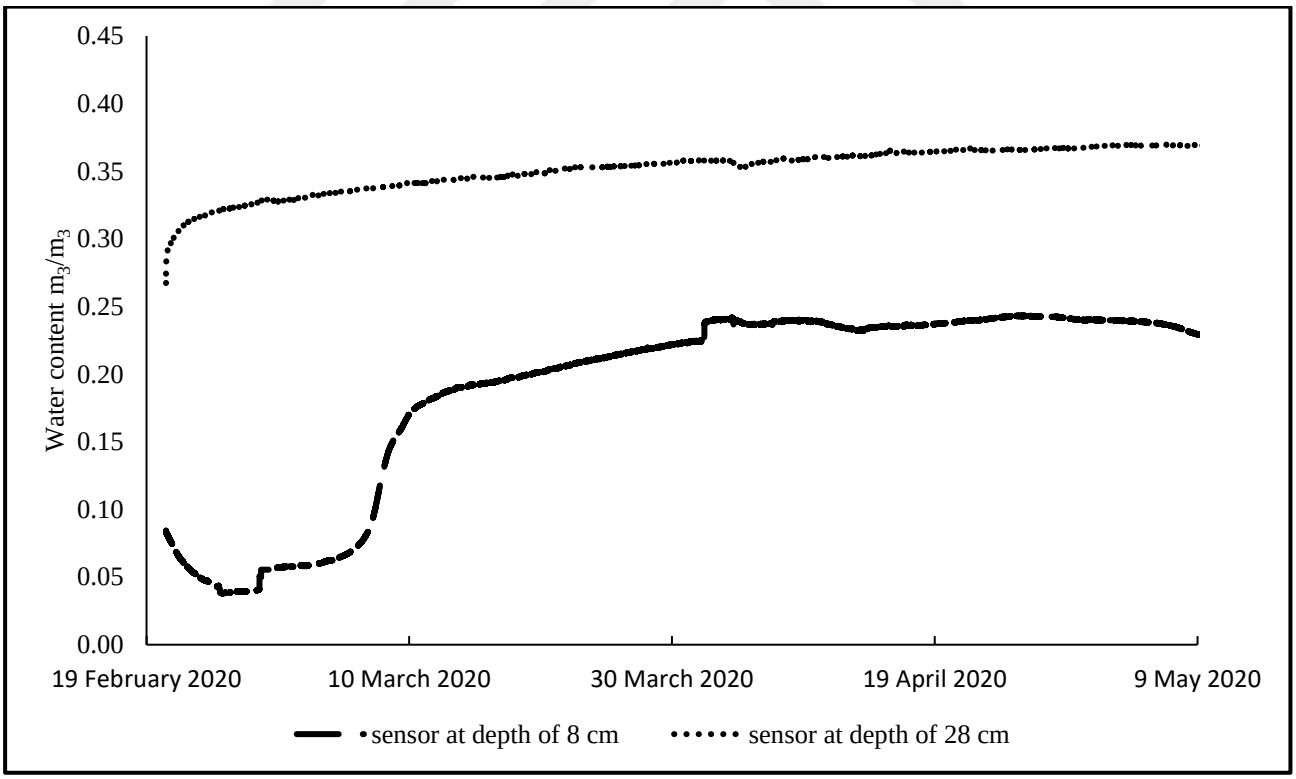

Figure 5.4. Moisture sensor measurements from column CA during experiment 1 (capillary rise without irrigation).

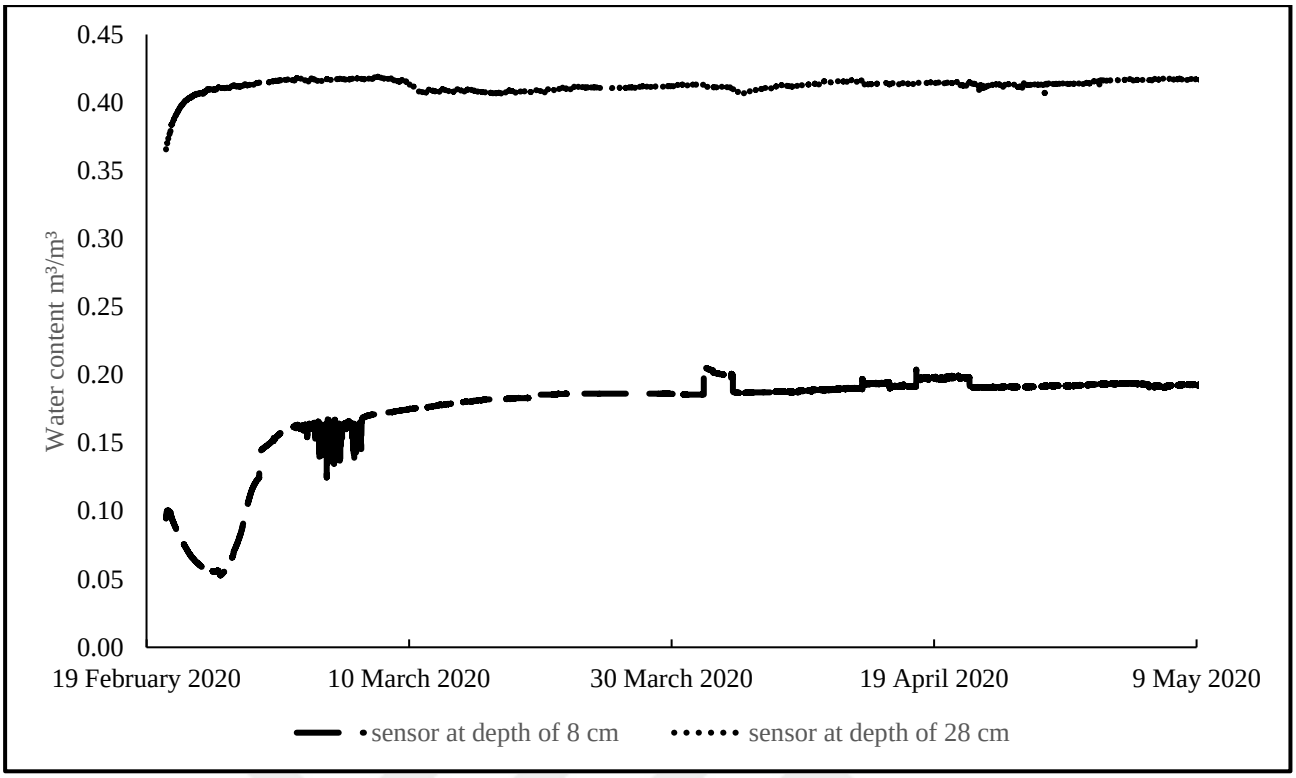

Figure 5.5. Moisture sensor measurements from column CB during experiment 1 (capillary rise without irrigation).

Experiment 2 was started by applying 1.5 L (~7.5 cm) of saline water to the surface of the columns which resulted in the first peak shown in Figure 5.6 and Figure 5.7. This amount was reduced to 1 L (~5 cm) in the following cycles to avoid excess water seeping through the entire column into the bottom tanks. The surface moisture for both columns CA and CB reached a peak between 0.45 to 0.55 m^3/m^3 moisture at the upper sensor at the end of each irrigation application followed by an immediate drop to a lower moisture level. This decrease in moisture level was due to the downward flow of the applied water and surface evaporation due to the constant temperature maintained at the top of the column. Moreover, it was observed that column CA returned to its original surface water content after each irrigation, whereas, column CB's moisture level after each irrigation cycle slightly increased from the previous cycles. Starting from 0.25 m^3/m^3 after the first cycle, the surface moisture level of CB increased to about 0.35 m^3/m^3 after the final cycle. This suggested that the existence of the hard compaction layer at the depth of 18 cm in CB, slowed down the infiltration and caused the soil to retain more moisture in the surface when compared with CA, the column with no compaction layer. A similar trend as that of the surface sensors was also recorded for the 28 cm depth. The moisture level at 28 cm was increased for CA upon every irrigation, however, for CB the irrigations did not lead to a sharp peak after the first cycle. This behaviour of column CB was again attributed to the presence of a compaction layer at the depth of 18 cm which created a hydraulic barrier, slowing

down infiltration and hence, resulting in a uniform increase in the moisture level in the depth below the compaction layer. However, a question was raised by the fact that the first irrigation in the column CB resulted in a peak but the followings did not. The differences between the first irrigation and the following were that the soil was drier at the initial irrigation and the irrigation consisted of 0.5 L more water than the following.

The soil moisture results obtained from experiment 2 demonstrates that agricultural soil compaction causes a greater accumulation of moisture in soil surface in comparison to a non-compacted soil profile. However, this is the result of the interaction of several factors such as the amount of applied irrigation, initial moisture and the soil hydraulic properties.

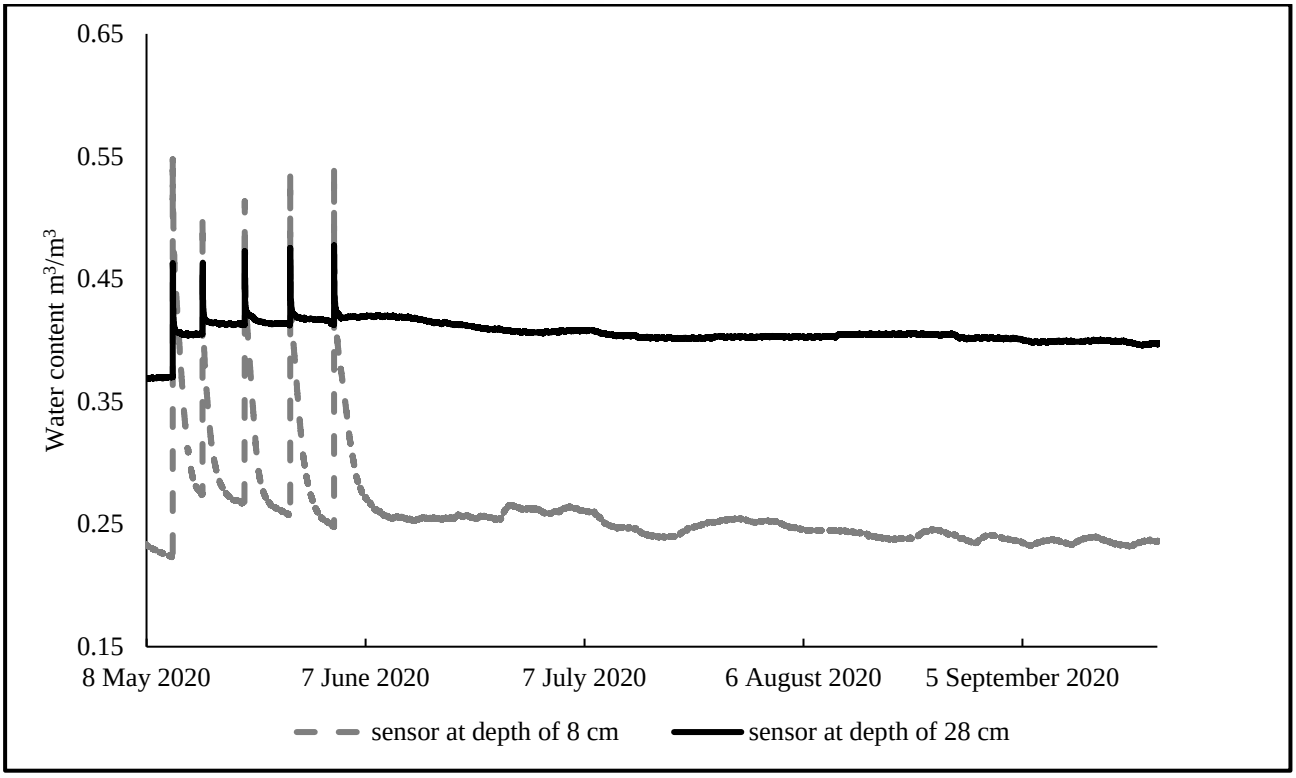

Figure 5.6. Moisture sensor measurements from column CA during experiment 2 (capillary rise with saline water flood irrigation).

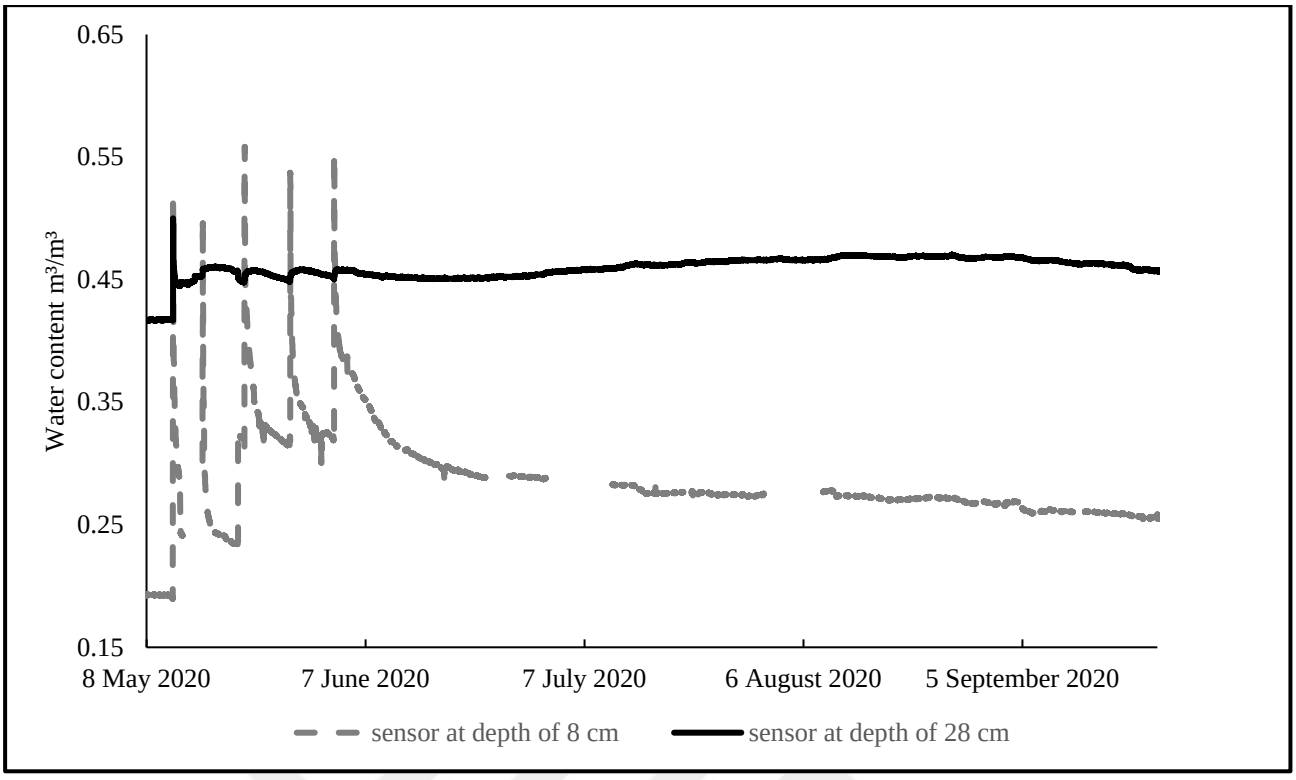

Figure 5.7. Moisture sensor measurements from column CB during experiment 2 (capillary rise with saline water flood irrigation).

Experiment 3 involved four drip irrigation cycles, each lasting for four days drip irrigation at the rate of 1.25 cm/h for 50 minutes. Every four peaks in consequent days shown in Figure 5.8 and Figure 5.9 illustrate one drip irrigation cycle performed during experiment 3.

Both columns CA and CB indicated that the drip irrigation cycles significantly impacted the water content at the surface layer. However, at 28 cm depth, the moisture was not significantly impacted by the drip irrigations. This response was due to the low rate of water inflow from drip irrigation being overcome by the surface evaporation, preventing moisture transport farther downwards through the profile.

With the drip irrigation condition, Column CB showed higher water content than that of CA, both at the surface and below its compaction layer. However, a comparison between drip irrigation and flood irrigation moisture measurements showed that the drip irrigations resulted in higher peaks than the flood irrigation only for the compacted column CB. The surface moisture peaks were between 0.50 to 0.55 m^3/m^3 for flood and drip irrigation in CA and flood irrigation in CB, while during the drip irrigation in CB most of the moisture peaks were above 0.55 m^3/m^3. Hence, it could be concluded that in our soil profile scenario with a shallow groundwater table, having a compaction

layer with drip irrigation led to a more significant increase in surface moisture than the application of flood irrigation. This conclusion is attributed to the lower infiltration velocity of the drip irrigation and the lower permeability of the compacted profile, allowing the moisture to remain above the surface layer of the soil. Nonetheless, due to the complexity of the interconnected processes (capillary, infiltration and evaporation) that are all dynamically affecting the soil moisture, further analysis is needed to validate this conclusion.

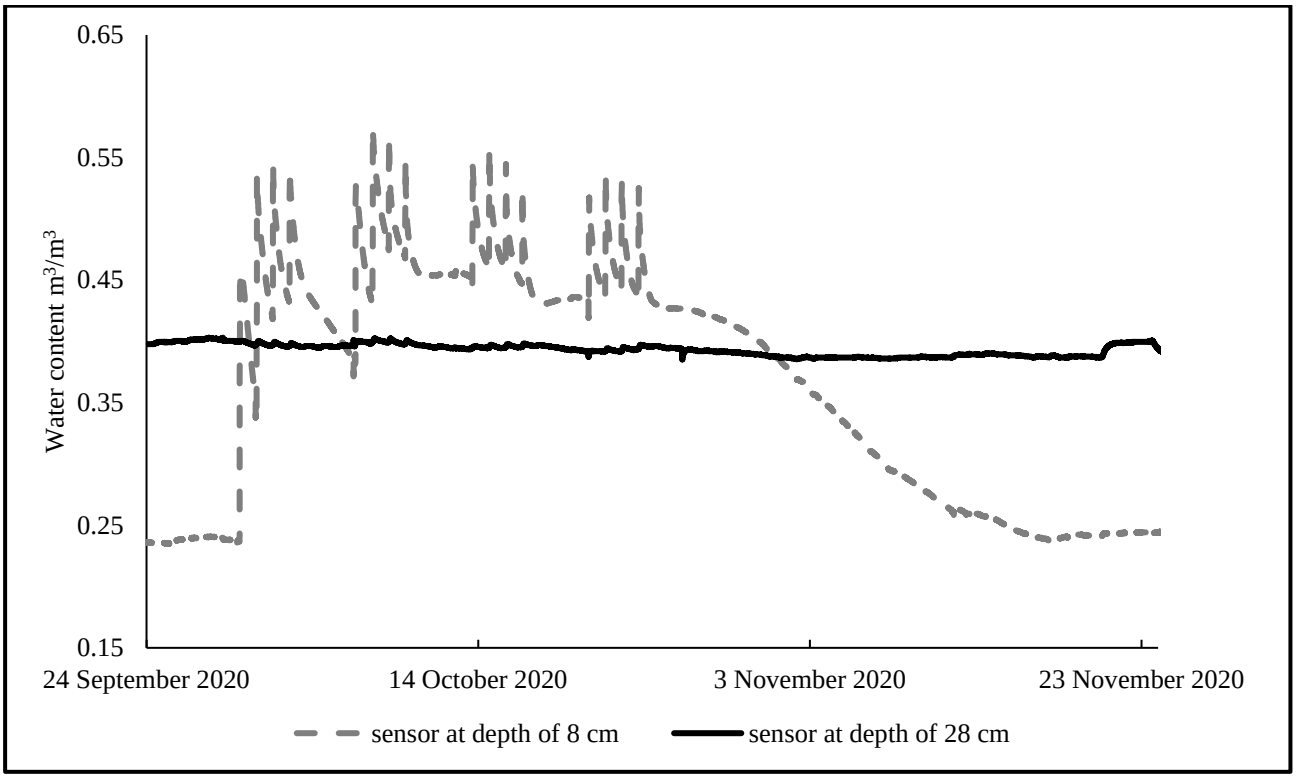

Figure 5.8. Moisture sensor measurements from column CA during experiment 3 (capillary rise with saline water drip irrigation).

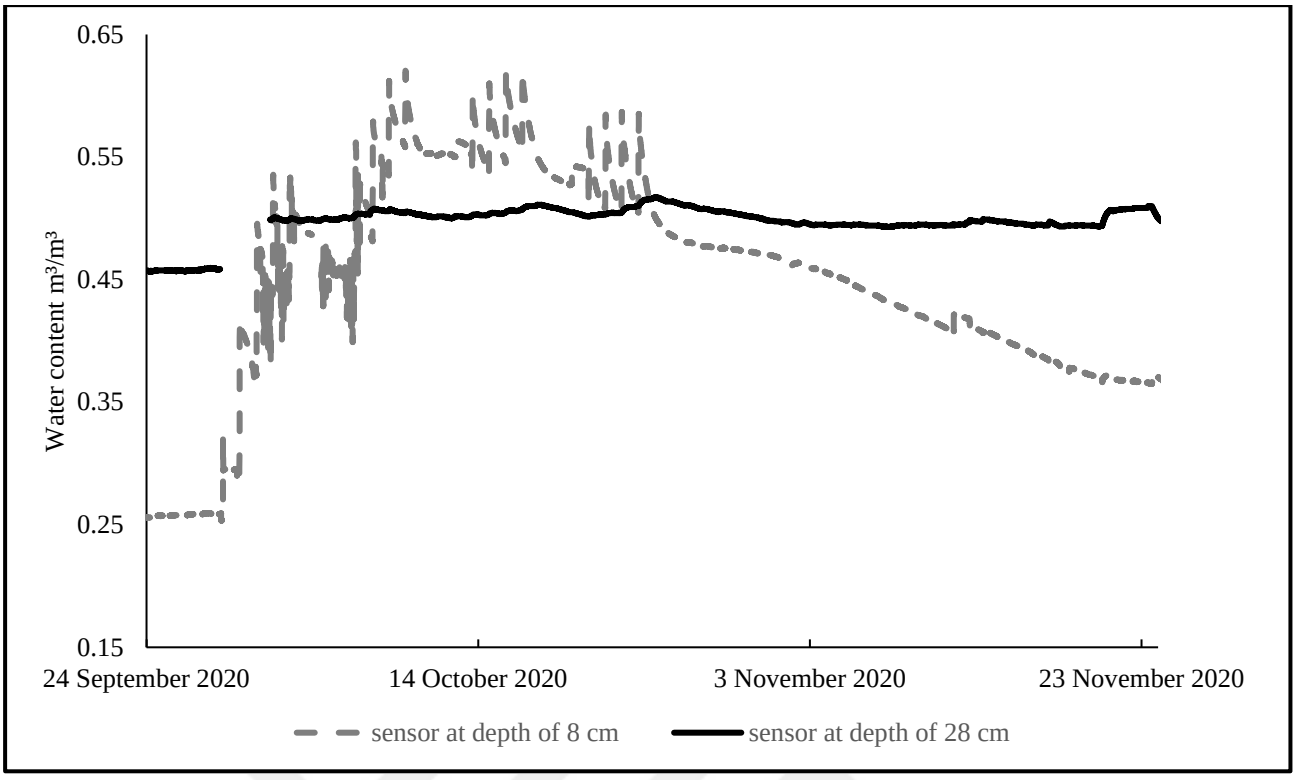

Figure 5.9. Moisture sensor measurements from column CB during experiment 3 (capillary rise with saline water drip irrigation).

The procedures in experiments 2 and 3 were repeated in experiments 4 and 5, respectively. The only difference between these 2 sets of experiments was the irrigation water quality. The former (experiments 2 and 3) used saline water for irrigation and whereas experiments 4 and 5 used freshwater (DI). Figure 5.7 to Figure 5.10 show soil moisture measurements during the 4th and 5th experiments for the compacted and uncompacted soil columns.

The patterns of change in water content in experiments 4 and 5 were closely similar to experiments 2 and 3. The moisture level during the flood irrigation with saline water and freshwater led to relatively similar peaks for the column CA, however, CB experienced a slightly higher level of surface soil moisture in the freshwater flood irrigation than the one with saline water. We can explain these variations in two ways. Firstly, the difference in the initial surface moisture conditions of experiment 2 and experiment 4 could explain why only the column with compaction (CB) encountered a higher level of surface soil moisture in the freshwater flood irrigation than the one with saline water. This is displayed in Figure 5.4 and Figure 5.11, where the initial moisture level of column CB was respectively around 0.25 m^3/m^3 for experiment 2 and 0.35 m^3/m^3 for experiment 4. The second reasoning for this was the possibility of changes in sodicity of the column CB leading to a lower permeability through the compaction layer.

A distinctive change of pattern observed during the freshwater irrigations (experiments 4 and 5) was that for the column CA the surface moisture peaks gradually decreased in each subsequent cycle. This indicated a change in the hydraulic properties of the topsoil. However, the explained pattern did not occur for column CB (Figure 5.7 to Figure 5.10). This change in hydraulic behaviour of column CA could suggest that the absence of the compaction layer might have resulted in the washing of the calcium and magnesium ions to the lower levels of the column during the DI water irrigations. Hence, changes in sodicity might have been the contributor to the reduction in peaks as shown in Figure 5.7 and Figure 5.9. The soil water analysis in the following sections will further divulge this hypothesis by showing the sodicity measurements of the soil profile.

Unlike the flood irrigation experiments, there were notable dissimilarities between surface moisture measurements of experiments 3 and 5. Column CA gradually dropped in surface moisture level after the first week of freshwater drip irrigation. In addition, column CB presented lower surface moisture content peaks in the 5th experiment than the third. These variations could be due to the change in the SAR in the columns after DI water flood irrigation in the 4th experiment.

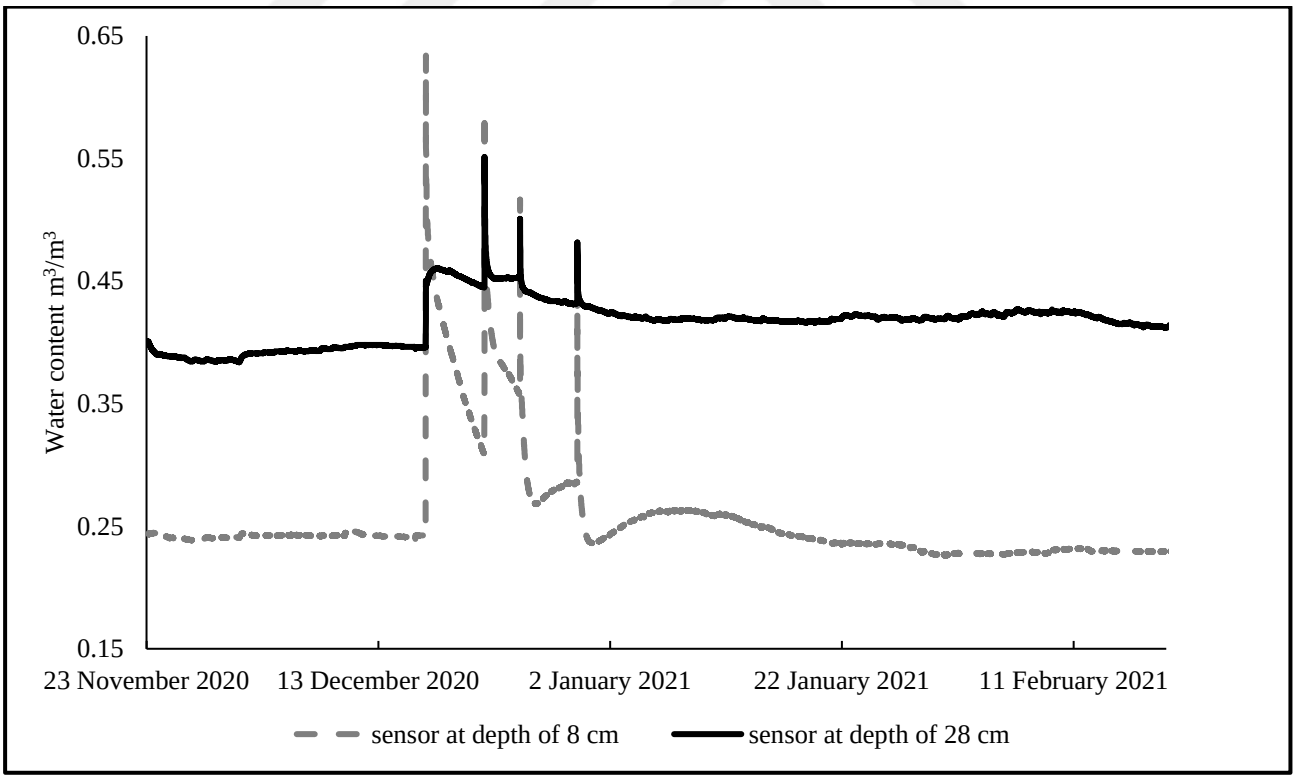

Figure 5.10. Moisture sensor measurements from column CA during experiment 4 (capillary rise with freshwater flood irrigation).

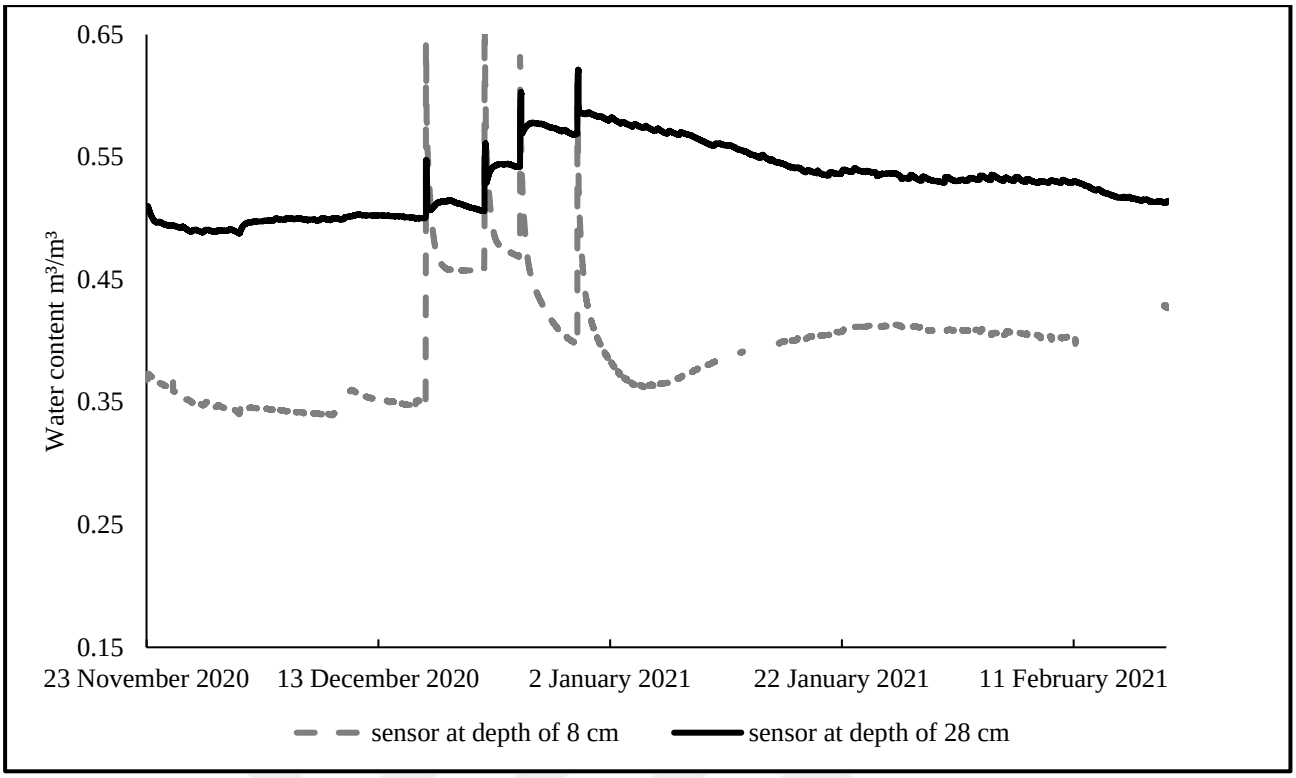

Figure 5.11. Moisture sensor measurements from column CB during experiment 4 (capillary rise with freshwater flood irrigation).

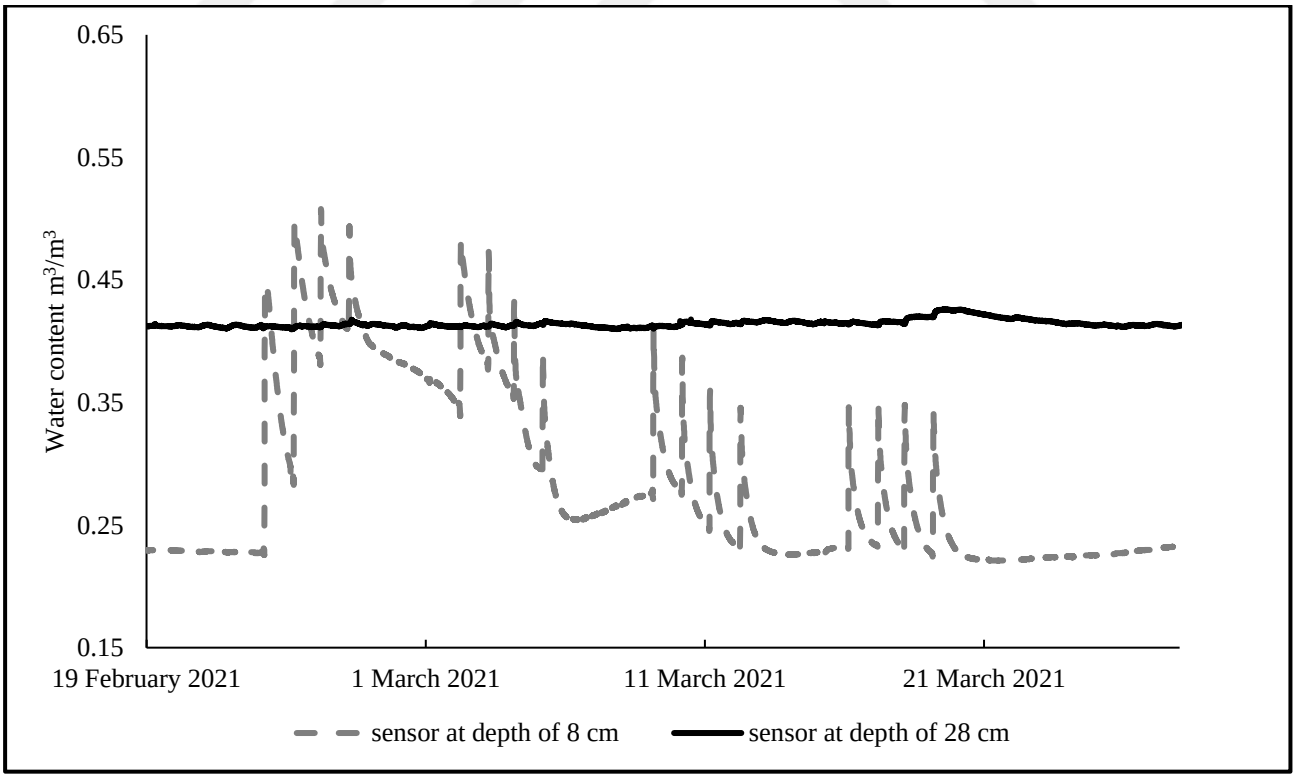

Figure 5.12. Moisture sensor measurements from column CA during experiment 5 (capillary rise with freshwater drip irrigation).

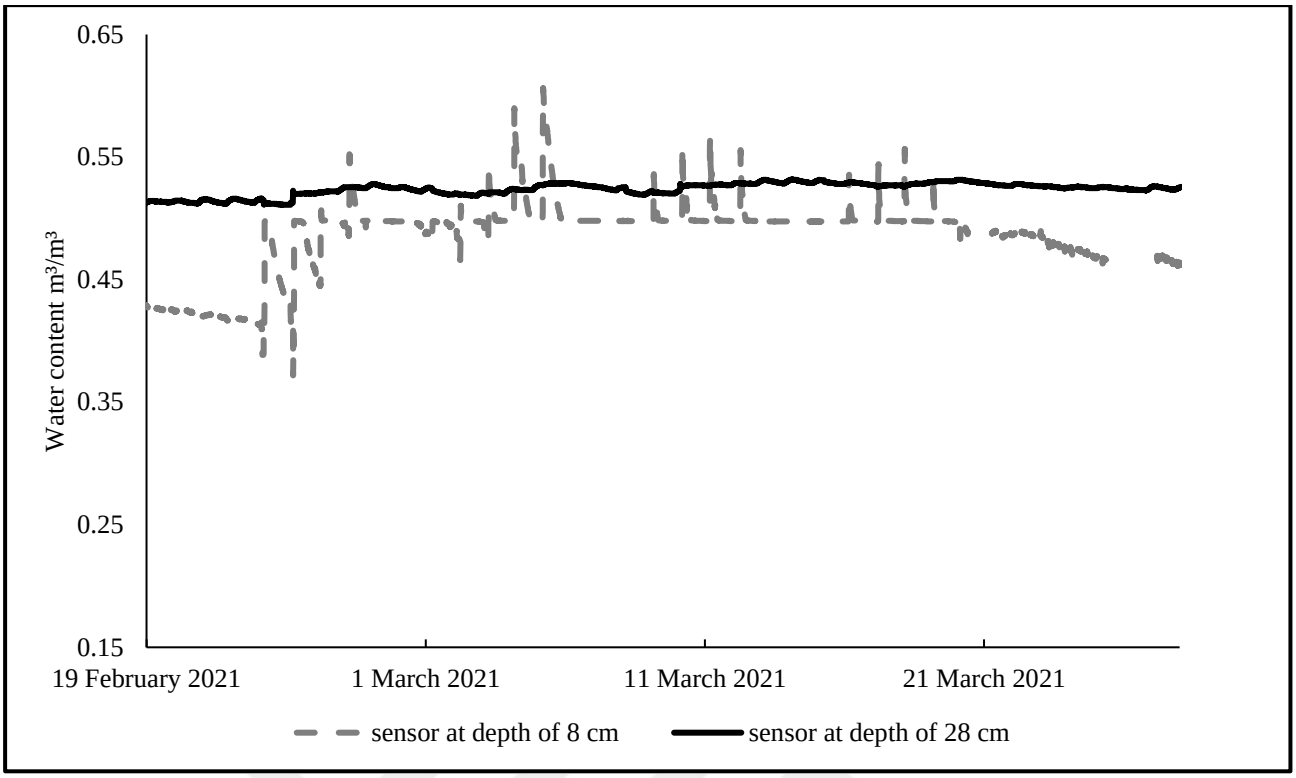

Figure 5.13. Moisture sensor measurements from column CB during experiment 5 (capillary rise with freshwater drip irrigation).

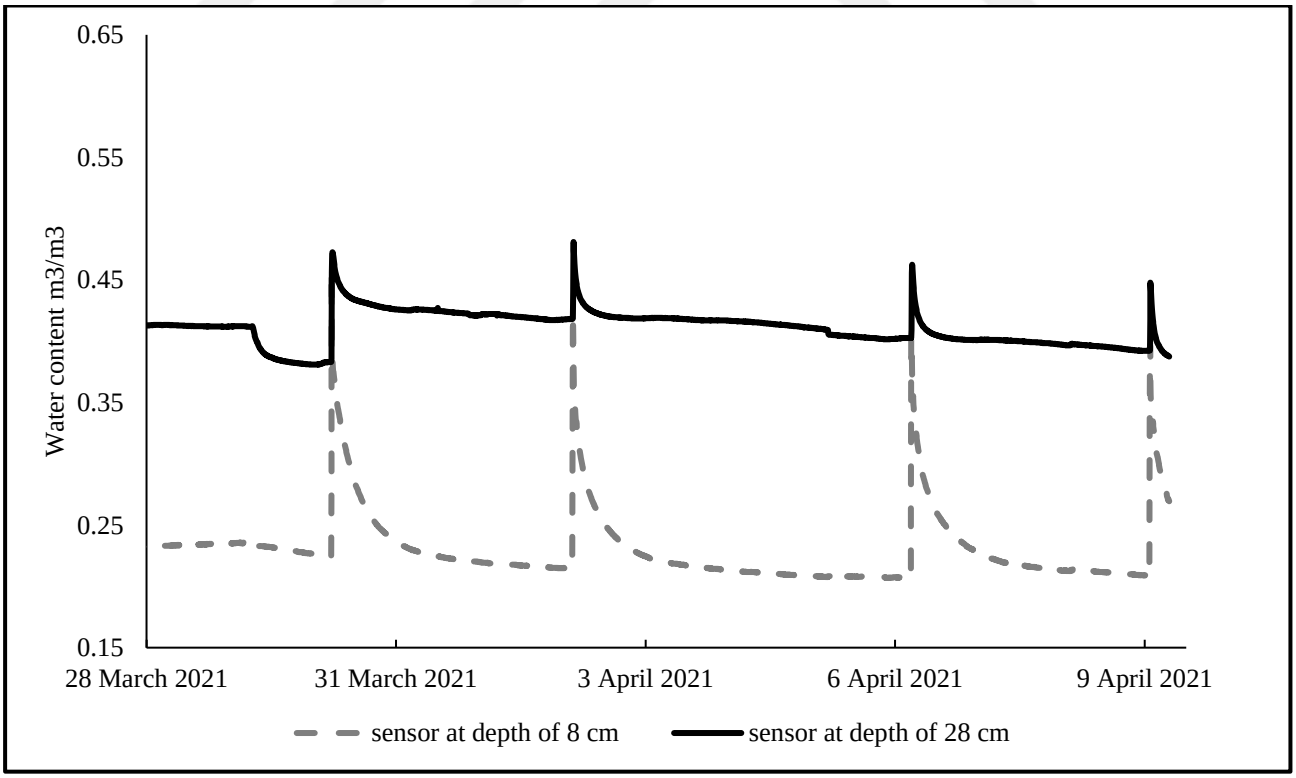

Figure 5.14. Moisture sensor measurements from column CA during experiment 6 (freshwater flood irrigation with free drainage).

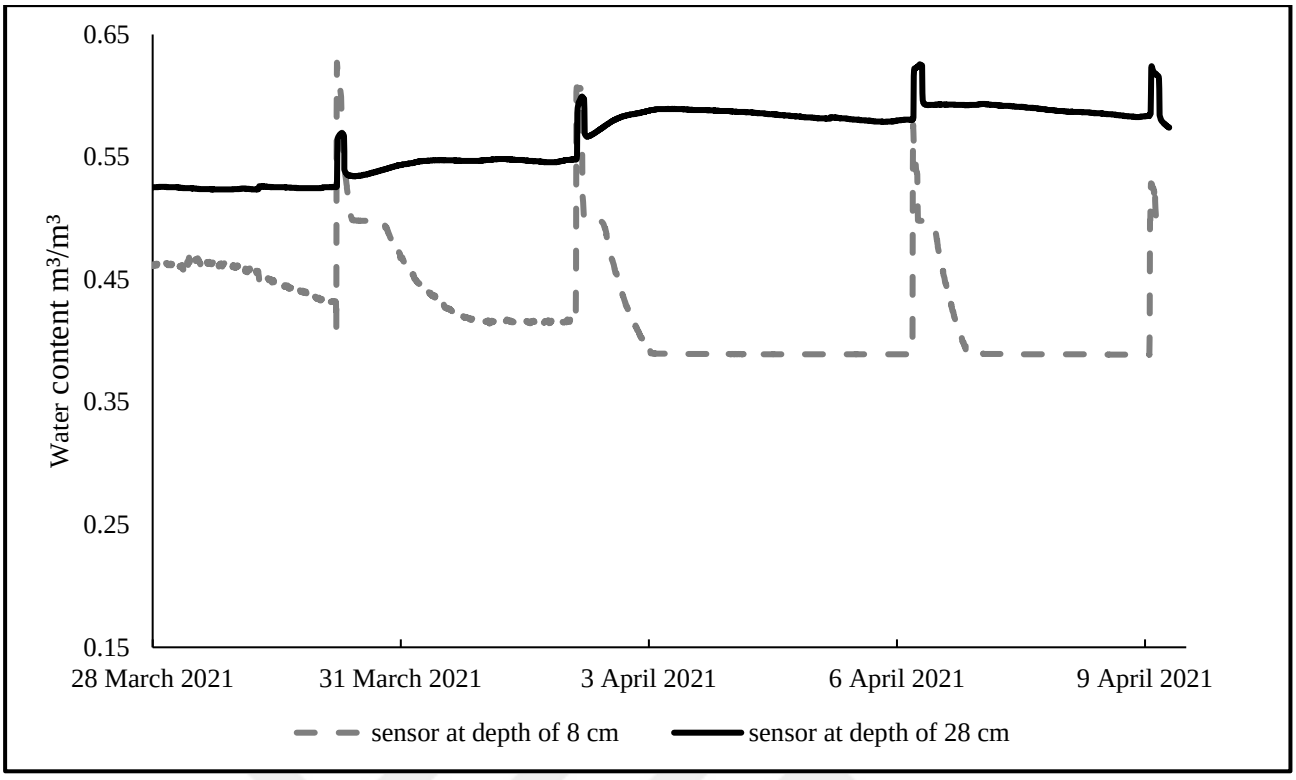

Figure 5.15. Moisture sensor measurements from column CB during experiment 6 (freshwater flood irrigation with free drainage).

This final experiment was performed in a similar setting as experiment 3 but with free drainage without the presence of the bottom aquifer (water tanks). This experiment provided us with the data to further understand the difference between having a shallow aquifer and a free drained soil profile.

As illustrated in Figure 5.11 and Figure 5.12, both CA and CB exposed a similar pattern of changes in water content. Nonetheless, the surface (8 cm) and subsurface (28 cm) moisture levels throughout the experiment were likely due to the compaction layer in column CB. Besides, the sharp drops in moisture after each irrigation indicated the influence of the free drainage on the water infiltration rate of the soil profiles affecting both 8 and 28 cm depths of moisture measurements.

The findings of the second and the final experiment suggest that the presence of soil compaction could result in a higher surface moisture level despite having free drainage or a shallow water table. This conclusion determines that having agricultural soil compaction can create a hydraulic barrier for the soil moisture to transport through the compacted layer even by having a soil drainage system.

An overall picture of the moisture level throughout all six experiments is presented in Figure 5.16. The above discussions about surface moisture are also illustrated in this figure. In addition, this

overview figure shows that the column with compaction layer (CB) hold higher surface moisture than the column with uniform density (CA) after the beginning of the first irrigation in experiment 2. This showed that before experiment 2 when the capillary rise was the only means of water transport within the column, the compaction layer slowed down the moisture movement towards the surface. On the other hand, once the irrigation started, the moisture level in the surface of CB became more than that of CA which indicates that the compaction layer acted as a barrier to hold the moisture longer in the surface in contrast to the column with uniform bulk density but without compaction.

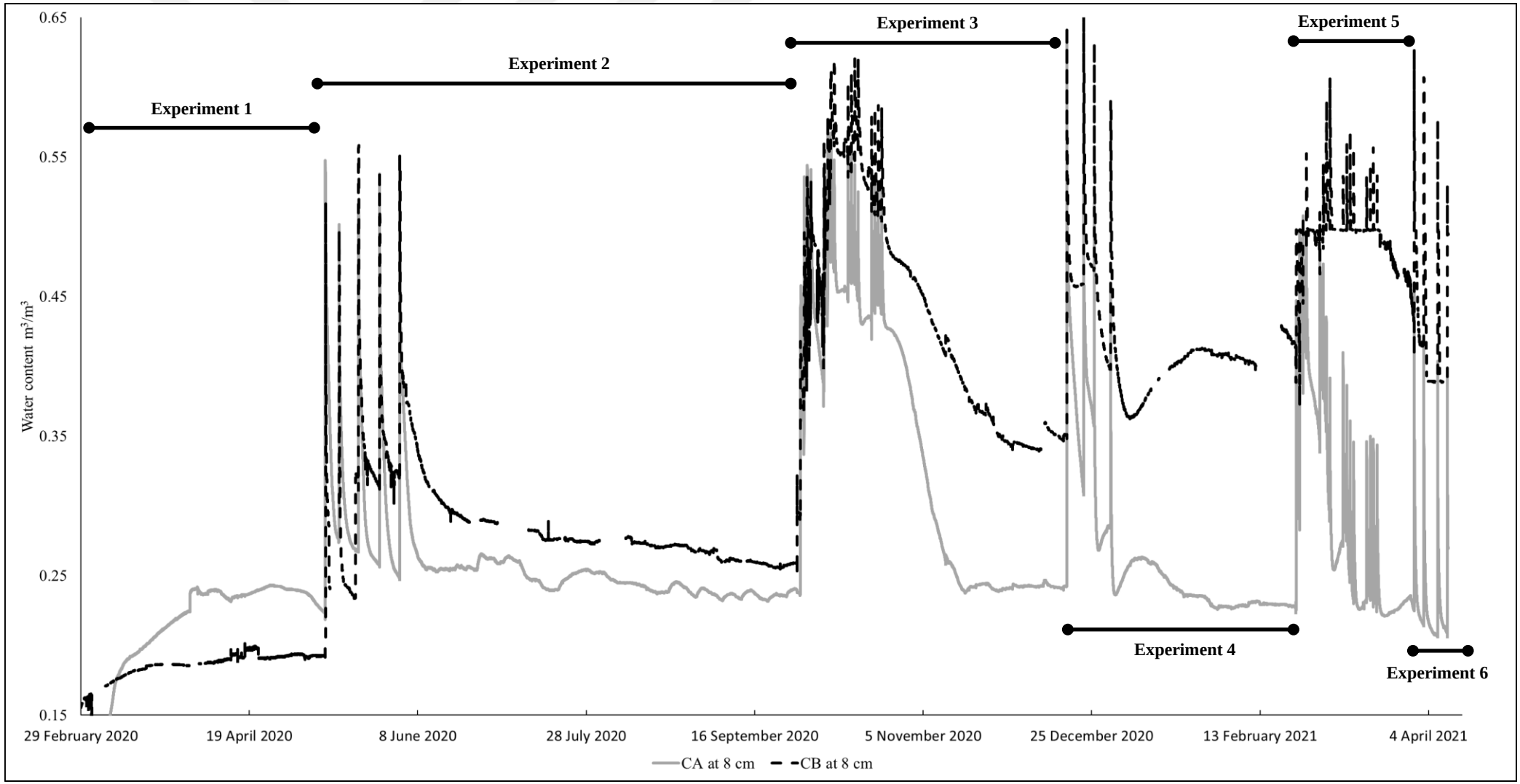

Figure 5.16. Comparison between moisture sensor measurements of column CA and CB throughout all the experiments.

5.3. Surface Soil Bulk Electrical Conductivity

The Teros 12 sensors continuously measured the surface (depth of 5 cm) EC_b which was a relative indication of the surface soil salinity. The numbers shown by these sensors represent a relative indication of the soil salinity (see Section 2.1). Nonetheless, these numbers can be compared across the measurements which have similar conditions.

The initial experiment - which only consisted of capillary rise action of the saline shallow water table (EC ~3.40 dS/cm) – resulted in a gradual increase in the bulk electrical conductivity and salinity of the surface soil in both columns (Figure 5.17). The measurements revealed a slightly higher increase (about 7%) in the surface EC_b for column CB (with compaction). These small differences might be due to slight differences in initial conditions of the columns such as the vertical placement of the sensors in the columns. Overall, it can be considered that at the end of experiment 1, the salinity levels are approximately the same for both columns.

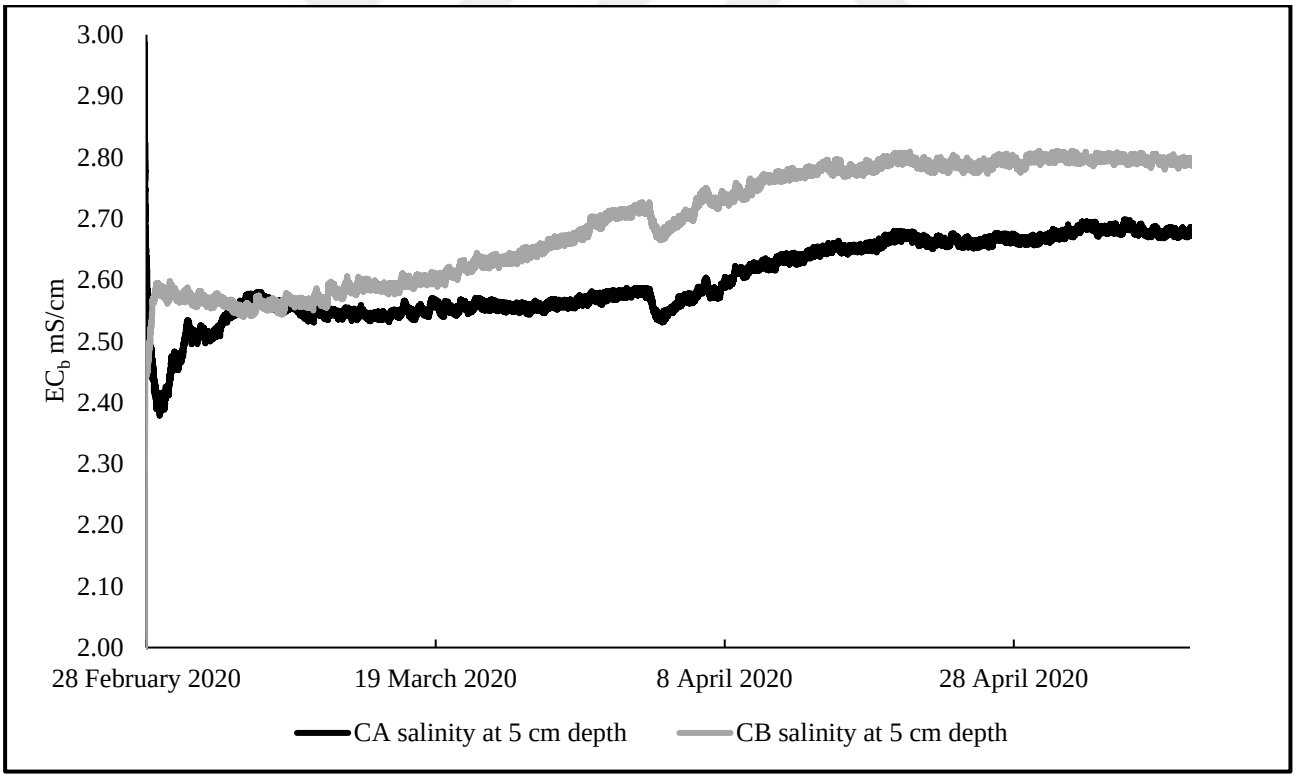

Figure 5.17. Surface bulk electrical conductivity measured by the Teros 12 sensor for columns CA and CB during experiment 1 (capillary rise without irrigation).

Since EC_b measurements are sensitive to soil moisture, EC_b measurements at peak moisture are examined which correspond to field capacity as seen with the moisture results from the previous

section. In other words, each peak shows the time when the irrigation water is just applied to the columns.

Experiment 2 begun by introducing saline water at the top boundary following a flood irrigation regime. Subsequently, experiment 3 utilized the same saline water amount and quality but the application was through a drip irrigation regime. Figure 5.18 and Figure 5.19 compare the EC_b measurements at the irrigation times between columns CA and CB in the surface soil during the experiment 2 and 3, respectively. Figure 5.20 and Figure 5.21 represent the EC_b measurements of experiment 4 and 5, respectively, which were performed in the same manner as the experiment 2 and 3 but with using DI water for irrigation. Figure 5.22 shows the EC_b corresponds to free drainage at the bottom boundary (experiment 6).

The surface EC_b results from flood irrigation cycles revealed that the saline water irrigation increased the conductivity from a value of 2.7 mS/cm (Figure 5.17) to a value of 8±2 mS/cm and was maintained at this level for both columns CA and CB as shown in Figure 5.18. Although the salinity (EC) of the applied irrigation was ~3.4 mS/cm, the salinity of the water did continue to increase up to this level, suggesting the bulk conductivity of the soil surface reached a relative equilibrium. This could be understood by the fact that the crystalized salts on the surface could only be dissolved up to the saturation level of the soil water. Because the applied water had a relatively high salinity (~3.4 mS/cm), this limited the ability of the infiltrated water to dissolve the crystallized salt in the soil columns.

The DI water flood irrigation (Figure 5.20) caused a gradual decrease in peaks for both columns. This shows the impact of the shallow groundwater table in preventing the salts from rapid leaching to deeper levels, whereas the capillary rise counter affects the leaching and transports salts back to the surface. Furthermore, the rapid reduction in the peak levels in Figure 5.22 - as compared to Figure 5.20- indicate that having free drainage greatly helps in washing the salts from the surface layers.

The differences between the peaks throughout the flood irrigation cycles (Figure 5.18 and Figure 5.20) oscillated with CB having a higher value in most instances. Hence, a clear difference between CA and CB could not be derived from the flood irrigation figures. One possible way to understand the differences between the two columns during these experiments is to examine the soil water and surface soil analyses to measure the changes between the two columns during these experiments. The results of these analyses are presented in the coming sections.

The bulk soil conductivity measurements during the drip irrigation cycles are shown in Figure 5.19 and Figure 5.21. The drip irrigation cycles with saline and DI water showed a similar trends as in flood irrigation cycles (Figure 5.18 and Figure 5.20), whereby the conductivity increased sharply and stayed relatively stable for the saline water irrigation, and gradually decreased throughout the DI water irrigation cycles.

The peaks in the drip irrigation cycles (Figure 5.19 and Figure 5.21) implied that the salinity levels in column CA reached a higher level than salinity levels in column CB during both drip irrigation experiments with saline and DI waters. Therefore, the presence of the compaction layer in column CB resulted in less salt accumulation on the surface of the profile. This could be explained by the slower rate of capillary rise driven salt transport in CB than in CA. This difference in transport rate resulted in a higher accumulation of precipitated salts in the surface of the CA column that led to higher EC_b peaks. In addition, Figure 5.22 shows the opposite effect in absence of the shallow aquifer where the surface conductivity decreases more gradually in the column CB than in CA. This shows that in a free drainage scenario the compaction layer in CB slows down the washing out salts to the deeper levels when compared with the profile without compaction (CA).

Given the above discussions, it can be concluded that agricultural compacted land can prevent salt transport to the soil surface in a scenario with a shallow aquifer in a clay loam profile. In such condition, flood irrigation can provide a better washing of salts from the surface layer. Overall, in the presence of a shallow head boundary changing the irrigation water quality does not significantly improve the salinization problems. On the other hand, for the irrigation patterns, 1) drip irrigation with saline water contributes to a higher surface salt accumulation than flood irrigation with saline water given the same volume of irrigation water; 2) drip irrigation with freshwater is less effective than flood irrigation in removing the surface salinity. The validity of these finding is further discussed and analysed from different aspects in the following sections.

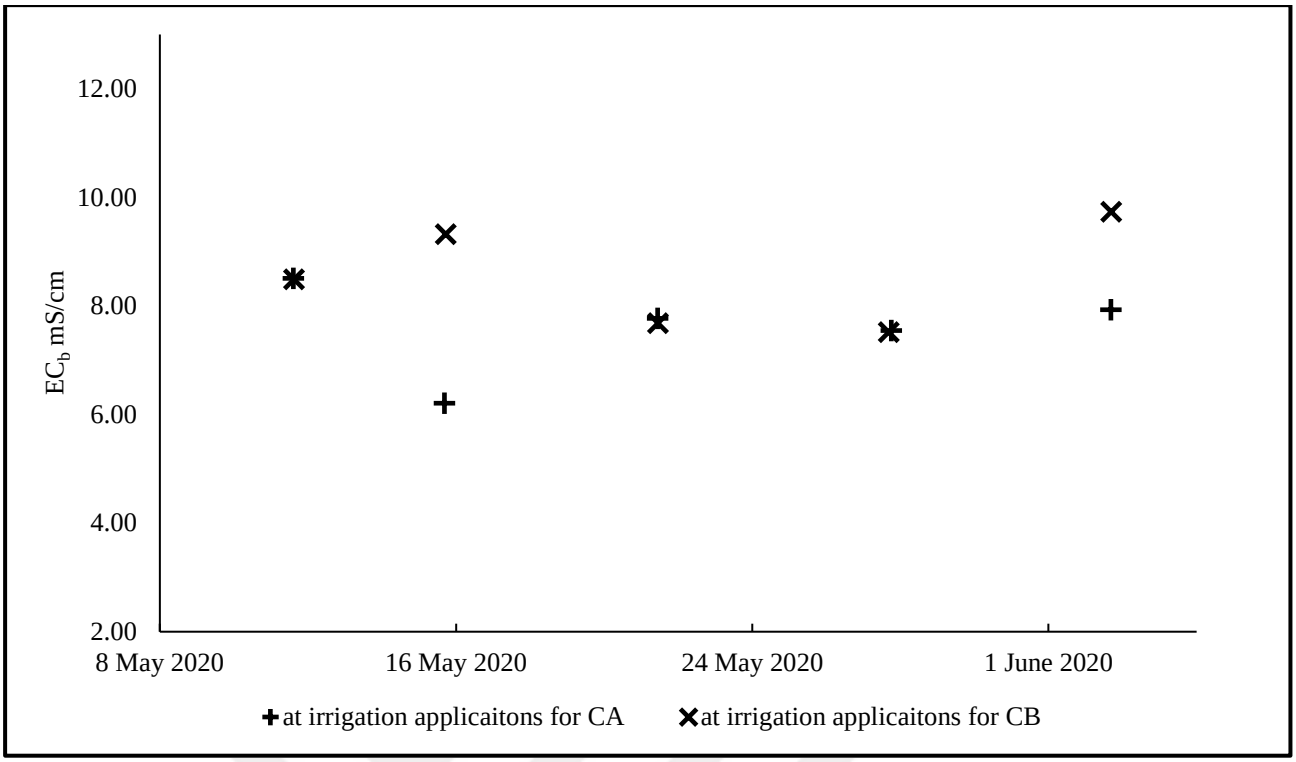

Figure 5.18. Surface bulk electrical conductivity at every irrigation instance measured by the Teros 12 sensor for columns CA and CB during experiment 2 (capillary rise with saline water flood irrigation).

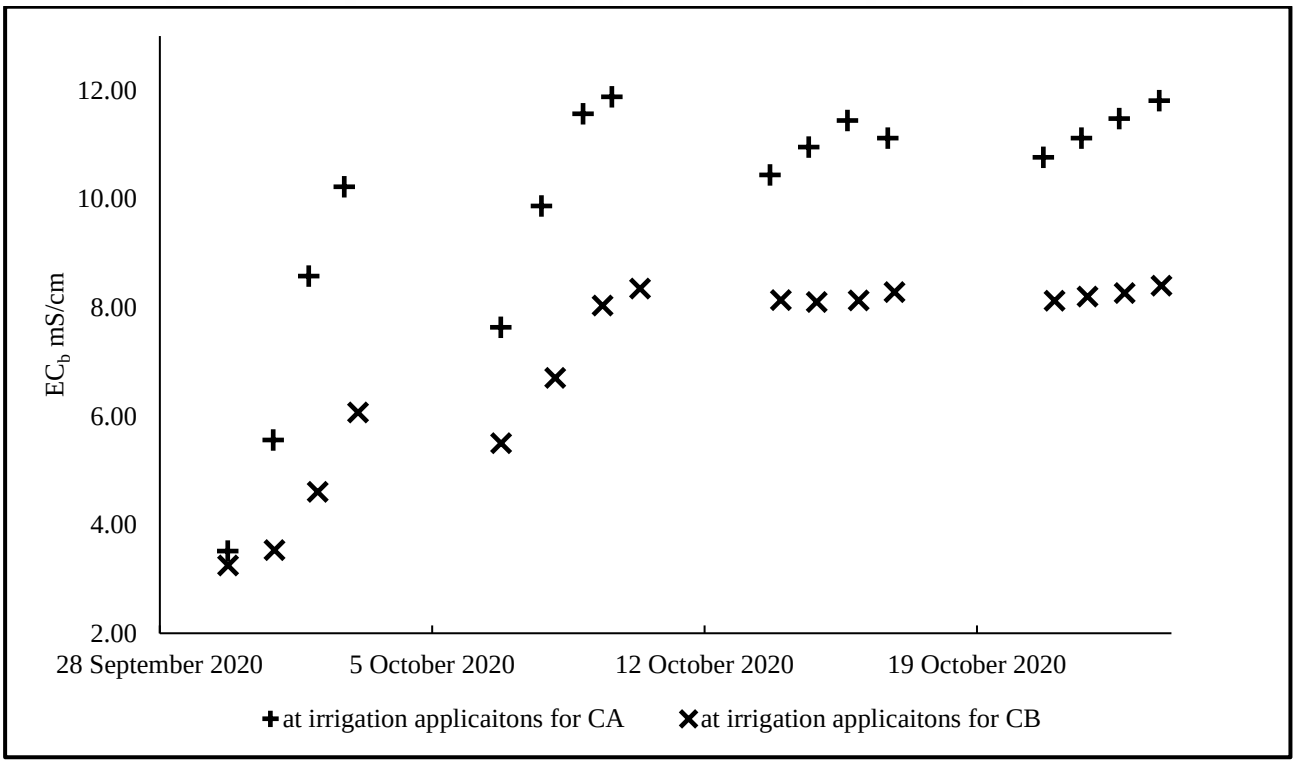

Figure 5.19. Surface bulk electrical conductivity at every irrigation instance measured by the 12 sensors for columns CA and CB during experiment 3 (capillary rise with saline water drip irrigation).

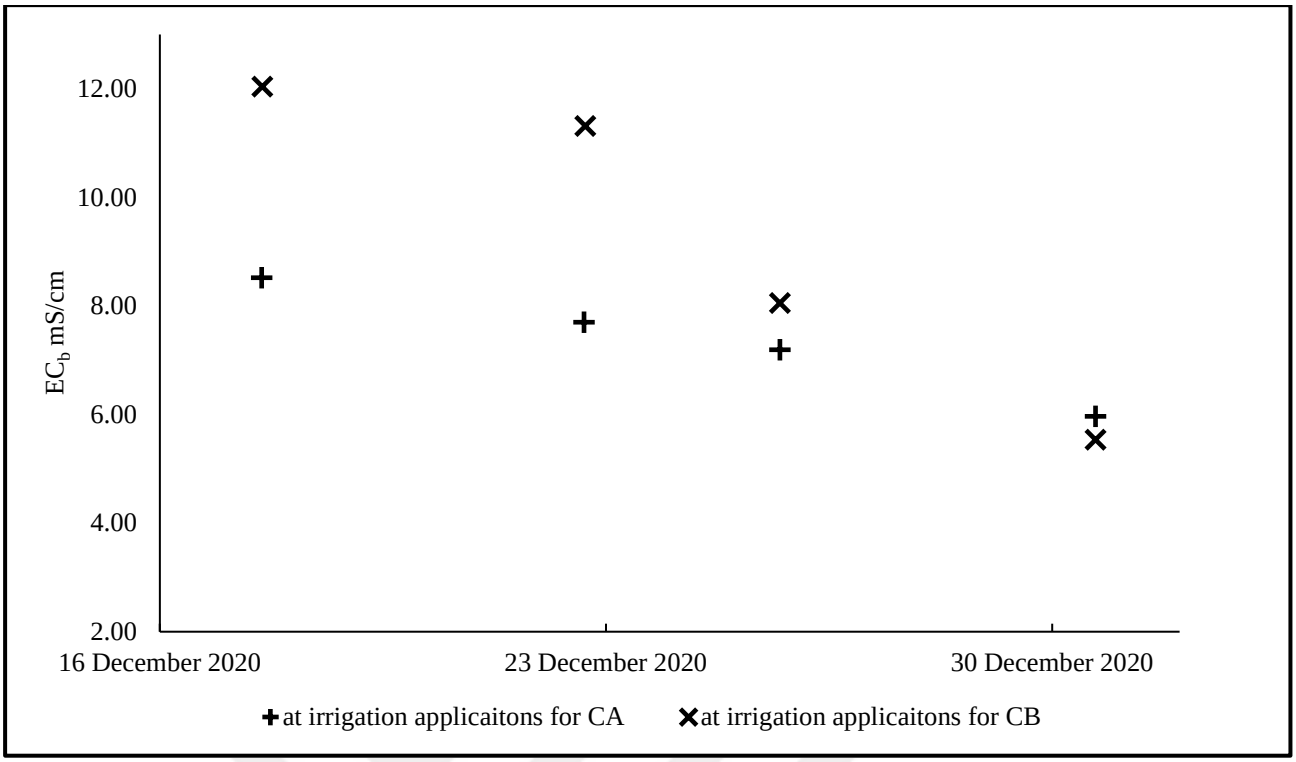

Figure 5.20. Surface bulk electrical conductivity at every irrigation instance measured by the Teros 12 sensor for columns CA and CB during experiment 4 (capillary rise with freshwater flood irrigation).

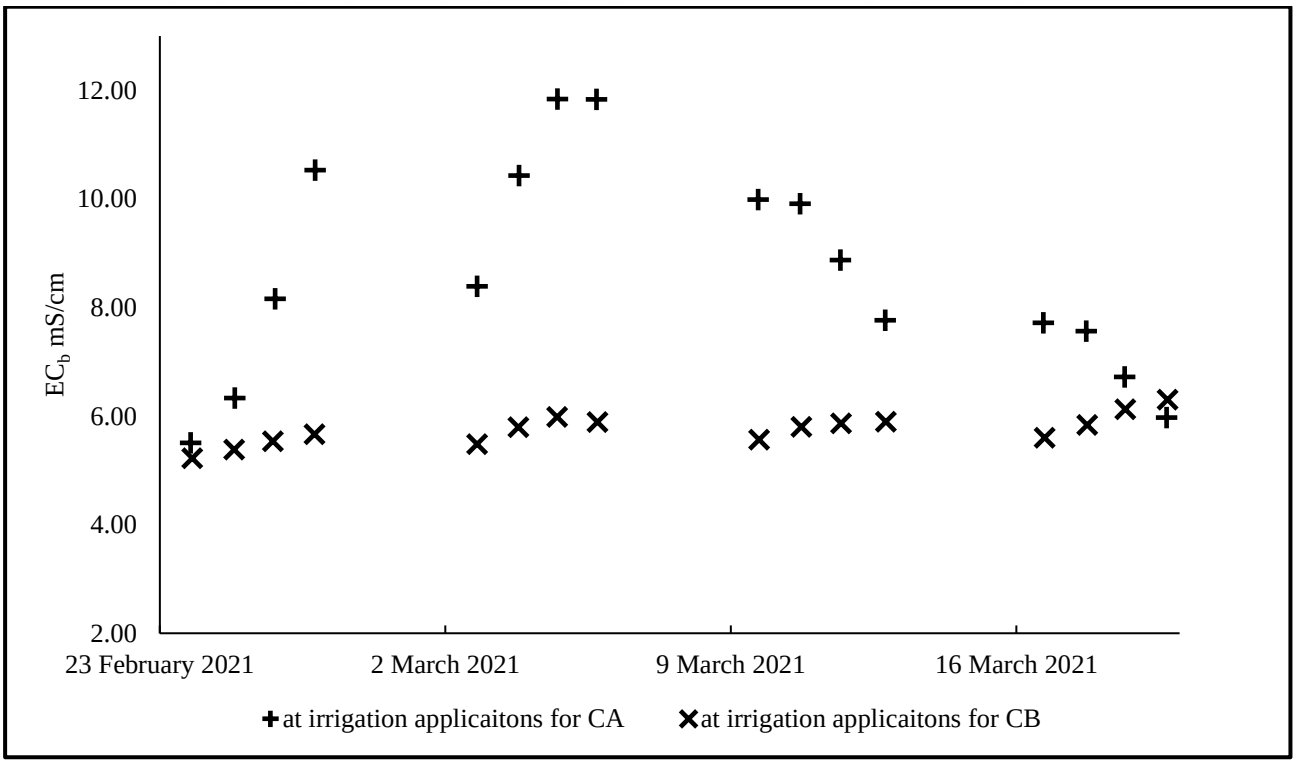

Figure 5.21. Surface bulk electrical conductivity at every irrigation instance measured by the Teros 12 sensor for columns CA and CB during experiment 5 (capillary rise with freshwater drip irrigation).

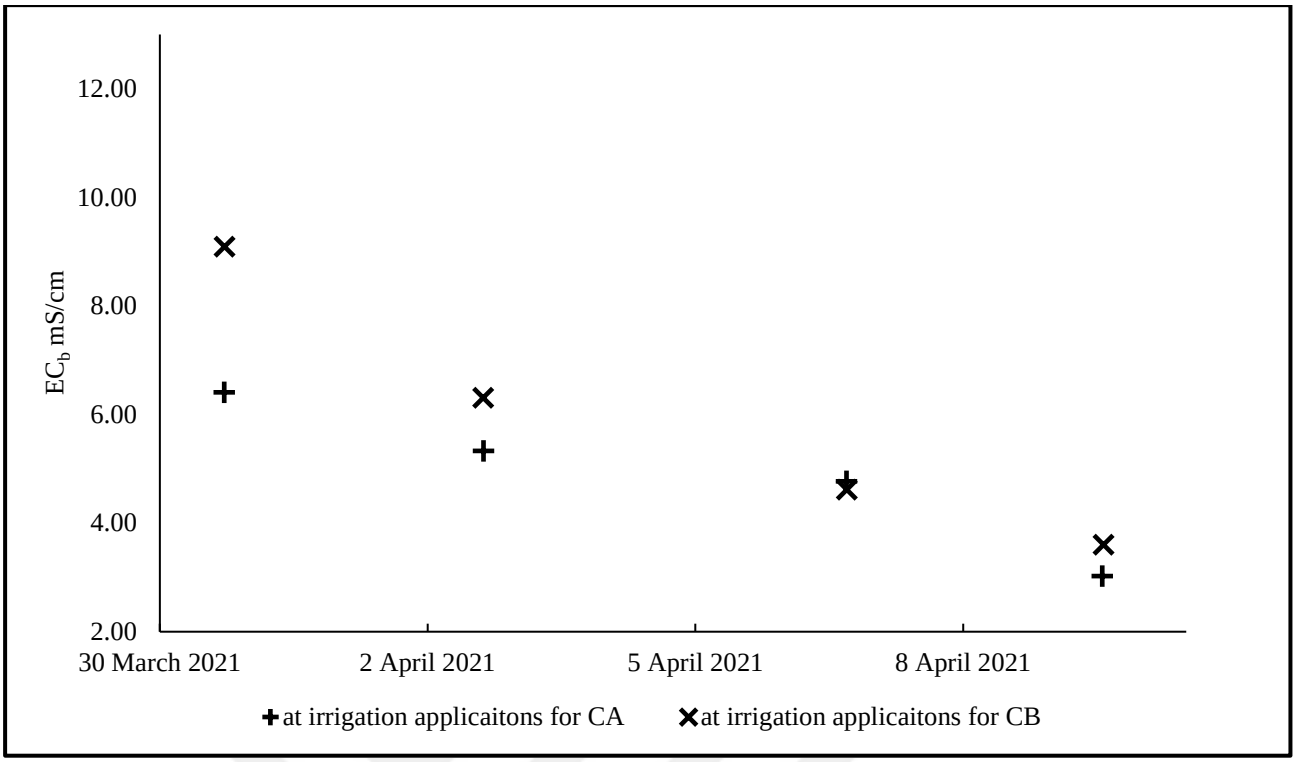

Figure 5.22. Surface bulk electrical conductivity at every irrigation instance measured by the Teros 12 sensor for columns CA and CB during experiment 6 (freshwater flood irrigation with free drainage).

5.4. Pressure/Tension Sensors

Soil pressure or water potential was measured at three depths of each column throughout the experiments. The pressure measurements could only be recorded when the soil moisture was above 0.25 m^3/m^3 as the T5 sensors could not function if air entered its shaft. Water potential values below -30 kPa were in the irreversible drying phase of the sensor shaft. There were missing data measurements which are due to the events when air entered the sensor shafts and a one-time fault of the datalogger recording on November 2020.

The middle and bottom sensor measurements were visualized separately due to the significant alternations in the surface sensor. Figure 5.23 and Figure 5.24 show the water potential levels for the middle and bottom sensors for columns CA and CB, respectively. The fluctuations represent the irrigation cycles. In all irrigation cycles, the water potential increased and got back to a steady level, this hold except for the final experiment in which the shallow groundwater table was missing. Therefore, the existence of a shallow water table assured a constant soil tension level through the profile. The changes in the tension for the middle and bottom measurement points were more

significant during irrigation from column CB than that of column CA. This can be due to the higher soil compaction (dry bulk density) of column CB in comparison to CA. In addition, the middle sensor (at the depth of 24 cm) showed higher water potential for column CB than that of CA. This suggested that CB had a greater moisture level at the depth just below the compaction layer as also suggested by the results presented in Section 5.2.

The surface water potential measurements during the first two experiments are not shown due to the low moisture content. In this regard, Figure 5.25 shows the surface water potential from experiment 3 to 6. The oscillations indicate either an irrigation application or drying out the sensor shaft. The higher level of water potential in column CB shows that the compaction layers impact in keeping the surface moisture hold longer than for CA, the column without compaction. This is a validation of the findings shown in Section 5.2.

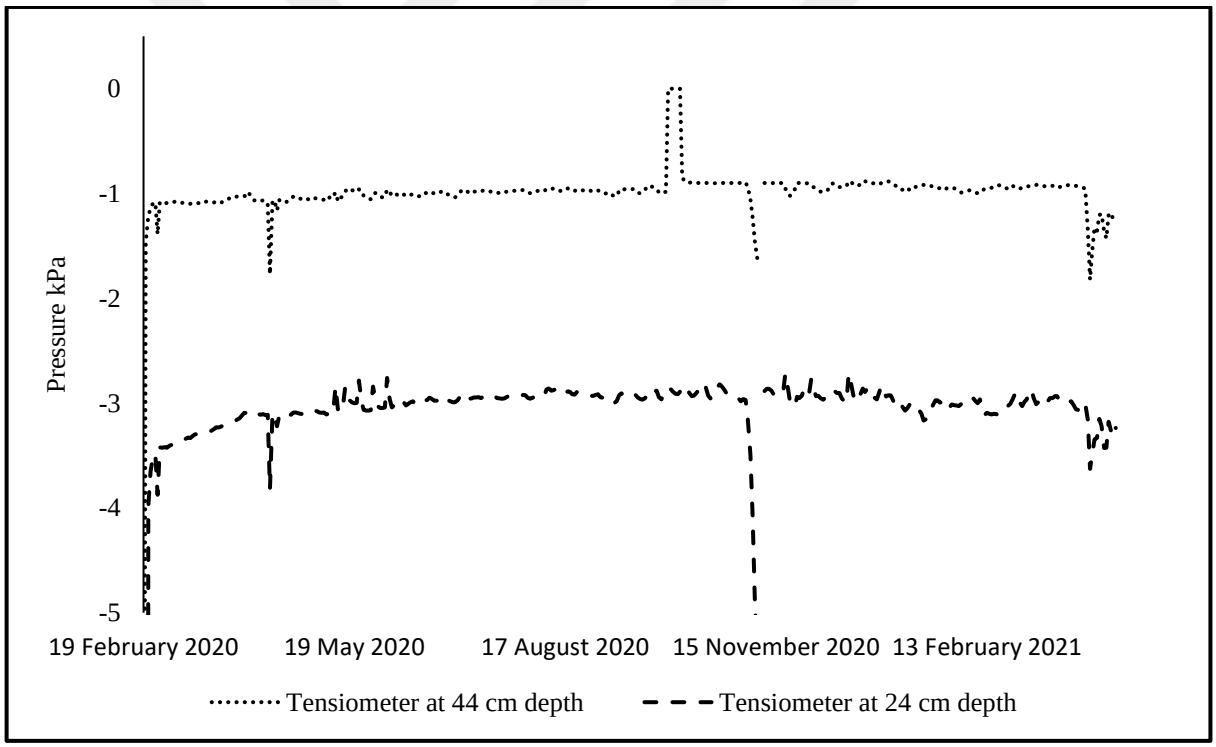

Figure 5.23. Soil tension measurements from middle and bottom sensors in column CA during experiment 1 to 6.

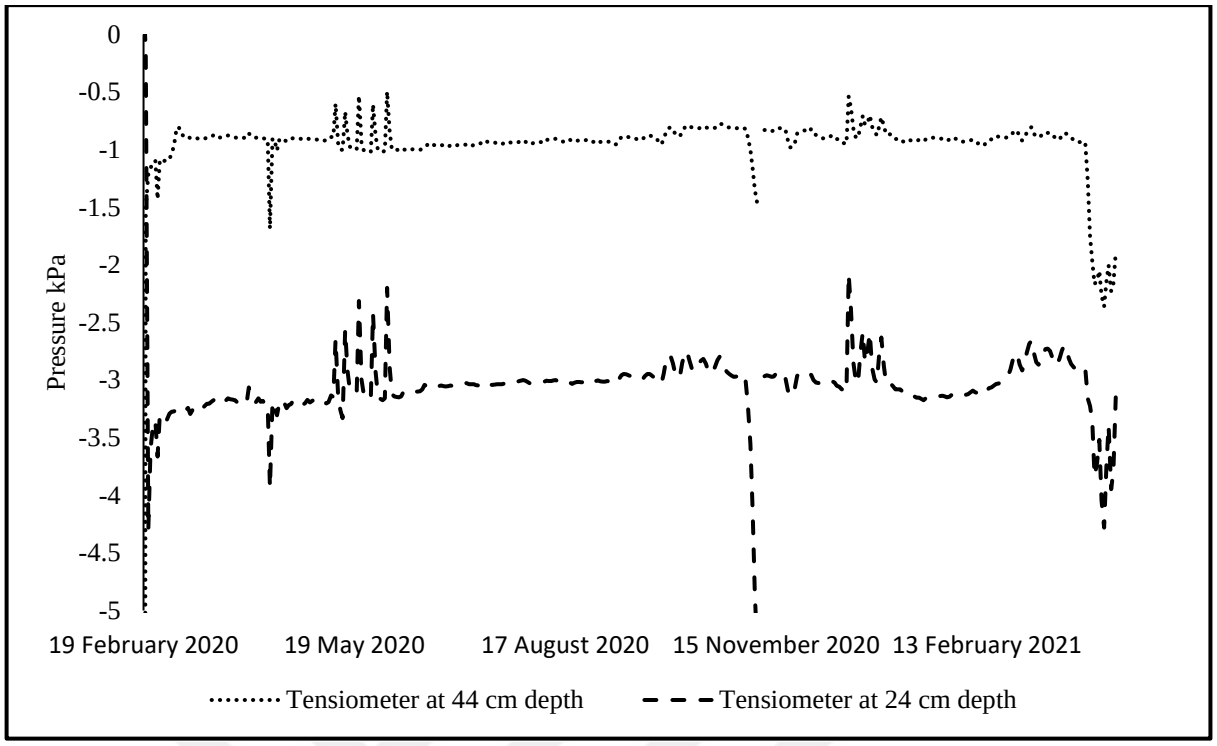

Figure 5.24. Soil tension measurements from middle and bottom sensors in column CB during experiment 1 to 6.

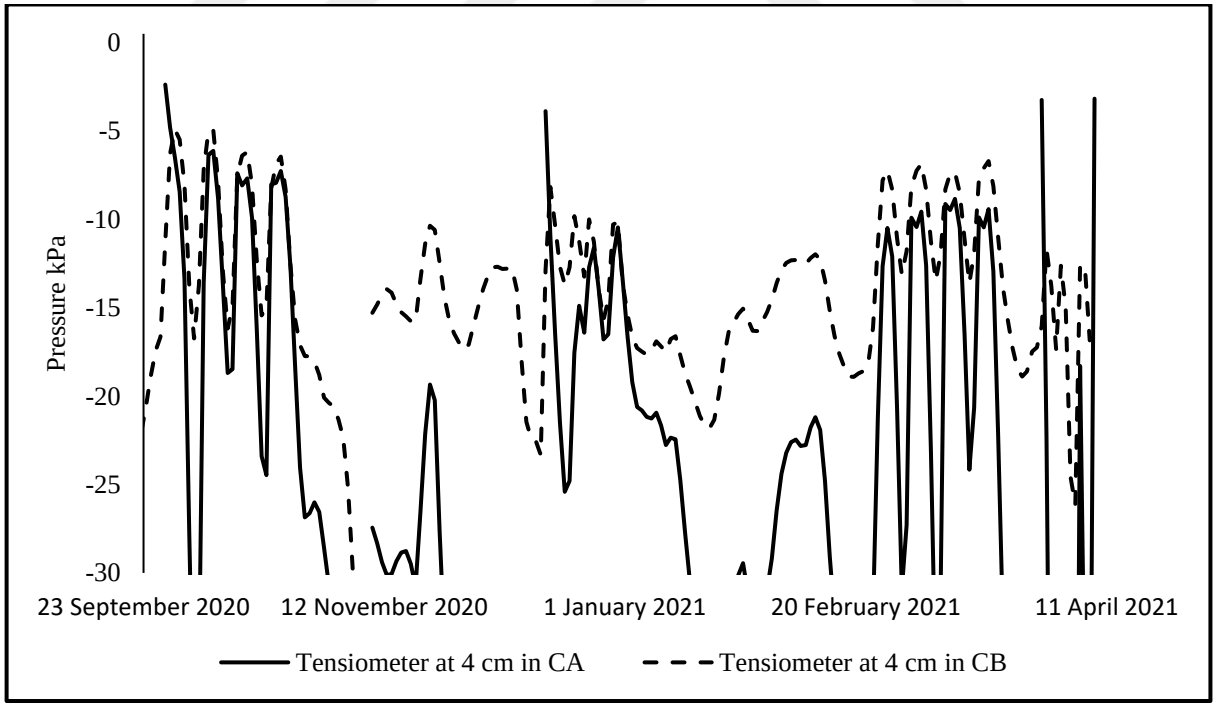

Figure 5.25. Soil tension comparison between surface sensors in column CA and CB during experiment 3 to 6.

5.5. Soil Moisture Analysis

Soil water samples were collected from 5 depths of the columns before every irrigation cycle throughout every experiment. These samples were later analysed using atomic absorption spectroscopy (AAS) to measure the concentration of the four cations: Na^{+}, Ca^{2+}, $Mg^{2+}$and K^{+}. The AAS measurements were performed in duplicates from each sample and the uncertainties were calculated accordingly. Nonetheless, only the mean concentrations were recorded for experiments 1 and 2 whereas, starting from the third experiment both duplicate measurements were recorded allowing for standard error calculation. In some instances, soil water could not be collected from the most top collection point due to the low surface moisture before the first irrigation cycles of each experiment. Furthermore, the measured concentration of the major cations was used to measure the SAR level by utilizing Eq.2.2. Table 5.3 to Table 5.6 present all the cation concentrations from the soil water analysis from samples collected from the suction cups at different depths of Experiments 1 to 6. In addition, Table 5.7 shows the SAR values calculated from the cation concentrations at each measurement.

To better view the impact of experiment runs on the salinity of the soil water across both CA (non-compacted) and CB (compacted) columns, the data from Table 5.4 to Table 5.7 were plotted in a series of charts (Figure 5.26 to Figure 5.30). These charts are dedicated to comparing the salinity across CA and CB relative to the cation concentration of the shallow water table (saline bottom tank).

An overall analysis of the results shown in Figure 5.26 to Figure 5.30 indicates that all the ions have relatively similar behaviour of change in different experimented scenarios. However, the comparison between the cation concentrations and the bottom tank concentrations proves to be different for different cations. For instance, magnesium levels in the soil water tend to be below the bottom tank for most cases, on the opposite hand, calcium and potassium levels exceeded the shallow saline water's initial concentration. The reason for this is the initial soluble concentration of sodium and potassium of the soil sample as presented earlier in Table 5.1. Sodium levels, however, tend to increase at the surface layer (0-16 cm) especially after the freshwater applications (from experiments 4 to 6).

Table 5.3. Magnesium concentrations measured by AAS after each experiment at various depths. The standard deviations from the two replicates are shown in brackets when available.

Mg^{2+} (mEq/L)		After experiment 1		After experiment 2		After experiment 3		After experiment 4		After experiment 5		After experiment 6	
Water tank	Depth (cm)	CA	CB	CA	CB	CA	CB	CA	CB	CA	CB	CA	CB
16.54	6	-	25.60	9.46	8.19	37.45 *(0.29)*	34.77 *(0.58)*	46.91 *(0.47)*	6.25 *(0.05)*	16.13 *(0.12)*	12.51 *(0.23)*	6.3 *(0.12)*	2.55 *(0.06)*
	16	4.86	5.43	7.94	8.89	15.55 *(0.35)*	21.15 *(0.06)*	16.83 *(0)*	12.55 *(0.12)*	10.95 *(0.12)*	11.07 *(0.17)*	13.21 *(0.06)*	2.3 *(0)*
	26	5.18	5.39	7.57	7.94	4.57 *(0.06)*	7.08 *(0.12)*	8.72 *(0.06)*	23.41 *(0.06)*	7.45 *(0.06)*	9.3 *(0.12)*	16.62 *(0.12)*	8.93 *(0)*
	36	5.06	5.10	6.91	6.54	4.28 *(0.12)*	5.88 *(0.06)*	7.61 *(0.17)*	13.17 *(0.12)*	7.16 *(0.12)*	7.32 *(0)*	12.06 *(0.06)*	14.61 *(0)*
	46	4.44	5.72	5.39	5.80	6.05 *(0.06)*	6.54 *(0.12)*	6.95 *(0.12)*	6.95 *(0)*	9.59 *(0.23)*	8.35 *(0.06)*	14.2 *(0.06)*	14.53 *(0.06)*

Table 5.4. Calcium concentrations measured by AAS after each experiment at various depths. The standard deviations from the two replicates are shown in brackets when available.

Ca^{2+} (mEq/L)		After experiment 1		After experiment 2		After experiment 3		After experiment 4		After experiment 5		After experiment 6	
Water tank	Depth (cm)	CA	CB	CA	CB	CA	CB	CA	CB	CA	CB	CA	CB
9.28	6	-	147.11	38.30	39.97	124.63 *(6)*	86.33 *(1.76)*	109.03 *(0.99)*	10.58 *(0.23)*	45.46 *(0.14)*	32.43 *(0.28)*	14.7 *(0.56)*	7.41 *(0.18)*
	16	26.10	29.74	37.25	42.66	73.48 *(2.33)*	100.72 *(0.39)*	86.1 *(2.33)*	60.73 *(1.13)*	54.17 *(0)*	49.2 *(0.92)*	59.93 *(0.21)*	10.58 *(0.14)*
	26	28.82	30.61	37.00	35.95	24.58 *(1.06)*	31.59 *(0.25)*	48.73 *(1.02)*	102.59 *(2.68)*	40.32 *(0.39)*	37.65 *(0.18)*	88.02 *(0.49)*	43.09 *(0.67)*
	36	27.25	29.24	31.89	27.17	22.16 *(1.52)*	26.05 *(0.67)*	39.47 *(1.27)*	53.42 *(0.92)*	36.23 *(0.81)*	26.7 *(0.49)*	61.55 *(0.88)*	61.5 *(0.25)*
	46	21.81	29.04	23.60	17.71	20.38 *(1.16)*	21.38 *(0.99)*	22.58 *(0.49)*	19.51 *(0.92)*	24.2 *(0.07)*	17.32 *(0.21)*	42.76 *(0.42)*	39.85 *(0.49)*

Table 5.5. Sodium concentrations measured by AAS after each experiment at various depths. The standard deviations from the two replicates are shown in brackets when available.

Na^+ (mEq/L)		After experiment 1		After experiment 2		After experiment 3		After experiment 4		After experiment 5		After experiment 6	
Water tank	Depth (cm)	CA	CB	CA	CB	CA	CB	CA	CB	CA	CB	CA	CB
13.05	6	-	7.54	12.39	6.76	55.04 *(1.6)*	11.15 *(0.68)*	71.04 *(1.29)*	20.83 *(1.91)*	26.26 *(1.29)*	26.26 *(0.37)*	13.48 *(0.03)*	3.37 *(0.06)*
	16	1.30	1.37	2.83	2.63	13.74 *(0.31)*	20.7 *(0.15)*	29.28 *(0.34)*	41 *(0.65)*	23.56 *(0.41)*	25.46 *(0.07)*	36.13 *(0.09)*	13.11 *(0.46)*
	26	1.95	1.77	2.42	2.19	8.7 *(0.46)*	10.5 *(0.46)*	16.87 *(0.52)*	31 *(0.46)*	20.4 *(0.55)*	18.26 *(0.74)*	35.11 *(0.31)*	22.5 *(0.03)*
	36	4.91	1.30	4.26	5.39	10.63 *(0.61)*	11.2 *(0)*	17.09 *(0.25)*	18.96 *(0.15)*	18.78 *(0.41)*	15 *(0.52)*	27.02 *(0.77)*	22.24 *(0.25)*
	46	9.33	1.97	8.65	9.70	11.7 *(0.52)*	0 *(0)*	14.54 *(0.71)*	14.17 *(0.95)*	16.7 *(0.81)*	15.57 *(0.26)*	22.17 *(0.25)*	20.48 *(0.15)*

Table 5.6. Potassium concentrations measured by AAS after each experiment at various depths. The standard deviations from the two replicates are shown in brackets when available.

K^+ (mEq/L)		After experiment 1		After experiment 2		After experiment 3		After experiment 4		After experiment 5		After experiment 6	
Water tank	Depth (cm)	CA	CB	CA	CB	CA	CB	CA	CB	CA	CB	CA	CB
0.00	6	-	2.67	1.51	1.49	2.89 *(0.04)*	2.52 *(0)*	2.68 *(0.08)*	0.94 *(0.01)*	1.56 *(0.02)*	1.42 *(0.03)*	1.05 *(0.03)*	0.63 *(0.01)*
	16	0.95	1.05	1.19	1.40	1.22 *(0.02)*	1.52 *(0.01)*	1.44 *(0)*	1.45 *(0.02)*	1.01 *(0)*	1.26 *(0.02)*	1.15 *(0)*	0.54 *(0.01)*
	26	0.36	0.30	0.41	0.42	0.35 *(0.01)*	0.37 *(0)*	0.57 *(0.02)*	0.82 *(0.01)*	0.45 *(0.01)*	0.53 *(0.01)*	0.73 *(0.03)*	0.5 *(0.01)*
	36	0.32	1.07	0.38	0.38	0.31 *(0)*	0.28 *(0)*	0.44 *(0.04)*	0.55 *(0.01)*	0.44 *(0)*	0.35 *(0.02)*	0.53 *(0)*	0.45 *(0)*
	46	0.44	0.33	0.33	0.25	0.27 *(0)*	0 *(0.37)*	0.27 *(0.03)*	0.3 *(0)*	0.34 *(0.02)*	0.25 *(0)*	0.4 *(0.01)*	0.3 *(0)*

Table 5.7. SAR values after each experiment at various depths. The standard deviations from the two replicas are shown in brackets when available.

SAR		After experiment 1		After experiment 2		After experiment 3		After experiment 4		After experiment 5		After experiment 6	
Water tank	Depth (cm)	CA	CB	CA	CB	CA	CB	CA	CB	CA	CB	CA	CB
6.42	6	-	1.43	4.48	2.44	10.81 *(0.52)*	2.53 *(0.18)*	14.22 *(0.32)*	12.69 *(1.26)*	8.37 *(0.43)*	9.79 *(0.19)*	7.35 *(0.14)*	2.67 *(0.08)*
	16	0.58	0.58	1.05	0.92	3.64 *(0.14)*	4.69 *(0.04)*	7.22 *(0.16)*	11.97 *(0.29)*	7.3 *(0.13)*	8.2 *(0.1)*	10.56 *(0.05)*	9.13 *(0.37)*
	26	0.84	0.74	0.91	0.83	4.03 *(0.29)*	4.22 *(0.21)*	5.56 *(0.22)*	6.9 *(0.18)*	7.38 *(0.23)*	6.66 *(0.29)*	8.58 *(0.1)*	7.8 *(0.06)*
	36	2.16	0.56	1.71	2.32	5.17 *(0.46)*	4.95 *(0.06)*	6.23 *(0.19)*	5.81 *(0.09)*	7.13 *(0.23)*	6.43 *(0.27)*	7.87 *(0.27)*	6.37 *(0.08)*
	46	4.55	0.84	4.02	5.00	5.69 *(0.39)*	0 *(0)*	6.69 *(0.39)*	6.89 *(0.58)*	7.18 *(0.38)*	7.68 *(0.17)*	7.35 *(0.11)*	6.94 *(0.09)*

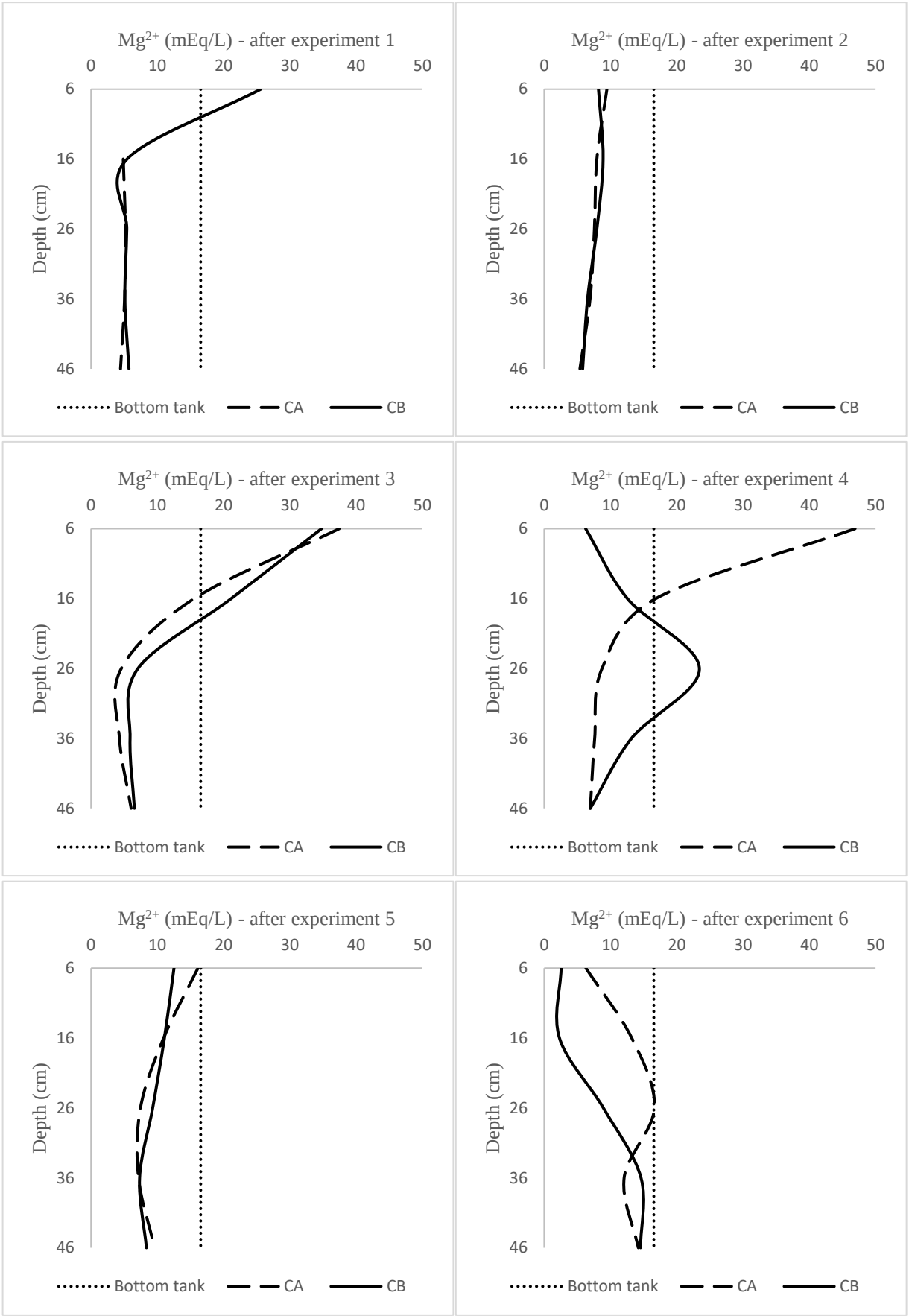

Figure 5.26. Comparison between CA, CB and bottom tank magnesium concentrations after each experiment at various depths.

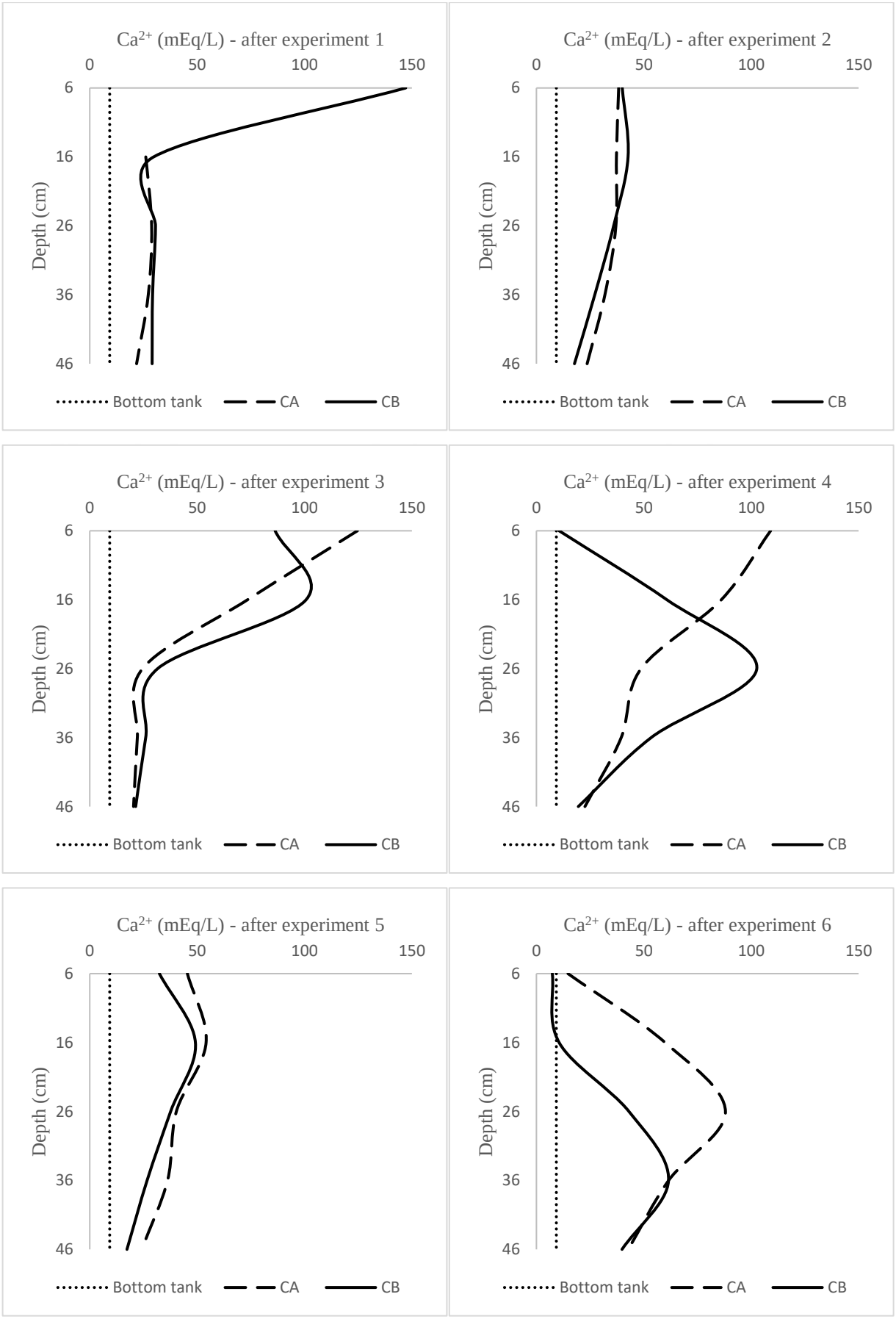

Figure 5.27. Comparison between CA, CB and bottom tank calcium concentrations after each experiment at various depths.

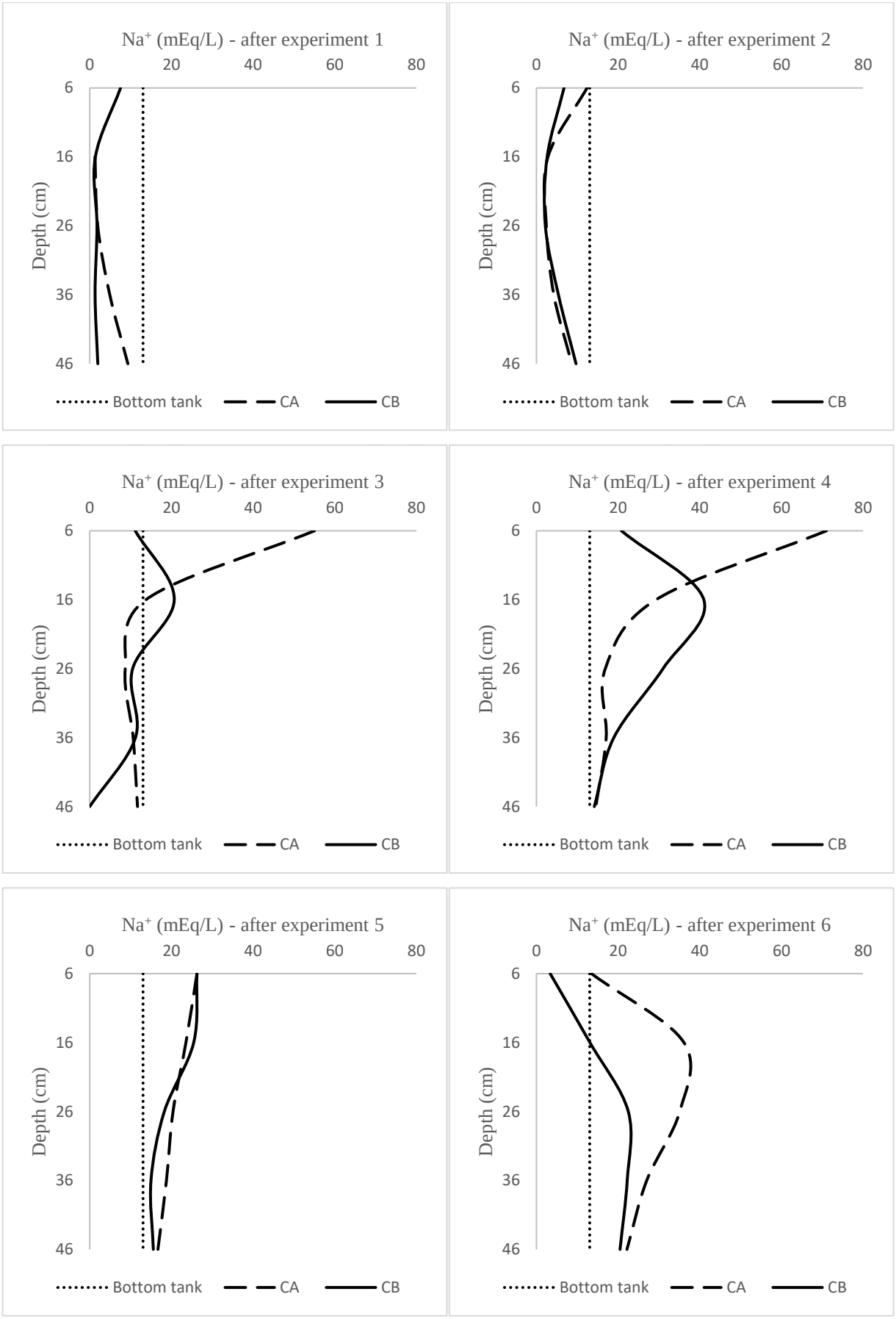

Figure 5.28. Comparison between CA, CB and bottom tank sodium concentrations after each experiment at various depths.

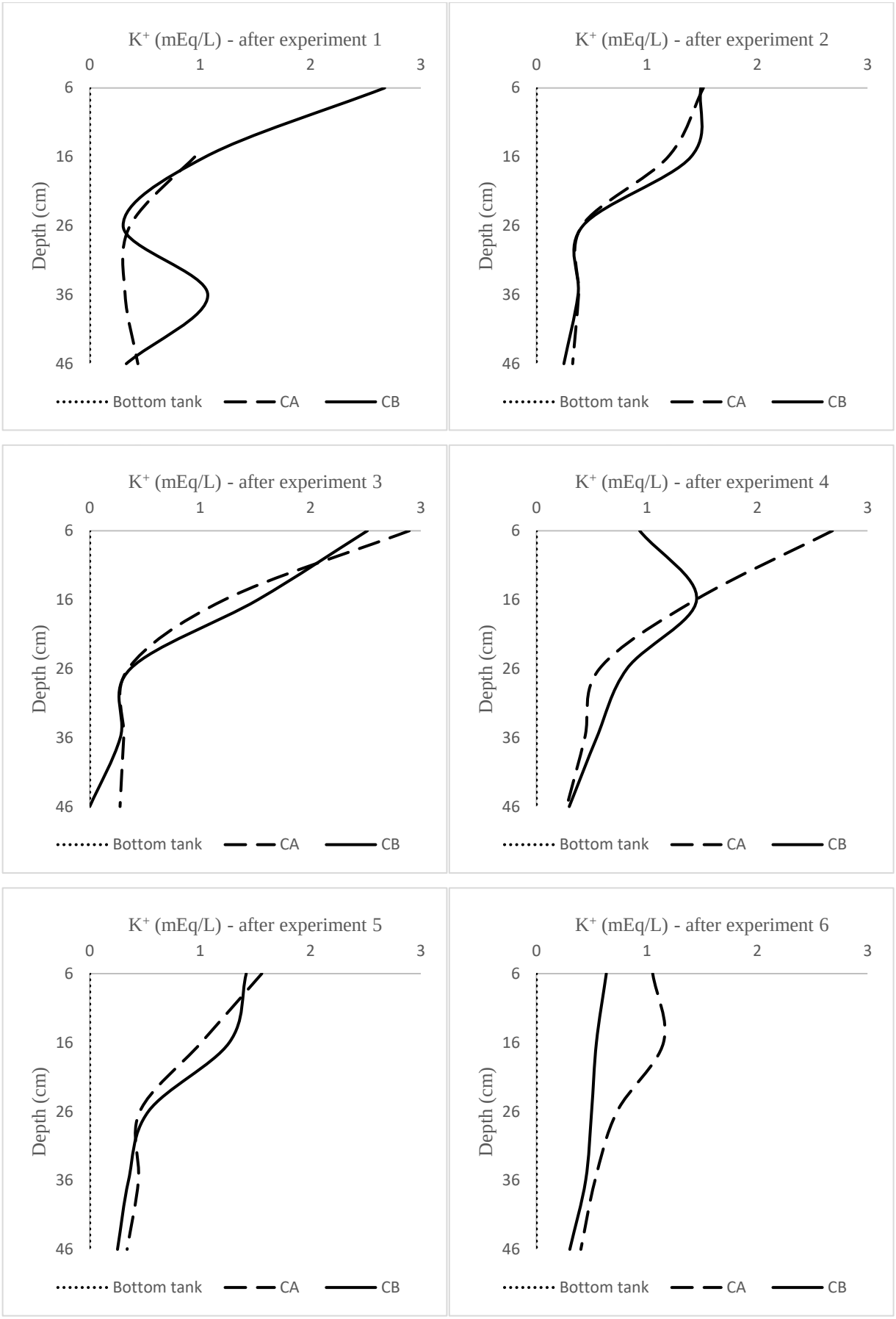

Figure 5.29. Comparison between CA, CB and saline bottom tank potassium concentrations measured by AAS after each experiment at various depths.

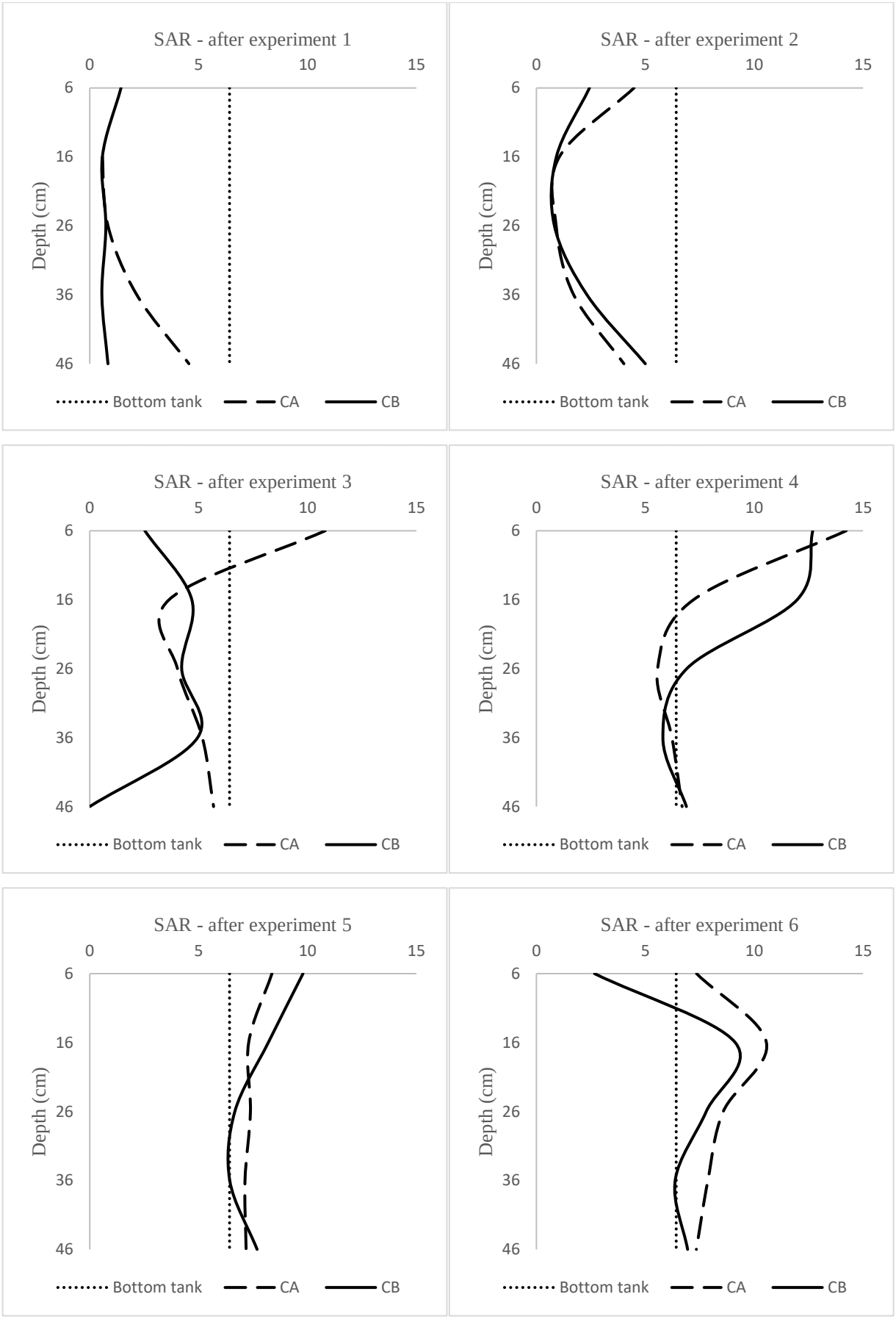

Figure 5.30. Comparison between CA, CB and bottom tank SAR values after each experiment at various depths.

Examination of the results presented in Figure 5.26 to Figure 5.30 suggests that after experiment 1 (surface irrigation and capillary action, no surface water application) both columns lead to an increase in the cation concentrations beyond the ion concentration in the bottom tank. This is due to the continuous upward migration of the moisture along with evaporation from the column surfaces leading to ion accumulation in the column. This is true even for K^+ which is not present in the bottom tank water, demonstrating capillarity combined with surface irrigation can lead to upward migration of ions from the shallow water as well as a redistribution of ions within the soil column.

After the saline flood irrigation cycles (experiment 2) the surface levels of all cations did not significantly increase, with both compacted and non-compacted columns behaving relatively similar for all 4 measured cations. However, the saline dripping irrigation cycles (experiment 3) resulted in different surface cation concentrations between CA and CB. This difference was explicitly seen in calcium and sodium levels. Whereas, CA, the non-compacted column, showed the highest concentration at the uppermost point (6 cm) and the deepest points (36 and 4 cm), CB, the compacted column, had a higher accumulation of salts at 16 cm which is just above the compaction layer. This result demonstrates the compaction layers involvement in creating a barrier accumulating salts just above it. The fact that this could only be seen during drip irrigation suggests that the velocity and mode of the applied water can play a role in the significance of the washing of salts within the profile.

The freshwater irrigations with the presence of the bottom tank (experiments 4 and 5) indicated an inverse impact than the saline water irrigation cycles. In the freshwater cycles, the flood irrigation applications resulted in a higher surface (6 cm) salts concentration for CA but a higher deeper (16 cm) salts concentrations for CB. Nonetheless, the freshwater drip irrigations (experiment 5) suggest no difference across both columns. This again shows the accumulation of salts above the compacted layer, but this time after the flood irrigation and not the drip irrigation cycles.

Experiment six which was freshwater flood irrigation with the absence of the bottom tank (free-drainage bottom boundary) showed the wash down of the cations to the deeper levels for all cations across both column CA and CB.

It is also observed that all ion concentrations can exceed the bottom tank concentrations. The demonstrates the potential accumulation of ions in the soil column when saline conditions along with high surface evaporation are present, a problem encountered in Konya and many other semi-arid

regions of the world. The column results also indicate rapid changes in the soil moisture salinity after only a few water application cycles.

These results suggest that the decision on which type of irrigation can be more beneficial washing down the salts has complex relationships with the irrigation water quality, the soil density distribution throughout the profile (having agricultural compaction) and the soil drainage at the bottom boundary. More specifically for the type of soil and the column experiment setup, it was shown that the most effective method of washing down the salts is to apply freshwater flood irrigation with free drainage at the bottom. In addition, drip irrigation with saline water was more beneficial for the compacted column (CB) in terms of having less surface salinity effect, while flood irrigation with freshwater was a better treatment for CB than CA. Experiments 2 and 5 showed no significant difference across CA and CB.

The measurements given in Figure 5.19 and the guidelines in Table 2.1 indicate that the SAR values presented in Figure 5.30 do not contribute to major changes in the soil's physical structure and water infiltration. This is mainly due to the high (>2.9 mS/cm) values of EC_b in the soil surface as presented in Figure 5.19 These non-sodic effects can also be linked to the high levels of salinity due to the presence of the saline shallow groundwater table from experiments 1 to 5. Future investigations are yet needed to understand the sodicity effects on the soil columns. These experiments could consist of further wash down of the salts in the soil columns to decrease the electrical conductivity below a threshold at which sodicity effects take place (see Table 2.1). In addition, sodic water irrigation cycles can also be tested to further understand the impact of sodicity on soil profiles.

5.6. HYDRUS-1D Numerical Simulations

The HYDRUS-1D modelling package was utilized to simulate the column experiments of this project. The reserve modelling feature of HYDRUS-1D was used to calibrate the model and find the optimum soil parameters in accordance with the sensor measurements. The reverse modelling was used since finding the correct initial properties of the column experiments are not as straightforward due to the uncertainties with soil compaction and the soil hydraulic characteristics. The initial AAS measurements were used as an estimation input parameter for the model (see Section 5.1). Table 5.8 shows the key parameters used for the HYDRUS modelling. In addition, Table 5.9 indicates the soil Van Genuchten parameters that were used for calibration of the Hydrus reverse modelling feature.

This section further consists of results of model calibration from HYDRUS-1D reverse modelling and discussion on the solute transport simulations.

Table 5.8. List of key parameters used in the HYDRUS-1D simulations

Hydraulic Model	"Van Genuchten Mualem"	
Depth (cm)	55[a]	
Duration (days)	420[a]	
Water content upper boundary condition	"Atmospheric BC with surface layer"[a]	
Water content lower boundary condition	"Constant water content"[a*] "Free drainage"[a#]	
Potential surface evaporation (cm/day)	0.7[a]	
Solute transport time weighing scheme	"Crank-nicholson scheme"	
Solute transport space weighting scheme	"Galerkin finite elements"	
Solute transport upper boundary condition	"Concentration flux BC"[a]	
Solute transport lower boundary condition	"Concentration BC"[a*] "Zero concentration gradient"[a#]	
Molecular diffusion coefficient (cm^2/day)	5.5[b]	
Longitudinal dispersivity (cm)	5.5[b]	
Bulk density (g/cm^3)	1.15 (L1)[a]	1.15 (L2)[a]
CEC (mEq/Kg)	489.46 (L1)[c]	677.87 (L2)[c]
Gapon constant [Ca/Mg]	0.337744 (L1)[c]	0.322641 (L1)[c]
Gapon constant [Ca/Na]	0.100307 (L1)[c]	0.106528 (L1)[c]
Gapon constant [Ca/K]	6.65881 (L1)[c]	4.90888 (L1)[c]
Adsorbed Ca^{2+} (mEq/Kg)	158.5 (L1)[c]	169.34 (L2)[c]
Adsorbed Mg^{2+} (mEq/Kg)	25.1 (L1)[c]	22.63 (L2)[c]
Adsorbed Na^{+} (mEq/Kg)	299.48 (L1)[c]	479.48 (L2)[c]
Adsorbed K^{+} (mEq/Kg)	13.27 (L1)[c]	10.85 (L2)[c]
Precipitated Calcite (mEq/Kg)	0.0179 (L1)[c]	0.0142 (L2)[c]
Bottom tank Ca^{2+} (mEq/L)	9.28[d]	
Bottom tank Mg^{2+} (mEq/L)	16.54[d]	
Bottom tank Na^{+} (mEq/L)	13.05[d]	
Bottom tank K^{+} (mEq/L)	0.00[d]	
Bottom tank Alkalinity (mEq/L)	6.52[d]	
Bottom tank SO_4 (mEq/L)	16.52[d]	
Bottom tank Cl (mEq/L)	27.32[d]	

[a] column experiments setup and lab conditions.

[b] suggested by David et al. (2018).

[c] AAS measurements of initial soil samples based on Table 5.1, Table 5.2, Eq. 2.10 and Eq. 2.11.

[d] salt composition used for synthesizing the bottom tanks' saline water.

[*] lower boundary conditions only for experiments 1 to 5.

[#] lower boundary conditions only for experiment 6.

Table 5.9. Initial estimate of soil hydraulic parameters used for HYDRUS-1D reverse modelling

Layer- Column(s)	L1 – CA & CB	L2 – CA	L2 - CB
Calibration parameters			
Θ_r	0.0982[e]	0.0962[e]	0.0901[e]
Θ_s	0.543[f]	0.531[f]	0.498[f]
Alpha (1/cm)	0.0327[f]	0.0282[f]	0.0257[f]
N	1.658[f]	2.5[f]	2.596[f]
K_s(cm/day)	277.9[f]	83.1[f]	41.5[f]

[e] neural network prediction tool from HYDRUS-1D.

[f] Hyprop soil retention curve measurements.

5.6.1. Hydraulic Simulations

The HYDRUS-1D reverse modelling option was utilized with the maximum (500) fitting iterations. The calibrations could only run for the first five experiments due to the inconsistency in the bottom boundary condition in experiment 6.

Initially, the scenario for column CA was solved and calibrated by the model. The calibration analysis results, including the fitted parameters within 95% confidence limits are presented in Table 5.10. The simulation results are compared to the moisture sensor measurement at two depths in Figure 5.31 and Figure 5.32.

Subsequently, since the top Layer (L1) was packed in the same manner in both columns, the calibrated parameters for L1 in Table 5.10 was fixed and not further fitted in the calibration analysis for the column CB. Henceforth, only the soil hydraulic parameters of the bottom layer (L2) were used as calibration parameters for HYDRUS-1D reverse modelling. The results of the calibration analysis are listed in Table 5.11. Figure 5.33 and Figure 5.34 illustrate the comparison between the calibrated model and the sensor measurements of the column experiments for CB.

As the error analysis in Table 5.10 and Table 5.11 suggest, the column CA calibrated model resulted in simulations that are greatly closer to the sensor measurements than the CB. This is mainly because of the degree of freedom given to the CA model to fit the parameters of the layer L1 which was eliminated for the CB analysis. This is a bottleneck for this calibration analysis and since the soil hydraulic parameters are sensitive to various factors, measuring the correct parameters requires analysis that was outside the span of this study. Nonetheless, the overall fitted model is

representative of the experimental setup. This model is further utilized for solute transport that is discussed further in this chapter.

The key parameters (Table 5.8) and the calibrated soil parameters (Table 5.10 and Table 5.11) were used to simulate experiment 6 with the free drainage bottom boundary. The initial moisture conditions for this experiment were set as the final moisture content at each cm depth of the column from the simulations of experiment 1 to 5. Figure 5.35 to Figure 5.38 show the changes in the simulations for experiment 6. The decrease in the moisture indicates the impact of the free drainage bottom boundary on the instability of the moisture across the columns.

Table 5.10. Non-linear least-squares analysis for column CA by HYDRUS-1D model.

Layer	95% Confidence limits				
	Variable	Value	S.E.Coeff.	Lower	Upper
L1 0 – 18 cm	Θ_r	0.13651	0.15354	-0.17358	0.44661
	Θ_s	0.62174	0.057714	0.50518	0.7383
	Alpha (1/cm)	0.047585	0.03187	-0.01678	0.11195
	N	1.598	0.71353	0.15692	3.0391
	K_s(cm/day)	413.08	423.67	-442.59	1268.7
L2 18 – 55 cm	Θ_r	0.18	0.12158	-0.06554	0.42554
	Θ_s	0.56432	0.17829	0.20424	0.9244
	Alpha (1/cm)	0.03613	0.011521	0.012861	0.0594
	N	2.395	2.8687	-3.3989	8.1889
	K_s(cm/day)	14.397	12.245	-10.334	39.128
R^2 for regression of predicted vs observed = 0.74219					
Mean Weighted Error = 0.007170					
Mean Weighted Absolute Error = 0.06086					
Root Mean Square Weighted Error = 0.07450					

Table 5.11. Non-linear least-squares analysis for column CB by HYDRUS-1D model.

Layer	95% Confidence limits				
	Variable	Value	S.E.Coeff.	Lower	Upper
L2 18 – 55 cm	Θ_r	0.18	0.085809	0.007265	0.35273
	Θ_s	0.6	0.056369	0.48653	0.71347
	Alpha (1/cm)	0.031246	0.00057836	0.033846	0.036175
	N	2.493	0.56279	1.3601	3.6259
	K_s(cm/day)	13	0.54069	11.912	14.088
R^2 for regression of predicted vs observed = 0.49603					
Mean Weighted Error = 0.04568					
Mean Weighted Absolute Error = 0.08917					
Root Mean Square Weighted Error = 0.1130					

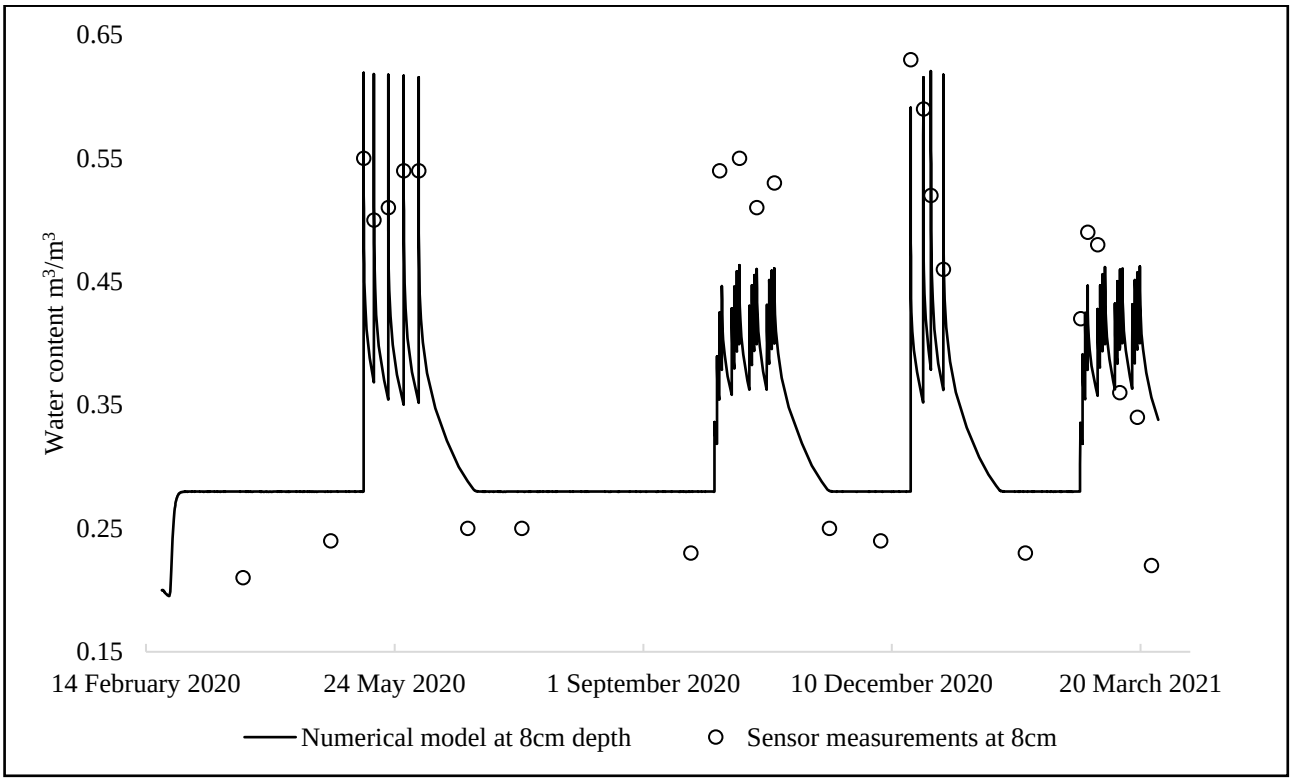

Figure 5.31. Calibrated HYDRUS-1D hydraulic model for column CA at depth of 8cm for experiments 1 to 5.

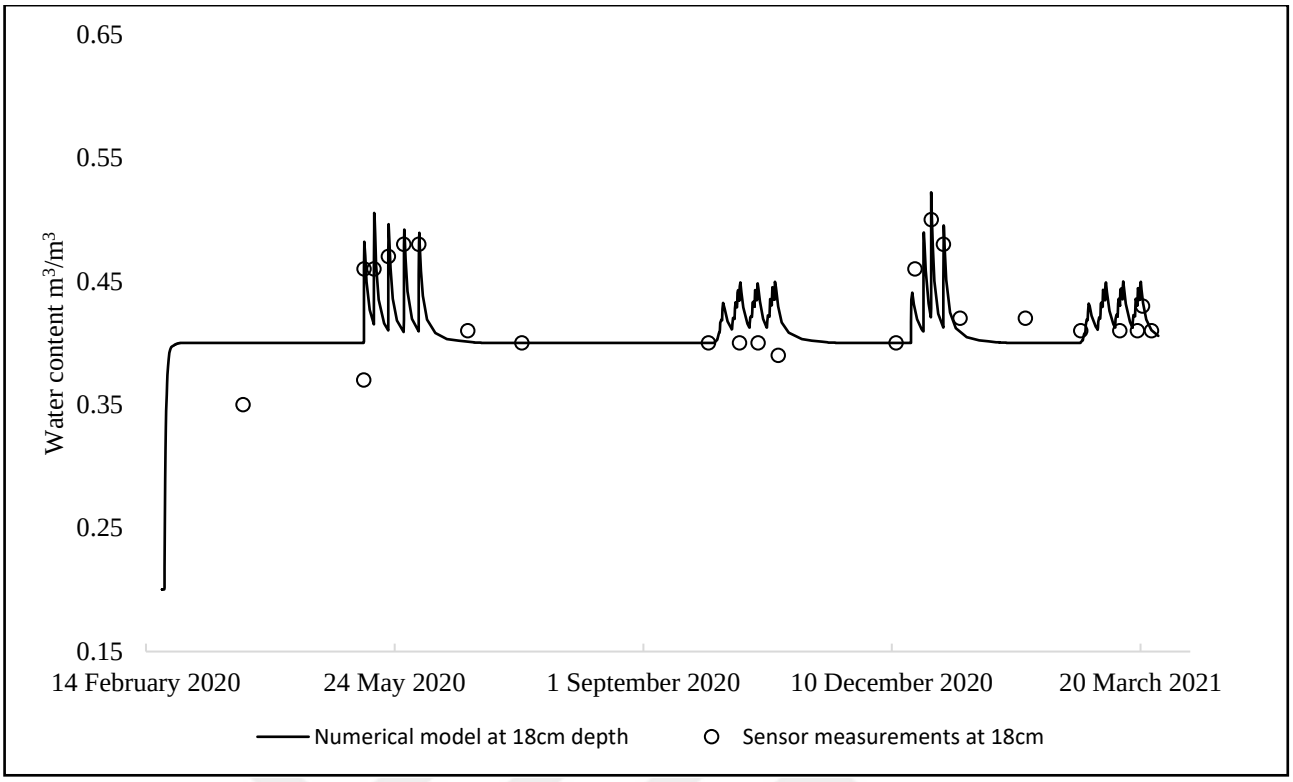

Figure 5.32. Calibrated HYDRUS-1D hydraulic model for column CA at depth of 18cm for experiments 1 to 5.

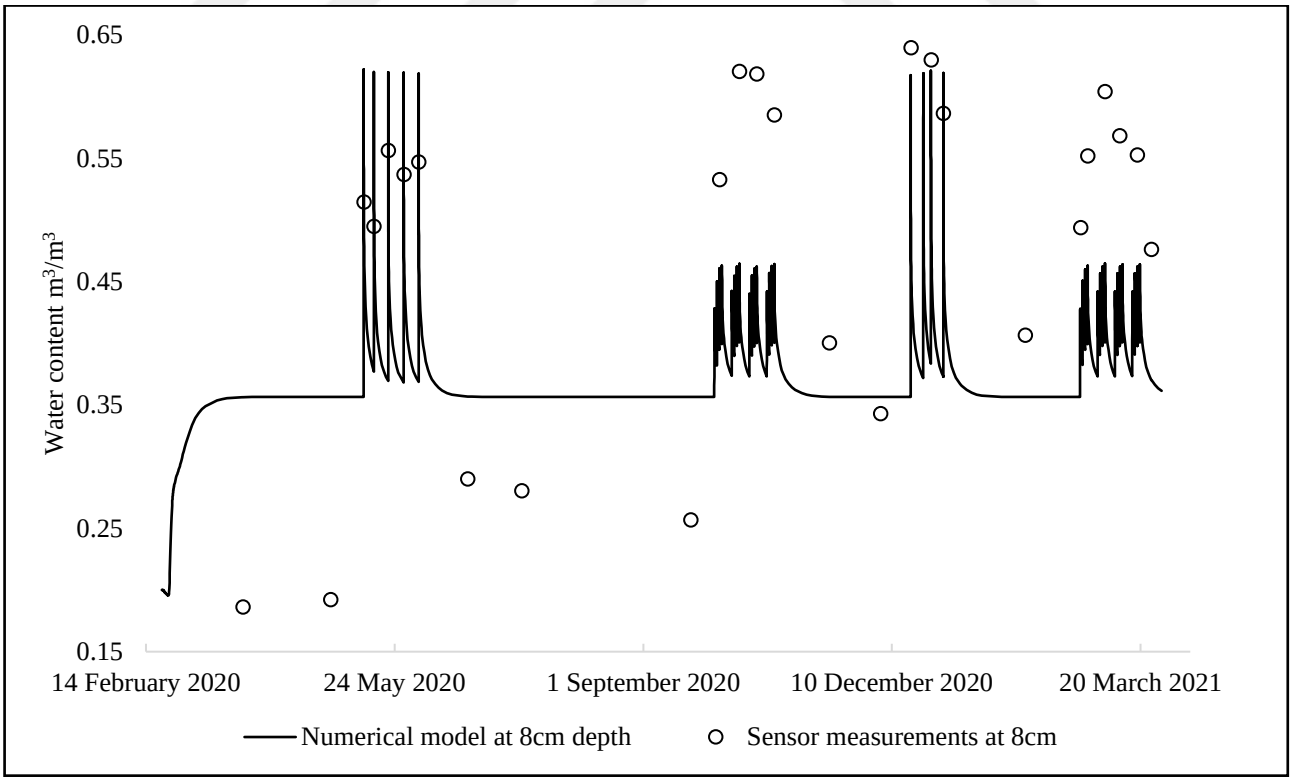

Figure 5.33. Calibrated HYDRUS-1D hydraulic model for column CB at depth of 8cm for experiments 1 to 5.

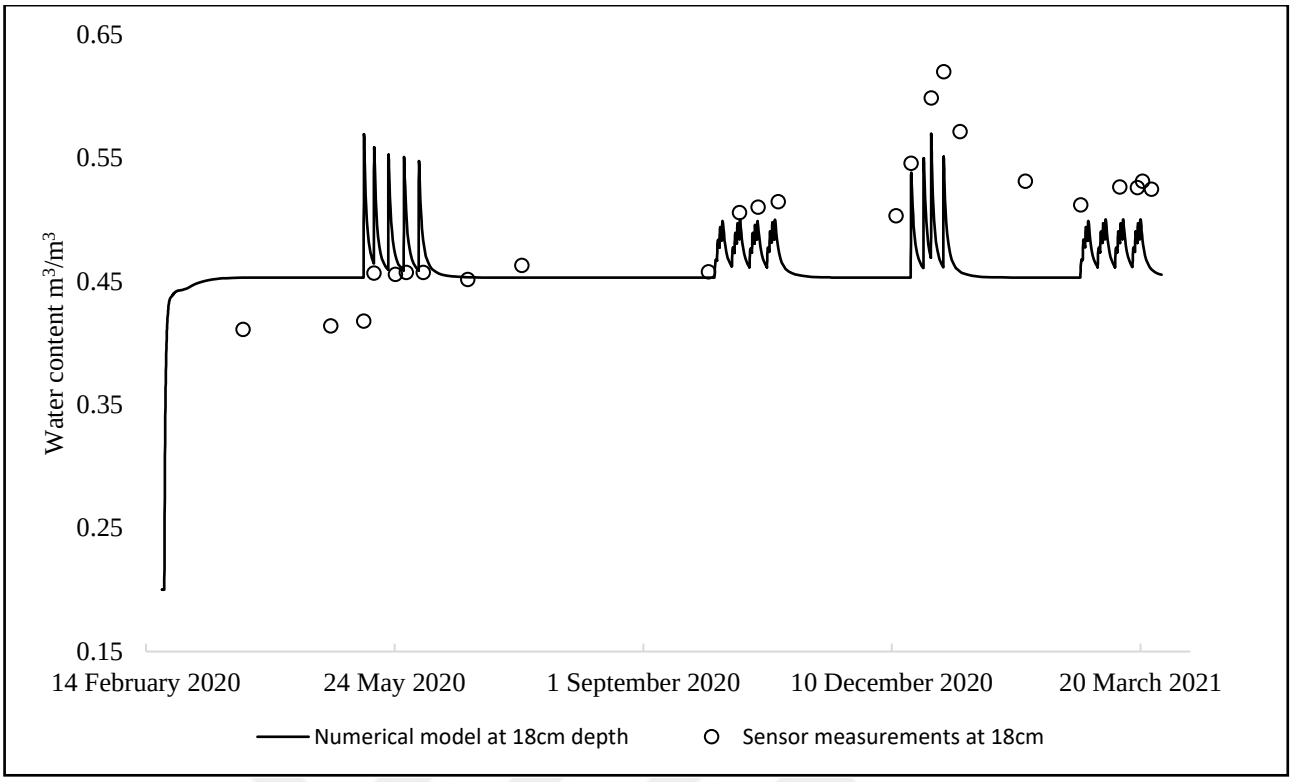

Figure 5.34. Calibrated HYDRUS-1D hydraulic model for column CB at depth of 18cm for experiments 1 to 5.

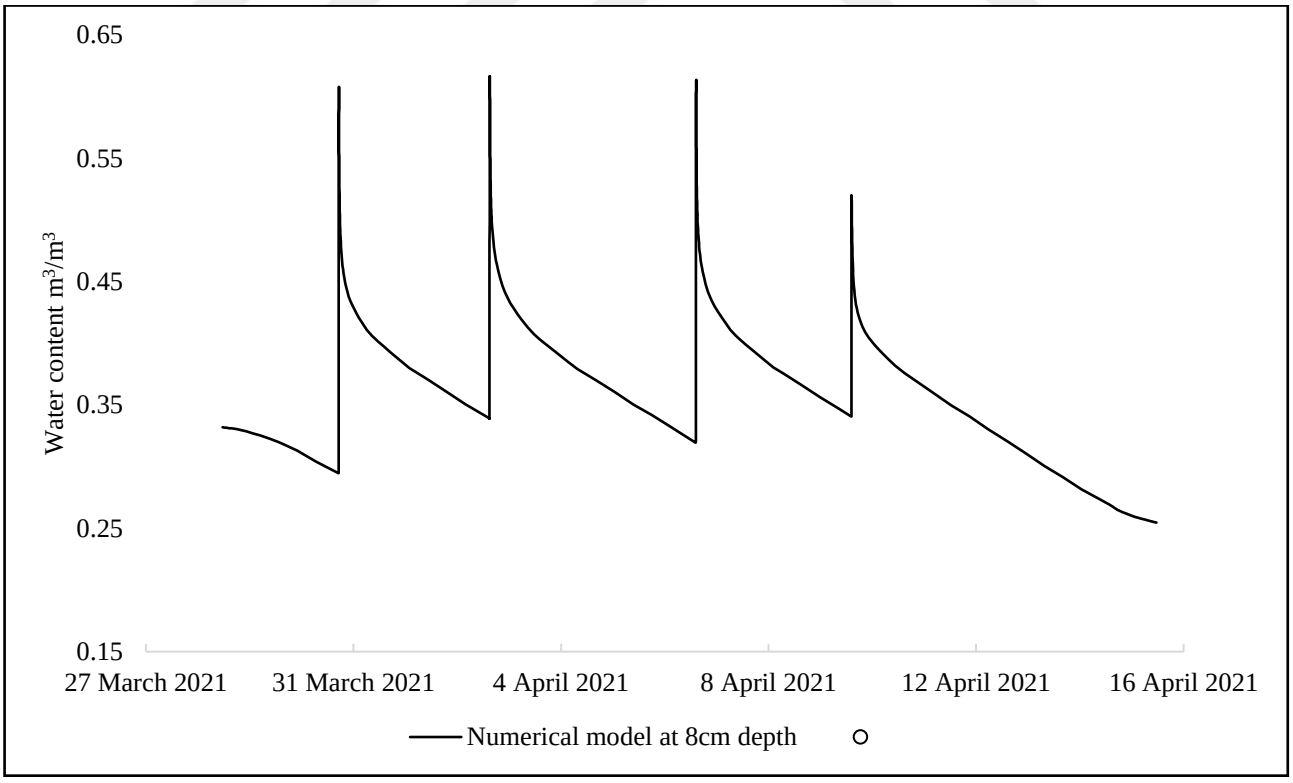

Figure 5.35. HYDRUS-1D hydraulic model simulation for column CA at depth of 8cm for experiment 6.

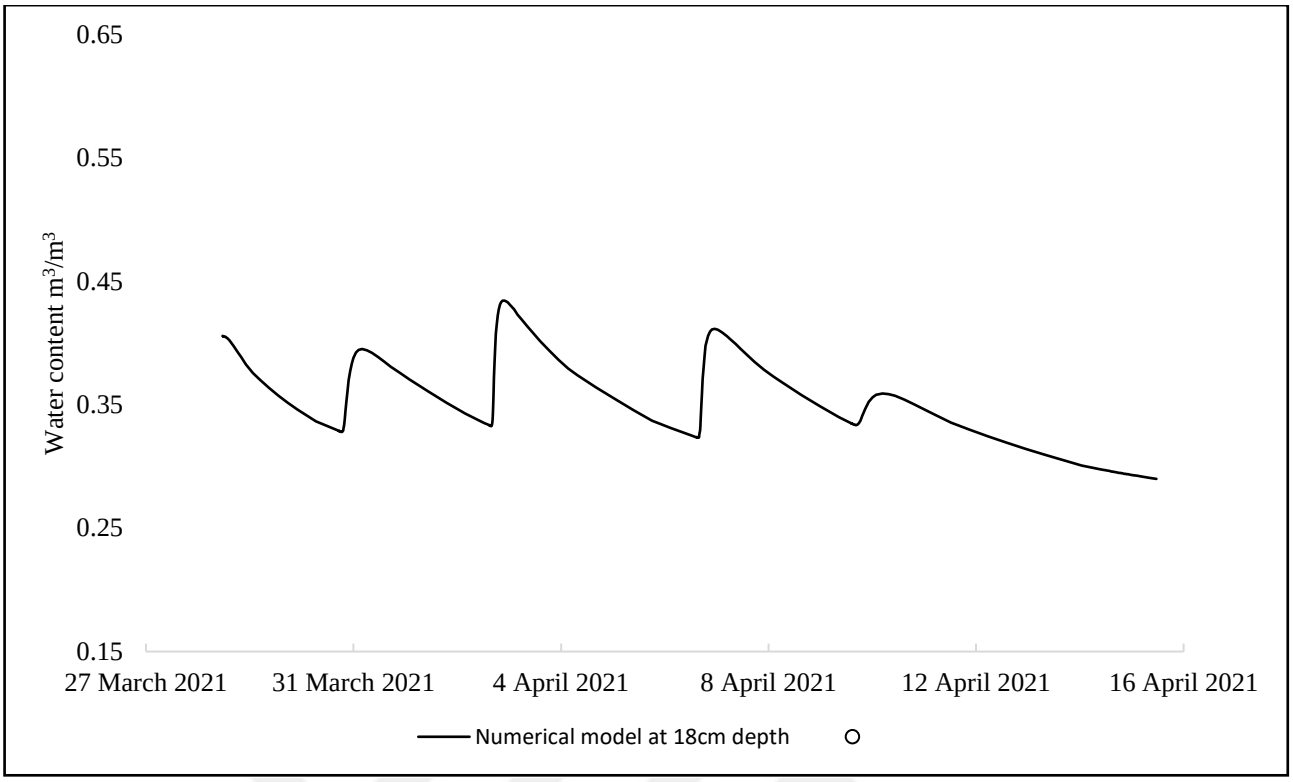

Figure 5.36. HYDRUS-1D hydraulic model simulation for column CA at depth of 18cm for experiment 6.

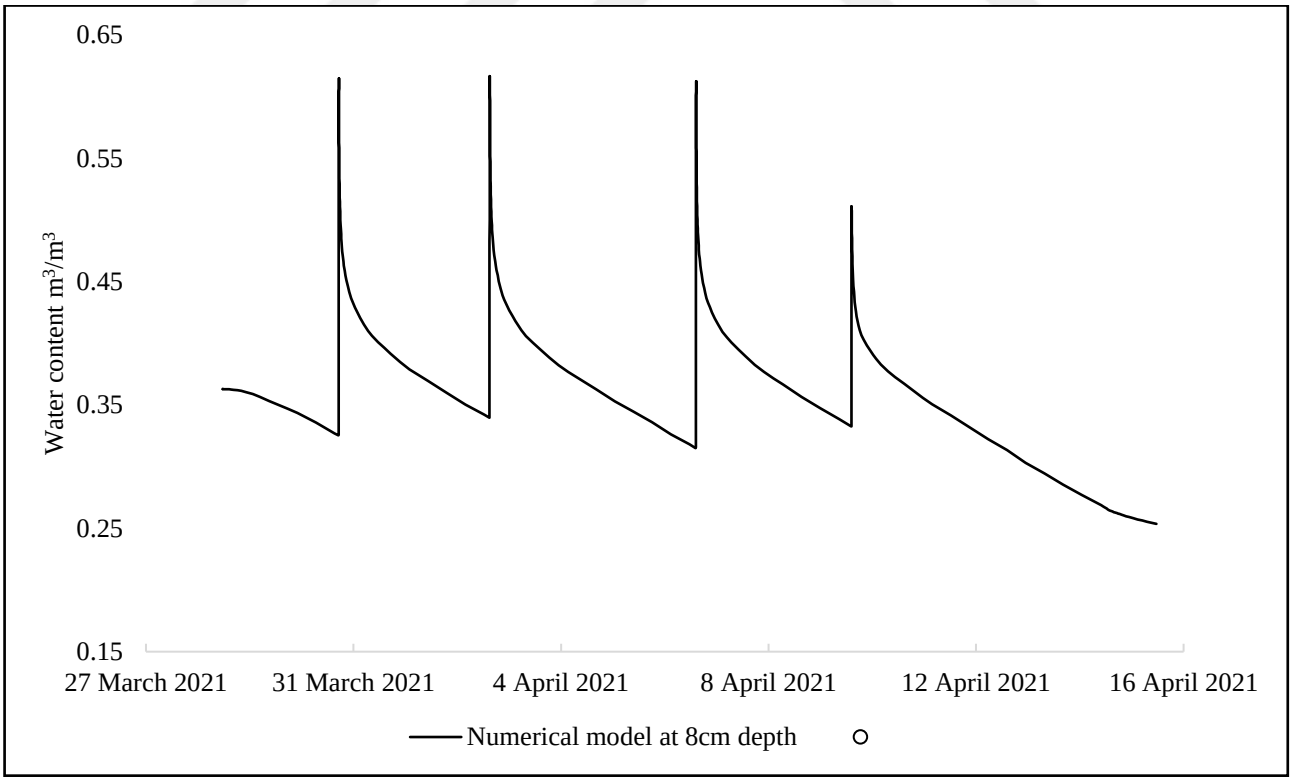

Figure 5.37. HYDRUS-1D hydraulic model simulation for column CB at depth of 8cm for experiment 6.

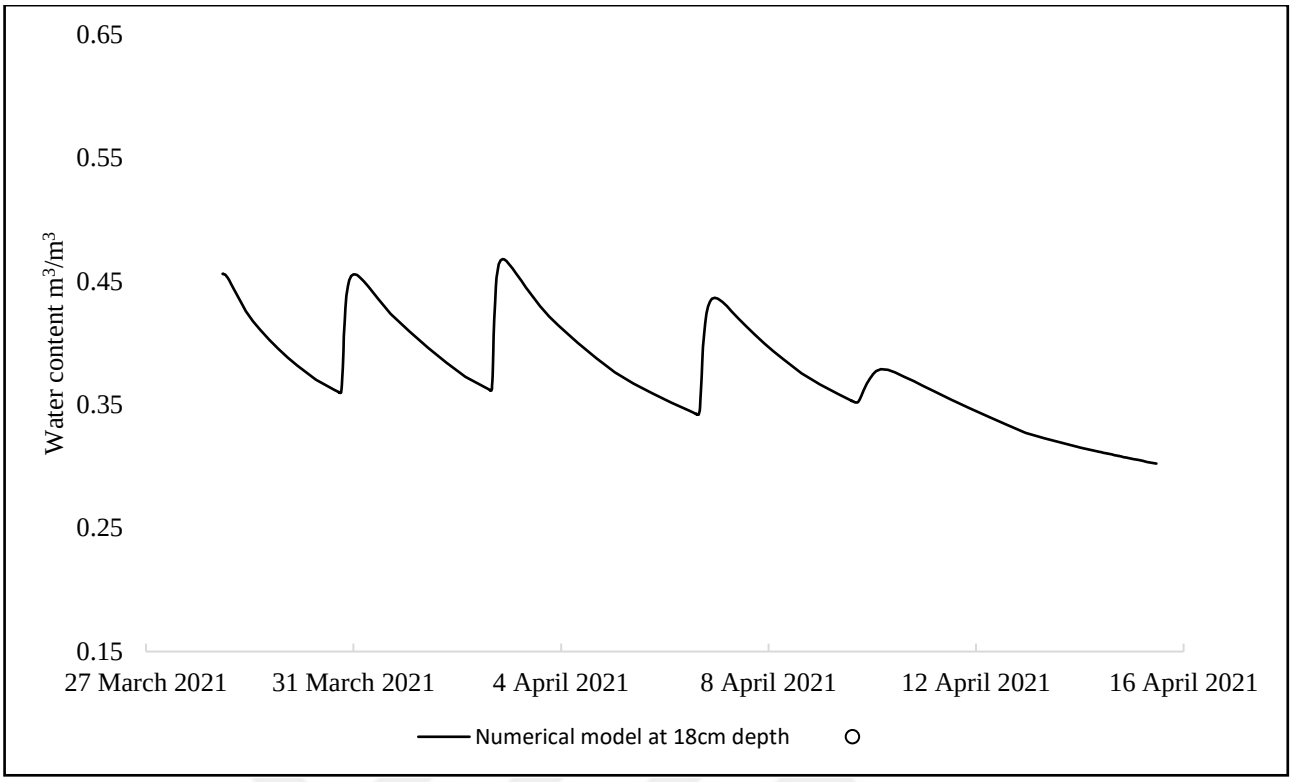

Figure 5.38. HYDRUS-1D hydraulic model simulation for column CB at depth of 18cm for experiment 6.

5.6.2. Solute Transport Simulations

The calibrated hydraulic parameters (Table 5.10 and Table 5.11) and the key parameters in Table 5.8 were utilized to run the HYDRUS-1D solute transport model. Due to the limitations to find the initial parameters for experiment 6 – which had a different bottom boundary condition than the first five experiments – the solute transport simulations were only performed for experiments 1 to 5.

Due to the lack of potassium ions (K^+) in the saline water used in the bottom tanks and for the irrigation cycles, the simulations resulted in zero potassium concentrations. Hence, the results in this section only focus on the three cat-ions, Mg^{2+}, Ca^{2+} and Na^+.

Figure 5.39 to Figure 5.41 compare the solute transport simulations and the measured cation concentration observed during the different column experiments. It is generally observed that the simulated values get closer to the measurements in the soil deeper levels. This is due to the diminished variation in water content of the bottom layers in comparison to the surface which underwent wider fluctuations due to the application of the irrigation cycles. Moreover, the modelling results exhibited less variation of cation concentrations with depth for both CA and CB columns compared to the observed data (discussed in Section 5.7.1). This is attributed mostly to the heterogeneity of physicochemical properties of soil column which was not fully accounted for in the model.

Nonetheless, the simulations do reveal some important features of the impact of irrigation on salt dynamics. Figure 5.42 to Figure 5.44 show the simulated cation concentrations plotted at the depth of 6 cm – which was the topsoil water collection point in the column experiments.

From February to May 2020, no irrigation was applied. Cation concentrations gradually increased due to surface evaporation and the capillary rise of saline water from the shallow water table. The first two sets of peaks in Figure 5.42 to Figure 5.44 correspond to experiments 2 and 3 with the saline irrigation cycles (May 2020 and October 2020). After both irrigation applications, cation ion concentrations continued to increase further due to the continuous evaporation from the surface. It is observed that the use of saline water for irrigation purposes had a much rapid and dramatic increase in cation concentrations in the topsoil than capillary rise from the shallow water table. The application of saline water serves as a means for the rapid and detrimental introduction of saline water to the topsoil.

A rapid decrease in cation concentration was also observed after the application of DI water (December 2020 and March 2021) through both flooding and drip irrigation. The declines shown after the last peaks in these 2 experiments are followed by a rapid incline towards the levels that were present before the freshwater application. The possible explanation for this is the re-distribution of salts to the surface by capillary rise after each peak that is caused by the irrigation. This demonstrates that the application amount of freshwater irrigation serves as a temporary reduction of topsoil salinity. Unless salts are drained from the soil column, the benefits of freshwater irrigation will be short-lived and ultimately reversed by the continuous evaporation at the surface combined with capillary action.

The flood irrigations with saline water (experiment 2) resulted in a sharp increase in all cations, with Ca^{2+} having the most increase. The reason for this difference in calcium is hypothesized to be due to the given calcite precipitated concentration throughout the soil profile which dissolved upon the irrigation cycles.

After a period of stability after experiment two, the second sets of peaks occurred as a response to the third experiment with drip irrigation cycles with saline water. In this experiment, the same increase in the surface salinity is observed from the simulation but only, it is accumulated in a longer period than the flood irrigation as expected from the duration of the irrigation cycles. The fact that both flood and drip irrigations resulted in a relatively same increase in the cation concentrations suggests that the amounts of salts added to the system has significance in the surface salinity, not the type of irrigation. In the conducted experiments the volume of water applied through flooding and drip irrigations were the same. However, in real practise by farmers, drip irrigation is applied to reduce the amount of irrigation water used in comparison to flood irrigation which requires an immense amount of water. Therefore, in the farmer scenarios applying drip irrigation would indeed decrease the total amount of salts added to the soil surface. Hence, it could be concluded that drip irrigation can be a better option for managing the surface salinity only if the total amount of salts added by this type of irrigation is less than the flood irrigation.

Experiments 4 and 5, shown respectively by the sets of peaks at December 2020 and March 2021 in Figure 5.42 to Figure 5.44 reveal the impact of freshwater (DI) irrigations on removing the soil surface cation concentrations or in other words, it indicates the changes in the surface salinity. The DI water irrigation effect on removing or pushing down the surface salts is shown by the simulations to be also dependent on the type of salinity. For instance, the Mg^{2+} concentrations reach as low as about 22 mEq/L during the DI flood irrigations (experiment 4), but it only decreases to about 30

mEq/L during the DI drip irrigation cycles (experiment 5). On the other hand, the duration of the period at which the surface salinity stays at minimum conditions is longer in the freshwater drip irrigation cycle in comparison to the flood irrigations with freshwater. This suggests that the amount of water and the frequency of its application in combination are directly proportional to the significance and endurance of washing salts to the lower depth of the soil profile. Hence, the type of plant, its growth period and its root system are important factors in deciding about the amount and frequency of freshwater irrigation as a treatment against salinization problems. For example, an agricultural profile with a specific plant may have a two-week period upon which the plant needs to receive enough fresh water for its intended growth. During this period the farmer can apply a sufficient amount of freshwater irrigation with a frequency to push the salts just below the root system of the agriculture plants. This brings an idea for further studies to develop a tool that can calculate the amount and frequency of the irrigation water needed to counteract salinization to get the maximum yield from lands with poor drainage (having shallow aquifers) and salinity problems.

The only study found which numerically modelled a column experiment scenario with a shallow groundwater table with HYDRUS-1D was Ibrahimi et al. (2014). The authors used a different approach to test the impact of the depth of the shallow water table by using bromine (Br) as a tracer element to measure the solute fate and transport. Ibrahimi et al. (2014) found out that applying low quantity but a frequent freshwater application can be used to push salinity below the top layer of the soil. This is consistent with our conclusion that is shown in the final sets of peaks in Figure 5.42 to Figure 5.44. It is important to note here that as long as the salts remain in the soil column (i.e., salts are not drained), the benefits of freshwater irrigation will be temporary with the salinity gradually increasing to its previous levels.

Overall, the column experiments and the simulations both suggest that in the presence of a saline shallow aquifer it is not likely to have a long-term solution against salinization for the specific soil type used in this study. Nonetheless, short-term solutions such as the application of freshwater can solve the farmers' issue regarding the reduction of yield upon salinity. The type of soil, the sort of plant and the availability of freshwater all play a role in the practicability of such short-term solution. It could be concluded that without having proper drainage the salinity within the profile would continue to accumulate while freshwater application being able to temporarily move and disperse the salts along with the depth of the profile.

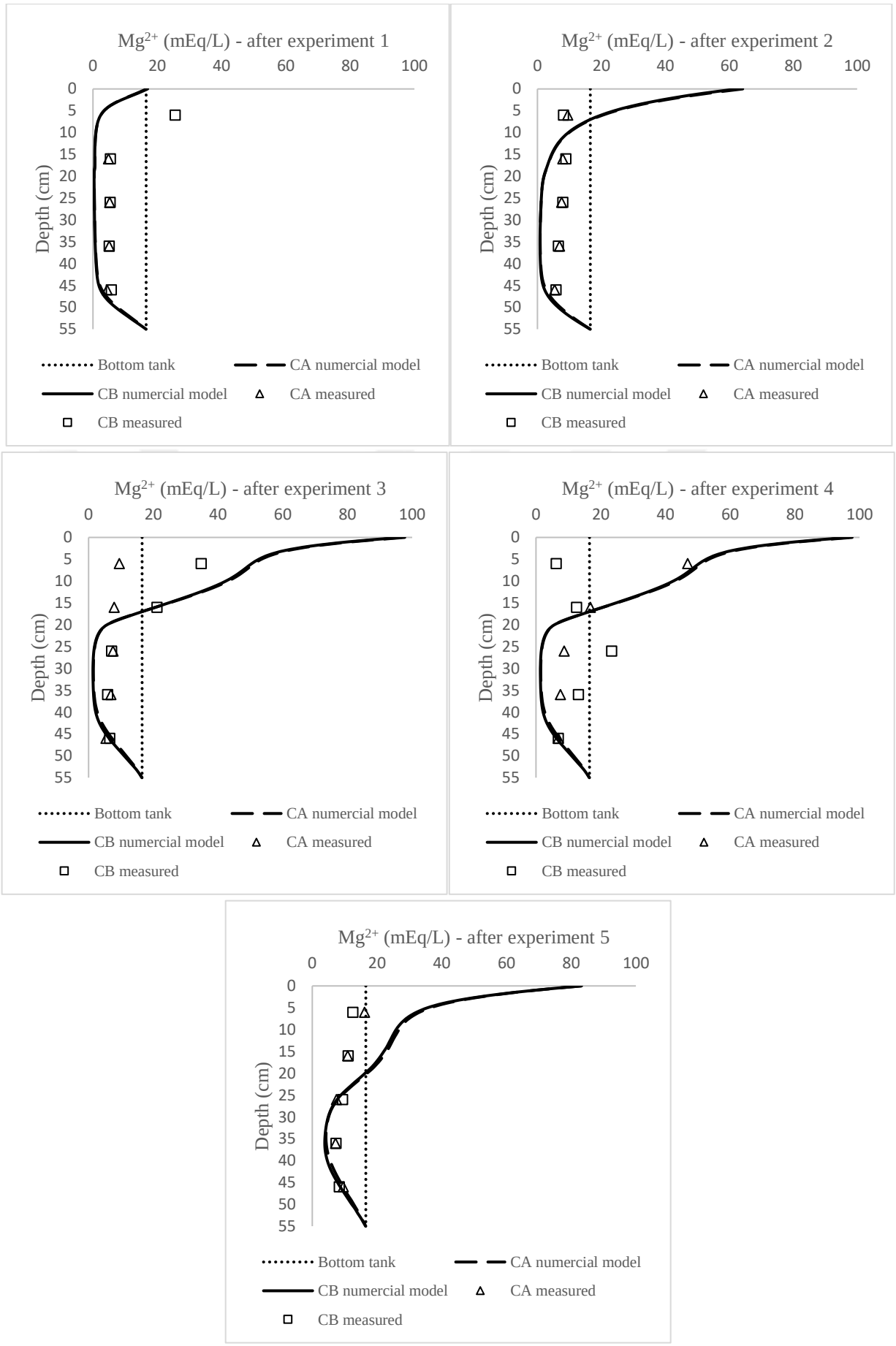

Figure 5.39. Comparisons between simulated and measured Mg^{2+} concentration profiles.

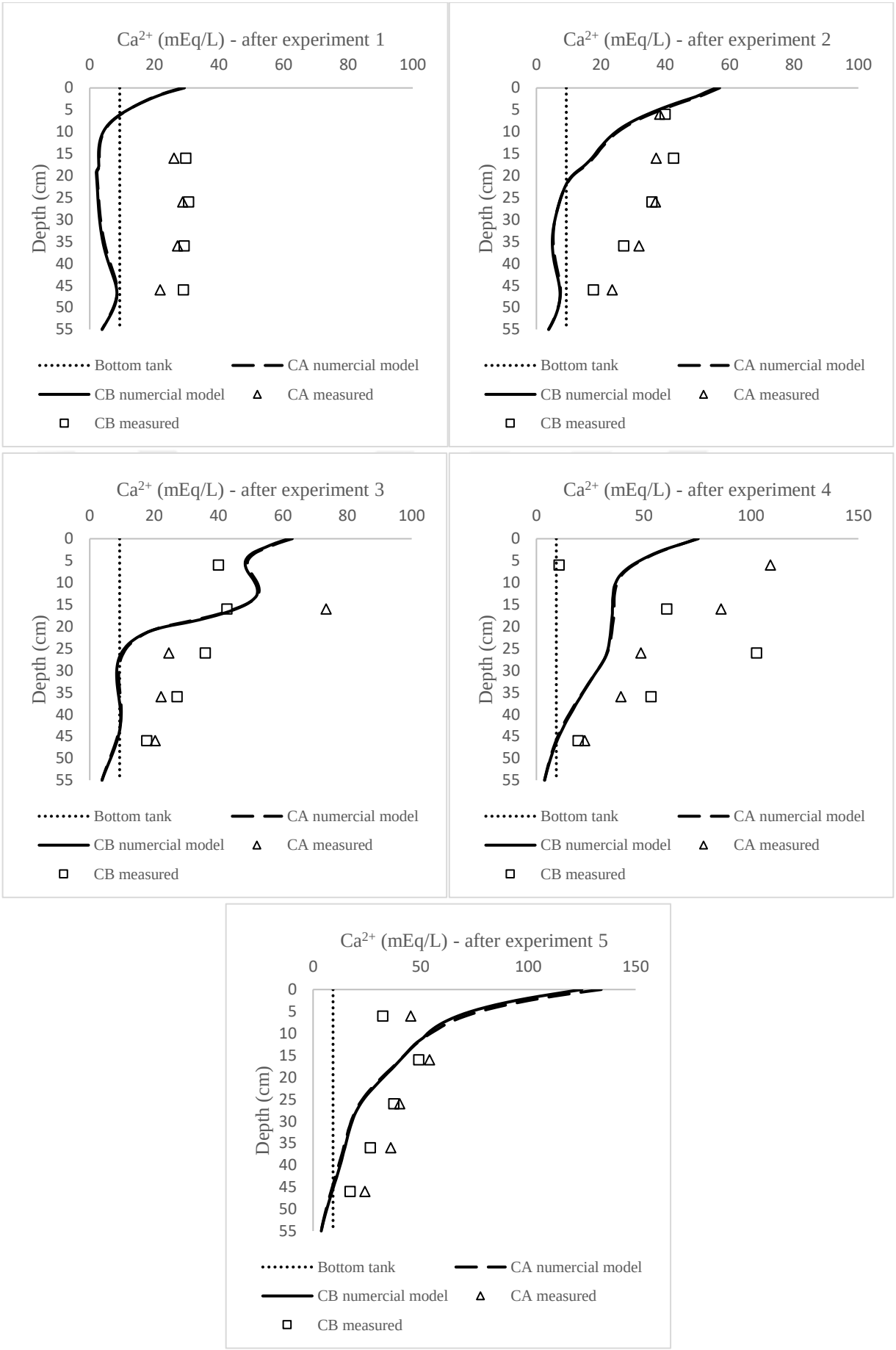

Figure 5.40. Comparisons between simulated and measured Ca^{2+} concentration profiles.

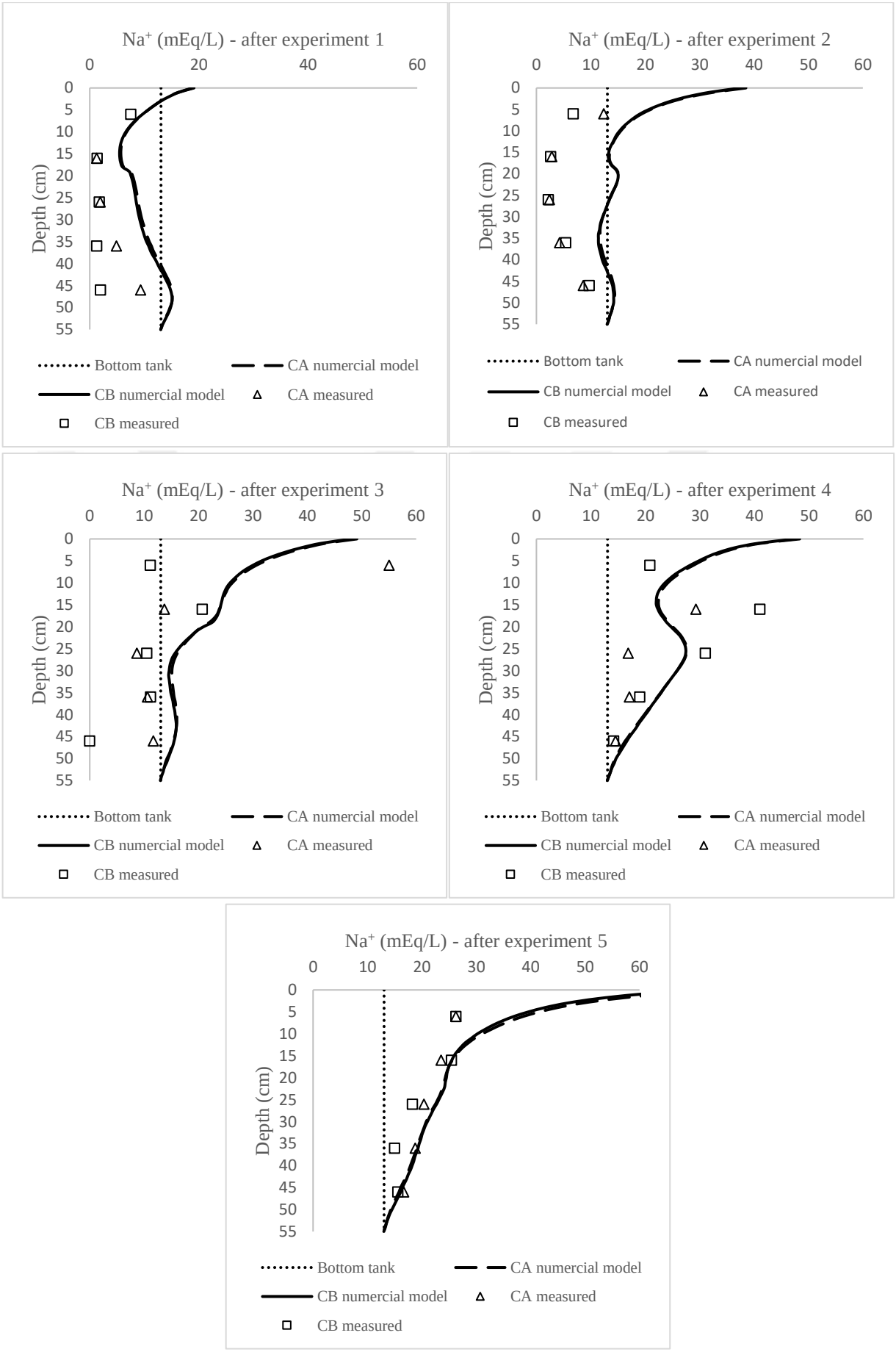

Figure 5.41. Comparisons between simulated and measured Na^+ concentration profiles.

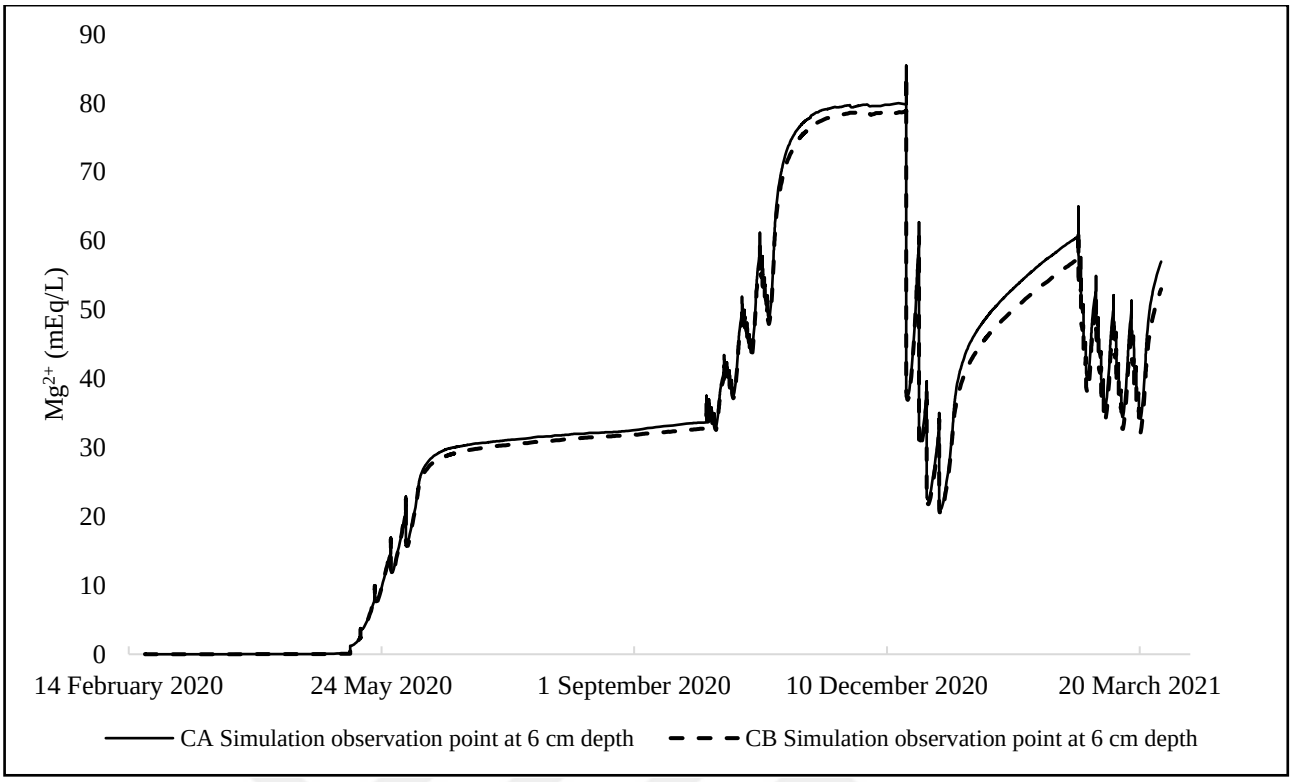

Figure 5.42. Simulated Mg^{2+} concentration in soil water through experiments 1 to 5.

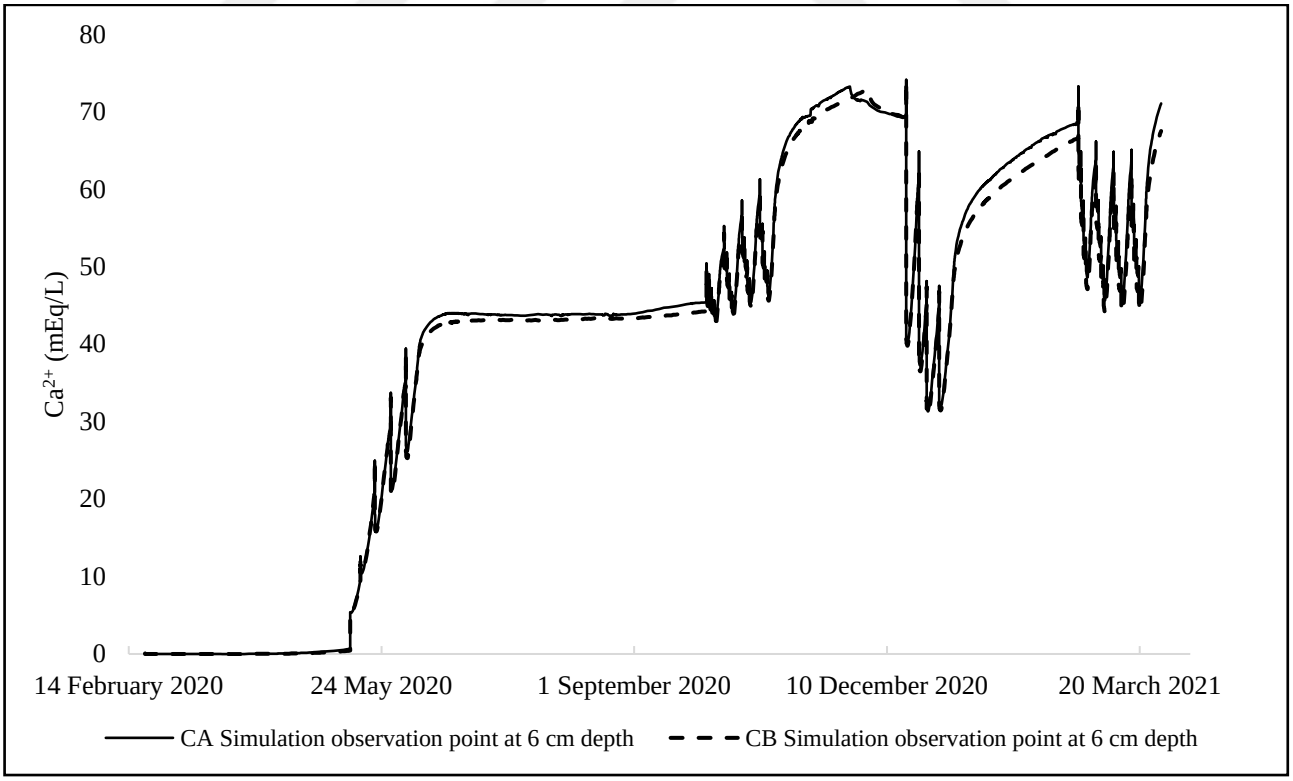

Figure 5.43. Simulated Ca^{2+} concentration in soil water through experiments 1 to 5.

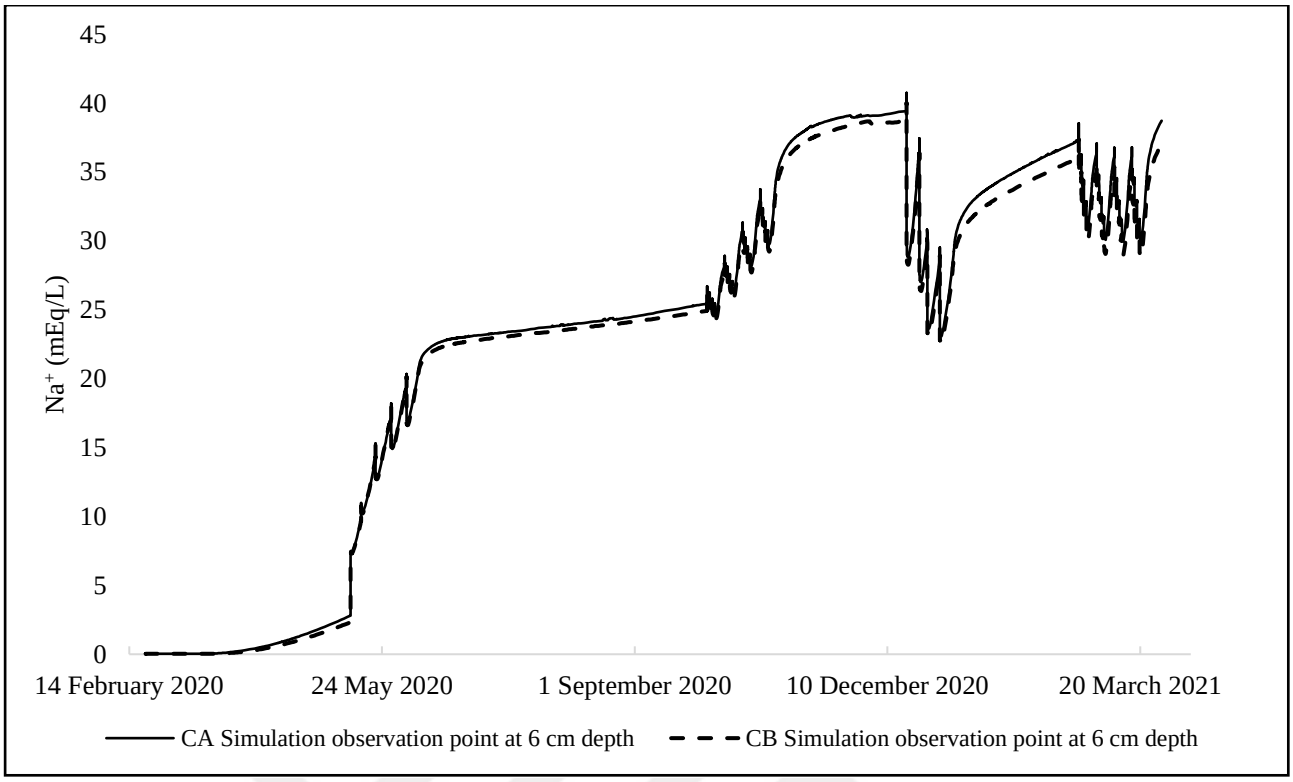

Figure 5.44. Simulated Na^+ concentration in soil water through experiments 1 to 5.

6. CONCLUSIONS

This two-year-long study examined the problem of soil salinization in arid and semi-arid environments in the presence of a saline shallow water table. Henceforth, a laboratory experimental setup was created to measure soil moisture and salt dynamics in a soil profile under different irrigation patterns. The soil used in the experiments was collected from an apple farm located in the Konya plain. The soils were transported to the laboratories at the Institute of Environmental Sciences at Bogazici University and packed into two soil columns. One column representing a soil profile with uniform bulk density and the other consisted of two layers with different compactions. A saline water tank was placed below each column to mimic a saline shallow aquifer.

Six different experiments were conducted on the soil columns to measure and examine the salinization phenomena by comparing different irrigation scenarios utilizing the soil column setup. Moisture and water potential were measured at various depths of the column, while the bulk electrical conductivity was recorded only at the surface by the designated soil sensors. In addition, soil water samples were collected at various depths at different instances throughout the experiments.

Moreover, a HYDRUS-1D numerical model (Simunek, et al. 2009) was developed to simulate the column experiments. The hydraulic model was calibrated with the initial soil measurements and the sensor measurements. The calibrated model was utilized as a base to run the HYDRUS-1D solute transport model to better understand the impact of irrigation type and soil compaction on the transient salinization processes.

The main findings of this study are:

- The rate of capillary rise in the soil profile with compaction was higher than that of the soil profile with uniform bulk density.
- Agricultural soil compaction can act as a hydraulic barrier limiting the soil moisture flow through the compacted layer.
- If the capillary rise is the only means of water transport within the column, the compaction layer speeds up the moisture movement towards the surface, while it decreases the magnitude of the transport.

- If irrigation is applied the compaction layer acts as a barrier to hold the moisture longer in the upper soil.
- Having a free drainage bottom boundary greatly helps in treating the surface salinization in comparison to having a shallow groundwater table.
- Agricultural compaction slows down the treatment of surface salinization in the case when a free drainage bottom boundary condition is present.
- Drip irrigation with freshwater is less effective than flood irrigation in pushing down the surface salinity to deeper levels.
- Drip irrigation with saline water contributes to a higher surface salt accumulation than flood irrigation with saline water given the same volume of irrigation water.
- The most effective method of washing down the salts within the tested scenarios is to apply freshwater flood irrigation with free drainage at the bottom.
- The soil compaction layer led to a more significant increase in surface moisture in drip irrigation than flood irrigation, given the clay-loam soil profile with a shallow groundwater table used in this study.
- The cumulative amount of salts added through the irrigation is the main contributor to the profile's salinity irrespective of the type of irrigation.
- Minimizing the amount of salts infiltrating the column by reducing the applied saline water can help in reducing the surface salinization problems.
- The amount of freshwater, as well as the frequency of its application can temporally push down the salinity to the lower soil layers in the presence of a shallow saline aquifer.
- The type of plant and its root system are important factors in deciding about the amount and frequency of freshwater irrigation as a treatment to fight salinization problems in profiles with a shallow groundwater table.
- In the presence of a saline shallow aquifer, it is not possible to have a long-term solution against salinization for the specific soil type used in this study
- Free drainage conditions are the single most important factor against salt accumulation, more so than the application of freshwater irrigation.
- The application of freshwater can only serve as a short-term solution to counter salinization problems in soil profiles with a saline shallow water table.

In conclusion, the capillary action from shallow water table along with surface evaporation can lead to significant accumulations of salts in the surface soils. Moreover, the agricultural compaction

layer greatly impacts the moisture distribution within the soil profile, hindering the infiltration, but at the same time, contributing to the capillary rise from the shallow aquifers. If the same amount of irrigation and water quality are applied, the mode of irrigation (drip vs flooding) had minimal effect on the salinity accumulation in the topsoil. However, drip irrigation proved to be a better option for managing the surface salinity because it uses water resources more efficiently with a less total amount of salts added by this type of irrigation compared to flood irrigation. This study concluded that without having proper drainage the salinity within the profile would only accumulate in the presence of a shallow saline aquifer. Furthermore, the numerical simulations show that short-term solutions such as the application of freshwater during the critical plant growth period can limit the accumulation of salts in agricultural soils. The type of soil, the kind of plant and the availability of fresh water all play a role in the practicability of such short-term solution.

This study could be further expanded in the future to investigate the salinization process of agricultural soil profiles with the aim of finding possible solutions to solve the agricultural salinization problems. Among the main points that can be improved in the future are:

- The number of irrigation scenarios and their replicas can increase in order to further testify the conclusion of the experiments. For instance, different irrigation water qualities, at different sequences can be tested for a range of soil types in the same setup to create a more complete picture of the system.
- Field experiments can be conducted to compare and validate the findings of laboratory experiments at the field scale under undisturbed soil conditions.
- Different profile heights can be tested to determine the impact of alternation in the depth of the shallow saline water table on the salinization processes.
- Effects of sodicity can be further explored throughout the experiments with a shallow aquifer. This can be analysed by changing the shallow aquifer and irrigation waters to be sodic.
- The hydraulic parameters and their changes can be measured in a more comprehensive setup to better calibrate the numerical model.
- The sensitivity of different parameters in the numerical model on soil moisture and salt dynamics can be tested to better understand the underlying flow and transport processes and to identify effective remedial actions.

In addition to the expansion of the current setup, this research suggests the possibility of the development of a practical tool to identify the optimal type of freshwater irrigation cycle in accordance with the soil type, cultivated crop and water availability to minimize the impact of salinity on agricultural yields of lands with salinization problems. The tool can be further expanded as a management program for farmers battling soil salinity, particularly in arid and semi-arid regions of the world.

REFERENCES

Abrol, I. P., Jai Singh Pal Yadav, and F. I. Massoud. 1988. Salt-affected soils and their management. Food & Agriculture Org.

Analytics, Clarivate. 2021. “Web of science.”, www. webofknowledge.com. Date accessed May 2021.

Bauder, Troy Allen, R. M. Waskom, P. L. Sutherland, J. G. Davis, R. H. Follett, and P. N. Soltanpour. 2011. Irrigation water quality criteria. Service in action, no. 0.506 ,Colorado State University. Libraries.

Baumhardt, R. L., C. W. Wendt, and J. Moore. 1992. Infiltration in response to water quality, tillage, and gypsum. Soil Science Society of America Journal, Soil Science Society of America, 56, 261–266.

Bin, L. 2005. Model-LEACHC and its Applications in Predicting the Soil Salinization and Alkalization. Journal of Anhui Agricultural Sciences 33, 2835.

Bjorneberg, D. L. 2013. Irrigation Methods. Reference Module in Earth Systems and Environmental Sciences. Irrigation Methods. Reference Module in Earth Systems and Environmental Sciences. Elsevier.

Blaine, Hanson. 1999. Upward Flow of Saline Shallow Groundwater. Agricultural salinity and drainage ,University of California Irrigation Program 83-86.

Bozdağ, Ayla. 2015. Combining AHP with GIS for assessment of irrigation water quality in Çumra irrigation district (Konya), Central Anatolia, Turkey. Environmental earth sciences, 73, 12, 8217-8236.

British Standards Institution. 2006. BS ISO 11464 Soil quality. Pretreatment of samples for physio-chemical analysis,

https://landingpage.bsigroup.com/LandingPage/Undated?UPI=000000000030090431. Date accessed May 2021.

Cardon, G. E., and J. Letey. 1992. Soil-based irrigation and salinity management model: II. Water and solute movement calculations. Soil Science Society of America Journal, Wiley Online Library 56, 1887–1892.

Chhabra, R. 2004. Classification of salt-affected soils. Arid Land Research and Management, Taylor & Francis, 19, 61–79.

David, Rassam, Šimůnek Jirka, Mallants Dirk, and Van Genuchten M Th. 2018. The HYDRUS-1D Software Package for Simulating the One-Dimensional Movement of Water, Heat, and Multiple Solutes in Variably-Saturated Media: Tutorial. CSIRO Land and Water, Australia, 183.

Ding, Jihui, Ibrahim Mtolera, Dongli She, Tao Ma, Kaiwen Chen, and Shuang'En Yu. 2020. Effects of Saline Water Irrigation and Biochar Amendment on Okra Growth and Nutrient Leaching in Coastal Saline Soils. Communications in Soil Science and Plant Analysis, Taylor & Francis, 1–15.

Dıvrak, Buket Bahar, Galena Is, and Ceren Ayas. 2007. Complementary Financing for Environment in the Context of Accession – Innovative Resources: National Report Turkey. A project for the European Commission (contract 070201/2006/443879/MAR/E3). WWF Turkey.

Dudley, L. M., and R. J. Hanks. 1991. Manual for the SOWACH model. Dept. of Plant, Soil and Biometeorology., Utah State University, Logan, Utah.

Eaton, Frank M. 1950. Significance of carbonates in irrigation waters. Soil science, LWW 69, 123–134.

Ezlit, Younes D., Rod J. Smith, and Steven R. Raine. 2010. A review of salinity and sodicity in irrigation, University of Southern Queensland.

Ferretti, Giacomo, Dario Di Giuseppe, Barbara Faccini, and Massimo Coltorti. 2018. Mitigation of sodium risk in a sandy agricultural soil by the use of natural zeolites. Environmental monitoring and assessment, Springer 190, 646.

Ghamarnia, Houshang, and Zahra Jalili. 2014. Shallow saline groundwater use by Black cumin (Nigella sativa L.) in the presence of surface water in a semi-arid region. Agricultural water management, Elsevier 132, 89–100.

Gonçalves, Maria C., Jirka Šim\uunek, Tiago B. Ramos, José C. Martins, Maria J. Neves, and Fernando P. Pires. 2006. Multicomponent solute transport in soil lysimeters irrigated with waters of different quality. Water Resources Research, Wiley Online Library, 42.

Hamza, M. A., and W. K. Anderson. 2005. Soil compaction in cropping systems: A review of the nature, causes and possible solutions. Soil and tillage research, Elsevier, 82, 121–145.

Hoffman, Glenn J. 1985. Drainage required to manage salinity. Journal of Irrigation and Drainage Engineering, American Society of Civil Engineers, 111, 199–206.

Hutmacher, R. B., J. E. Ayars, S. S. Vail, A. D. Bravo, D. Dettinger, and R. A. Schoneman. 1996. Uptake of shallow groundwater by cotton: growth stage, groundwater salinity effects in column lysimeters. Agricultural Water Management, Elsevier, 31, 205–223.

Ibrahimi, Mohamed Khaled, Tsuyoshi Miyazaki, Taku Nishimura, and Hiromi Imoto. 2014. Contribution of shallow groundwater rapid fluctuation to soil salinization under arid and semiarid climate. Arabian Journal of Geosciences, Springer 7, 3901–3911.

Institution, British Standards. 2018. BS EN ISO 23470 Soil quality. Determination of effective cation exchange capacity (CEC) and exchangeable cations using a hexamminecobalt trichloride solution. https://bsol.bsigroup.com/Bibliographic/BibliographicInfoData/000000000030333247. Date accessed May 2021.

Jones, R. J. A., and Luca Montanarella. 2001. Subsoil Compaction: A hidden form of Soil Sealing in Europe, European Soil Bureau, JRC.

Jorenush, M. H., and A. R. Sepaskhah. 2003. Modelling capillary rise and soil salinity for shallow saline water table under irrigated and non-irrigated conditions. Agricultural water management, Elsevier, 61, 125–141.

Kellogg, Charles Edwin. 1937. Soil survey manual. US Department of Agriculture.

Kobayashi, Tetsuo, Daisuke Yokoyama, Kenji Ebihara, Yasutaka Sonoda, Yoshinobu Sakata, Kazuki Urayama, Hiroyuki Cho, Hisashi Yoshikoshi, and Masaharu Kitano. 2008. Column Experiments on the Salt Accumulation in Adjoining Different–Textured Soil Profiles with a Shallow Water Table. Journal of the Faculty of Agriculture, Kyushu University 53, 529–534.

Lal, R. 1994. Water management in various crop production systems related to soil tillage. Soil and tillage research, Elsevier, 30, 169–185.

Li, Yufang, Mingsi Li, Hongguang Liu, and Wenbao Qin. 2021. Influence of soil texture on the process of subsurface drainage in saturated-unsaturated zones. International Journal of Agricultural and Biological Engineering, 14, 82–89.

Lu, N., and W. J. Likos. 2004. Rate of capillary rise in soil. Journal of geotechnical and Geoenvironmental engineering, American Society of Civil Engineers, 130, 646–650.

Malash, N. M., T. J. Flowers, and R. Ragab. 2008. Effect of irrigation methods, management and salinity of irrigation water on tomato yield, soil moisture and salinity distribution. Irrigation Science, Springer, 26 313–323.

Malicki, MA, and RT Walczak. 1999. Evaluating soil salinity status from bulk electrical conductivity and permittivity. European Journal of Soil Science, Wiley Online Library, 50, 3, 510-514.

McGarry, D. 2003. Tillage and soil compaction. In Conservation agriculture, 307–316. Springer.

Moghbel, Farzam, Behrouz Mostafazadeh-Fard, S. A. M. M. Maibodyand, Esmaeil Landi, and others. 2017. Salinity management for irrigation with saline-sodic wastewater under corn cultivation. Soil and Environment, Soil Science Society of Pakistan, 36, 120–130.

Nachshon, Uri. 2018. Cropland soil salinization and associated hydrology: Trends, processes and examples. Water, 10, 8, 1030.

Nakagawa, K., T. Hosokawa, S.-I. Wada, K. Momii, K. Jinno, and Ronny Berndtsson. 2010. Modelling reactive solute transport from groundwater to soil surface under evaporation. Hydrological Processes: An International Journal, Wiley Online Library, 24, 608–617.

Nassar, I. N., and Robert Horton. 1999. Salinity and compaction effects on soil water evaporation and water and solute distributions. Soil Science Society of America Journal, Soil Science Society, 63, 752–758.

of the United Nations. Crop, Agriculture Organization, and Grassland Service. 2003. Explore On-farm: On-farm Trials for Adapting and Adopting Good Agricultural Practices. Food & Agriculture Org.

Oosterbaan, R. J. 2001. SALTMOD; description of principles, user manual, and examples of application, Version 1.1. Tech. rep., ILRI.

Ozbahce, Aynur, and Ali Fuat Tari. 2010. Effects of different emitter space and water stress on yield and quality of processing tomato under semi-arid climate conditions. Agricultural Water Management, Elsevier, 97, 1405–1410.

Pessarakli, Mohammed, and Istvan Szabolcs. 1999. Soil salinity and sodicity as particular plant/crop stress factors. Handbook of plant and crop stress, Marcel Dekker New York, NY 2.

Qadir, M., R. H. Qureshi, and N. Ahmad. 1996. Reclamation of a saline-sodic soil by gypsum and Leptochloa fusca. Geoderma, Elsevier, 74, 207–217.

Radcliffe, David E, and Jiri Simunek. 2018. Soil physics with HYDRUS: Modeling and applications. CRC press.

Rengasamy, P., and K. A. Olsson. 1993. Irrigation and sodicity. Soil Research, CSIRO, 31, 821–837.

Rengasamy, Pichu. 2010. Soil processes affecting crop production in salt-affected soils. Functional Plant Biology, CSIRO, 37, 613–620.

Rengasamy, Pichu. 2006. World salinization with emphasis on Australia. Journal of experimental botany, Oxford University Press, 57, 1017–1023.

Rhoades, J. D. 1993. Electrical conductivity methods for measuring and mapping soil salinity. Vol. 49, in Advances in agronomy, 201–251.

Rhodes, Christopher J. 2012. Feeding and healing the world: through regenerative agriculture and permaculture. Science progress, SAGE Publications Sage UK: London, England, 95. 345–446.

Richards, Lorenzo Adolph. 1954. Diagnosis and improvement of saline and alkali soils. Vol. 78. LWW.

Seelig, Bruce. 2000. Salinity and sodicity in North Dakota soils, North Dakota State University.

Seleiman, Mahmoud F., Ahmed Kheir, Sami Al-Dhumri, Abdulaziz G. Alghamdi, El-Said H. Omar, Hesham M. Aboelsoud, Kamel A. Abdella, and Waleed H. Abou El Hassan. 2019. Exploring Optimal Tillage Improved Soil Characteristics and Productivity of Wheat Irrigated with Different Water Qualities. Agronomy Multidisciplinary Digital Publishing Institute, 9, 233.

Shahid, Shabbir A., Mohammad Zaman, and Lee Heng. 2018. Soil Salinity: Historical Perspectives and a World Overview of the Problem. In Guideline for Salinity Assessment, Mitigation and Adaptation Using Nuclear and Related Techniques. Springer International Publishing. https://doi.org/10.1007/978-3-319-96190-3_2.

Shainberg, Isaac, John Letey, and others. 1984. Response of soils to sodic and saline conditions. Hilgardia, University of California, Agriculture and Natural Resources, 52, 1–57.

Simunek, J., M. Šejna, H. Saito, M. Sakai, and M. T. Van Genuchten. 2009. The HYDRUS-1D software package for simulating the one-dimensional movement of water, heat, and multiple solutes in variably-saturated media, version 4.08. University of California, Riverside, Dept. of Environmental Sciences HYDRUS Software Series, 3, 330.

Simunek, Jirka, Diederik Jacques, Scott A. Bradford, and Martinus Th van Genuchten. 2013. Numerical modeling of contaminant transport using HYDRUS and its specialized modules. Journal of the Indian institute of science, 93, 265–284.

Singh, Purnendu N., and Wesley W. Wallender. 2010. Effects of soil water salinity on field soil hydraulic functions. Journal of Irrigation and Drainage Engineering American Society of Civil Engineers, 137, 295–303.

Skaggs, R. Wayne, M. A. Youssef, and G. M. Chescheir. 2012. DRAINMOD: Model use, calibration, and validation. Transactions of the ASABE, American Society of Agricultural and Biological Engineers, 55, 1509–1522.

Stitt, R. E., D. K. Cassel, S. B. Weed, and L. A. Nelson. 1982. Mechanical Impedance of Tillage Pans in Atlantic Coastal Plains Soils and Relationships with Soil Physical, Chemical, and Mineralogical Properties 1. Soil Science Society of America Journal, Soil Science Society of America, 46, 100–106.

Suarez, Donald L., and J. Šimůnek. 1997. UNSATCHEM: Unsaturated water and solute transport model with equilibrium and kinetic chemistry. Soil Science Society of America Journal, Wiley Online Library, 61, 1633–1646.

Thellier, Catherine, Garrison Sposito, and Kenneth M. Holtzclaw. 1990. Chemical effects of saline irrigation water on a San Joaquin Valley soil: I. Column studies. Journal of environmental quality, American Society of Agronomy, Crop Science Society of America, and Soil, 19, 50–55.

Tiwari, Priyanka , and Arun Goel. 2013. Review of computer based software tools for salinity management in agricultural lands.. Journal of Indian Water Resources Society 33, 4, 24-32.

USDA. 2008. Soil Quality Indicators. USDA. https://www.nrcs.usda.gov/Internet/FSE_DOCUMENTS/nrcs142p2_053256.pdf. Date accessed June 2021.

van Dam, Jos C. 2000. Field-scale water flow and solute transport: SWAP model concepts, parameter estimation and case studies.

Van der Zee, S. E. A. T. M., S. H. H. Shah, C. G. R. Van Uffelen, Peter A. C. Raats, and N. Dal Ferro. 2010. Soil sodicity as a result of periodical drought. Agricultural Water Management, Elsevier, 97, 41–49.

Vargas, R., Evgeniĭa Ivanovna Pankova, S. A. Balyuk, P. V. Krasilnikov, and G. M. Khasankhanova. 2018. Handbook for saline soil management. FAO/LMSU.

Wang, Qingjie, Caiyun Lu, Hongwen Li, Jin He, Khokan Kumer Sarker, Rabi G. Rasaily, Zhonghui Liang, Xiaodong Qiao, Hui Li, and Allen David Jack Mchugh. 2014. The effects of no-tillage with subsoiling on soil properties and maize yield: 12-Year experiment on alkaline soils of Northeast China. Soil and Tillage Research, Elsevier, 137, 43–49.

Warrence, Nikos J., James W. Bauder, and Krista E. Pearson. 2002. Basics of salinity and sodicity effects on soil physical properties. Departement of Land Resources and Environmental Sciences, Montana State University-Bozeman, MT, Citeseer 1–29.

Weil, R. R., and N. C. Brady. 2017. The Nature and Properties of Soils, Global Edition. Pearson Prentice Hall: Harlow, UK.

Weill, Sylvain, Emmanuel Mouche, and Jérémy Patin. 2009. A generalized Richards equation for surface/subsurface flow modelling. Journal of Hydrology 366, 1, 9-20.

Yadav, Sangeeta, Mohd Irfan, Aqil Ahmad, and Shamsul Hayat. 2011. Causes of salinity and plant manifestations to salt stress: a review. Journal of Environmental Biology, Triveni Enterprises, 32, 667.

Yang, Ting, Jirka Šim\uunek, Minghao Mo, Blake Mccullough-Sanden, Hossein Shahrokhnia, Setrag Cherchian, and Laosheng Wu. 2019. Assessing salinity leaching efficiency in three soils by the HYDRUS-1D and-2D simulations. Soil and Tillage Research, Elsevier, 194, 104342.

Yue, Y., W. N. Guo, Q. M. Lin, G. T. Li, and X. R. Zhao. 2016. Improving salt leaching in a simulated saline soil column by three biochars derived from rice straw (Oryza sativa L.), sunflower straw

(Helianthus annuus), and cow manure. Journal of Soil and Water Conservation, Soil and Water Conservation Society, 71, 467–475.

Zhang, He, L. I. Yan, M. E. N. G. Ya-li, C. A. O. Nan, L. I. Duan-sheng, Z. H. O. U. Zhi-guo, C. H. E. N. Bing-lin, and D. O. U. Fu-gen. 2019. The effects of soil moisture and salinity as functions of groundwater depth on wheat growth and yield in coastal saline soils. Journal of Integrative Agriculture, Elsevier, 18, 2472–2482.